Enabling Exploration with Small Radioisotope Power Systems

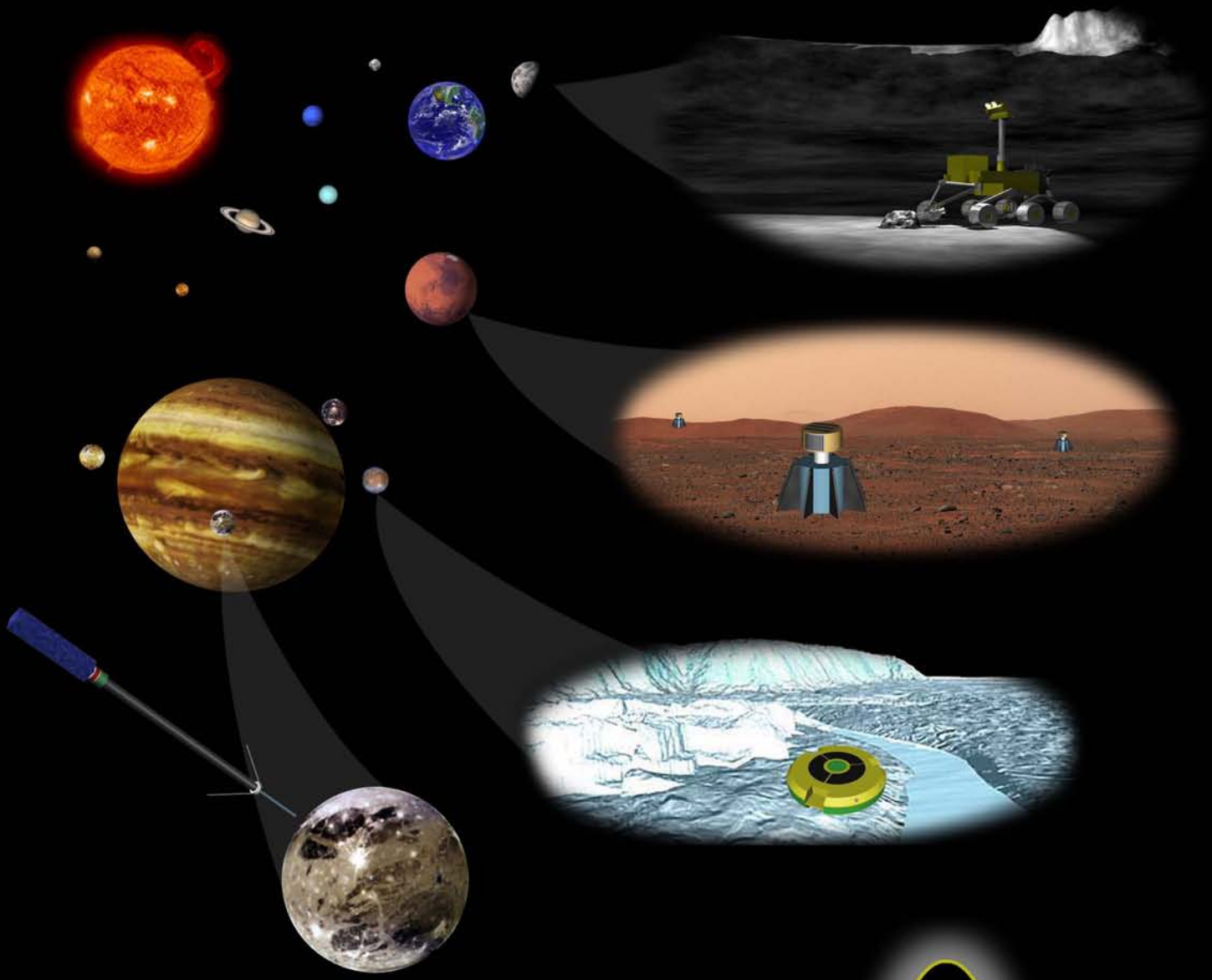

JPL Pub 04-10

Enabling Exploration with Small Radioisotope Power Systems

Requested by

George R. Schmidt
NASA Office of Space Science

Written by

Robert D. Abelson (Editor)	JPL/Caltech
Tibor S. Balint	JPL/Caltech
Kathryn E. Marshall	JPL/Caltech
Heros Noravian	Analytix/DOE
James E. Randolph	JPL/Caltech
Celeste M. Satter	JPL/Caltech
George R. Schmidt	NASA HQ
James H. Shirley	JPL/Caltech

September 2004

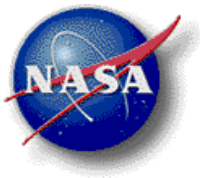

JPL

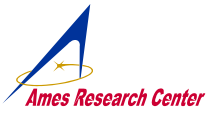

GSFC

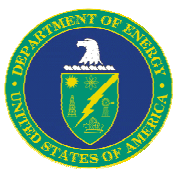

Prepared by the Jet Propulsion Laboratory, California Institute of Technology and the U.S. Department of Energy through an agreement with the National Aeronautics and Space Administration.

Table of Contents

List of Figures

List of Tables

1. SUMMARY

1.1 BACKGROUND

Radioisotope Power Systems (RPSs) generate electrical power by converting the heat released from the nuclear decay of radioactive isotopes into electricity. First used in space by the United States in 1961, these devices have consistently demonstrated unique capabilities over other types of space power systems for applications up to a kilowatt, and studies have indicated that these benefits may extend to at least applications requiring up to several kilowatts [1]. A key advantage is their ability to operate continuously, independent of orientation to and distance from the Sun. Radioisotope systems are also long-lived, rugged, compact, highly reliable, and relatively insensitive to radiation and other environmental effects. As such, they are ideally suited for missions involving autonomous operations in the extreme environments of space and planetary surfaces.

Table 1-1 lists the 28 U.S. space missions that have safely flown radioisotope energy sources since 1961. Four of these missions flew radioisotope heater units only, whereas twenty-one successfully used RPSs to produce power for scientific instruments and spacecraft operations. Some of the most notable RPS flights are the Apollo lunar missions, the Viking Mars landers, and the Pioneer, Voyager, Ulysses, Galileo and Cassini outer planetary probes. The different RPS units that the U.S. has developed and flown over the years have all provided electrical power levels ranging from ten to several hundred watts. The current system, the General Purpose Heat Source (GPHS)-Radioisotope Thermoelectric Generator (RTG), typically generates 285 watts of electrical power (We) at the beginning of its life (BOL). Two new units currently under development, the Multi-Mission RTG (MMRTG) and Stirling Radioisotope Generator (SRG), will each provide at least 110 We at BOL.

The increased use of smaller spacecraft over the last decade, in combination with studies of potential science applications, has suggested the need for RPSs yielding much lower power levels. Radioisotope generators lend themselves to small, long-lived power applications mainly because the rate of heat production per unit mass of fuel is independent of the size of the system. In fact, development of generators with power levels as low as tens of milliwatts appears to be quite feasible using existing plutonium-238 (Pu-238) heat sources and thermoelectric energy conversion technology. Such RPS power supplies have the potential to extend the capability of small science payloads and instruments, and to enable applications such as:

- Long-lived meteorological/seismological stations broadly distributed across planetary surfaces
- Small landers at extreme latitudes or in regions of low solar flux
- Surface and atmosphere-based mobility systems
- Subsurface probes, including impactors and autonomous boring devices
- Deep space micro-spacecraft and sub-satellites

Such units could also find application in future human exploration missions involving use of monitoring stations and autonomous devices, similar to the ALSEP units deployed on the Moon during the Apollo program.

Although flight-qualified RPS units in this size and power range do not presently exist, their potential to support a broad range of exploration tasks has led NASA and the Department of Energy (DOE) to consider the development of small-RPS units such that they might be available for missions by the early part of next decade. Starting in 2003, NASA's Office of Space Science and DOE convened a series of studies and technical interchange meetings to review the potential applications, associated requirements, and methodology for pursuing development of small-RPS.

Table 1-1. U.S. Space Missions Using Radioisotopes for Electrical and Thermal Power [2]

#	Spacecraft	Principal Energy Source (#)	Destination/ Application	Launch Year	Status
1	Transit 4A	SNAP-3B7 RTG (1)	Earth Orbit/ Navigation Satellite	1961	RTG operated for 15 yrs. Satellite now shut down.
2	Trandit 4B	SNAP-3B8 RTG (1)	Earth Orbit / Navigation Satellite	1961	RTG operated for 9 yrs. Operation intermittent after 1962 high alt test. Last signal in 1971.
3	Transit 5BN-1	SNAP-9A RTG (1)	Earth Orbit / Navigation Satellite	1963	RTG operated as planned. Non-RTG electrical problems on satellite caused failure after 9 months.
4	Transit 5BN-2	SNAP-9A RTG (1)	Earth Orbit / Navigation Satellite	1963	RTG operated for over 6 yrs. Satellite lost navigational capability after 1.5 yrs.
5	Transit 5BN-3 [1]	SNAP-9A RTG (1)	Earth Orbit / Navigation Satellite	1964	Mission aborted because of launch vehicle failure.
6	Nimbus B-1 [2]	SNAP-19B2 RTG (2)	Earth Orbit / Navigation Satellite	1968	Mission aborted because of range safety destruct. RTG heat sources recovered and recycled.
7	Nimbus III	SNAP-19B3 RTG (2)	Earth Orbit / Navigation Satellite	1969	RTGs operated for over 2.5 yrs. No data taken after that.
8	Apollo 11	ALRH Heater	Lunar Surface / Science Payload	1969	Heater units for seismic experimental package. Station shut down Aug 3, 1969.
9	Apollo 12	SNAP-27 RTG (1)	Lunar Surface / Science Payload	1969	RTG operated for about 8 years until station was shut down.
10	Apollo 13 [3]	SNAP-27 RTG (1)	Lunar Surface / Science Payload	1970	Mission aborted. RTG reentered intact with no release of Pu-238. Currently located at bottom of Tonga Trench.
11	Apollo 14	SNAP-27 RTG (1)	Lunar Surface / Science Payload	1971	RTG operated for over 6.5 years until station was shut down.
12	Apollo 15	SNAP-27 RTG (1)	Lunar Surface / Science Payload	1971	RTG operated for over 6 years until station was shut down.
13	Pioneer 10	SNAP-19 RTG (4)	Planetary / Payload & Spacecraft	1972	RTGs still operating. Spacecraft now well beyond orbit of Pluto.
14	Apollo 16	SNAP-27 RTG (1)	Planetary / Payload & Spacecraft	1972	RTG operated for about 5.5 years until station was shut down.
15	Triad-01-1X	Transit-RTG (1)	Earth Orbit / Navigation Satellite	1972	RTG still operating as of mid-1990s.
16	Apollo 17	SNAP-27 RTG (1)	Planetary / Payload & Spacecraft	1972	RTG operated for almost 5 years until station was shut down.
17	Pioneer 11	SNAP-19 RTG (4)	Planetary / Payload & Spacecraft	1973	RTGs still operating. Spacecraft operated to Jupiter, Saturn and beyond.
18	Viking 1	SNAP-19 RTG (2)	Planetary / Payload & Spacecraft	1975	RTGs operated for over 6 years until lander was shut down.
19	Viking 2	SNAP-19 RTG (2)	Planetary / Payload & Spacecraft	1975	RTGs operated for over 4 years until relay link was lost.
20	LES 8, LES 9 [4]	MHW-RTG (4)	Earth Orbit / Com Satellites	1976	RTGs still operating as of mid-1990s.
21	Voyager 2	MHW-RTG (3)	Planetary / Payload & Spacecraft	1977	RTGs still operating. Spacecraft successfully operated to Jupiter, Saturn, Uranus, Neptune, and beyond.
22	Voyager 1	MHW-RTG (3)	Planetary / Payload & Spacecraft	1977	RTGs still operating. Spacecraft successfully operated to Jupiter, Saturn, and beyond.
23	Galileo	GPHS-RTG (2) RHU Heater (120)	Planetary / Payload & Spacecraft	1989	RTGs continued to operate until 2003, when spacecraft was intentionally deorbited into Jupiter atmosphere.
24	Ulysses	GPHS-RTG (1)	Planetary / Payload & Spacecraft	1990	RTG continues to operate successfully after 14 years. Spacecraft conducting polar solar orbits.
25	Mars Pathfinder	RHU Heater (3)	Planetary / Payload & Spacecraft	1996	Heater units used to maintain payload temperature. Units still presumed active.
26	Cassini	GPHS-RTG (3) RHU Heater (117)	Planetary / Payload & Spacecraft	1997	RTGs continue to operate successfully after 7 years. Spacecraft entered Saturn orbit in 2004.
27	Mars MER Spirit	RHU Heater (8)	Mars Surface Rover Electronicst	2003	Heater units still operational and used to maintain payload temperature.
28	Mars MER Opportunity	RHU Heater (8)	Mars Surface Rover Electronics	2003	Heater units still operational and used to maintain payload temperature.

[1] Mission was aborted due to launch vehicle failure. RTG burned up on reentry as designed.
[2] Mission was aborted due to launch vehicle failure. RTG heat sources recovered, recycled and used on subsequent mission.
[3] Mission aborted on way to Moon. RTG reentered Earth atmosphere intact with no release of Pu-238. It is currently located deep in the Tonga Trench in the South Pacific Ocean.
[4] Mission consisted of two RPS-powered communications satellites (LES 8 and 9) launched on a single launch vehicle.

1.2 PURPOSE

The purpose of this report is to provide an initial reference document to support further definition of science community needs for small-RPS flight systems. It describes the most recent results of the ongoing NASA/DOE studies, and provides information for review by potential users that might take advantage of these types of power systems. This is extremely important since any future decision to proceed with the development of such units will require a strong identified need from the space science community and a well-defined set of power and operational requirements. NASA and DOE intend to use this document as a basis for soliciting information on additional small-RPS-enabled mission concepts, along with their respective power and operational requirements. This report is a first step in fleshing out a roadmap for potential future development and acquisition.

The report is divided into four parts. Section 1 summarizes the results of activities to date and provides possible options for future development. It includes the results of an initial survey of the Mars science community performed by NASA Ames Research Center (ARC), which polled potential investigators and members of the Mars Exploration Program Assessment Group (MEPAG) to assess their interests and needs for these types of systems. It also reviews the results of a recent Jet Propulsion Laboratory (JPL)-led study that extended the range of potential applications to include in-space and surface exploration of other planetary bodies. The preliminary set of mission options and technical requirements from these two activities provide a reference for engaging the science and user communities. The section also describes where efforts may be focused in support of future development.

The next three sections provide more details on small-RPS mission concepts, and describe possible technologies and designs for future power units. Section 2 describes the mission concepts examined in the JPL study, and identifies which space science programs could benefit from availability of these units. Section 3 describes the power conversion technologies that could, with modest to moderate levels of investment, be implemented in flight-qualified units by the early part of next decade. The final section presents and compares the performance of several milliwatt and multi-watt scale radioisotope generator concepts that have been developed over the last several years.

1.3 RESULTS

The results of initial surveys and studies point to many scientifically valuable mission concepts and applications that could benefit from or be enabled by small, reliable, long-lived RPSs. An important assumption in all the efforts to date has been the use of existing plutonium fuel capsule designs, since testing and evaluating new fuel configurations would likely impose excessive costs on any future development. This led to the categorization of small-RPS according to the power level groupings shown in Figure. 1-1. The upper end of small-RPS power capability (10 to 20 watts (We)) was best achieved by designing systems around single General Purpose Heat Source (GPHS) modules, which are the thermal building blocks used in current RTGs. The lower end of power output (40 to 100 milliwatts (mWe)) could be met with systems based on one to several Radioisotope Heater Unit (RHU) fuel capsules. The mid-range (100 mWe to several watts) could be accommodated by a number of options, including heat source assemblies composed of multiple RHU fuel capsules and fractional GPHS units based on one or two GPHS fuel capsules. Thermoelectrics were considered to be the most viable technology for thermal-to-electric power conversion, although Stirling cycles could offer unique advantages at the lower and middle ranges of power.

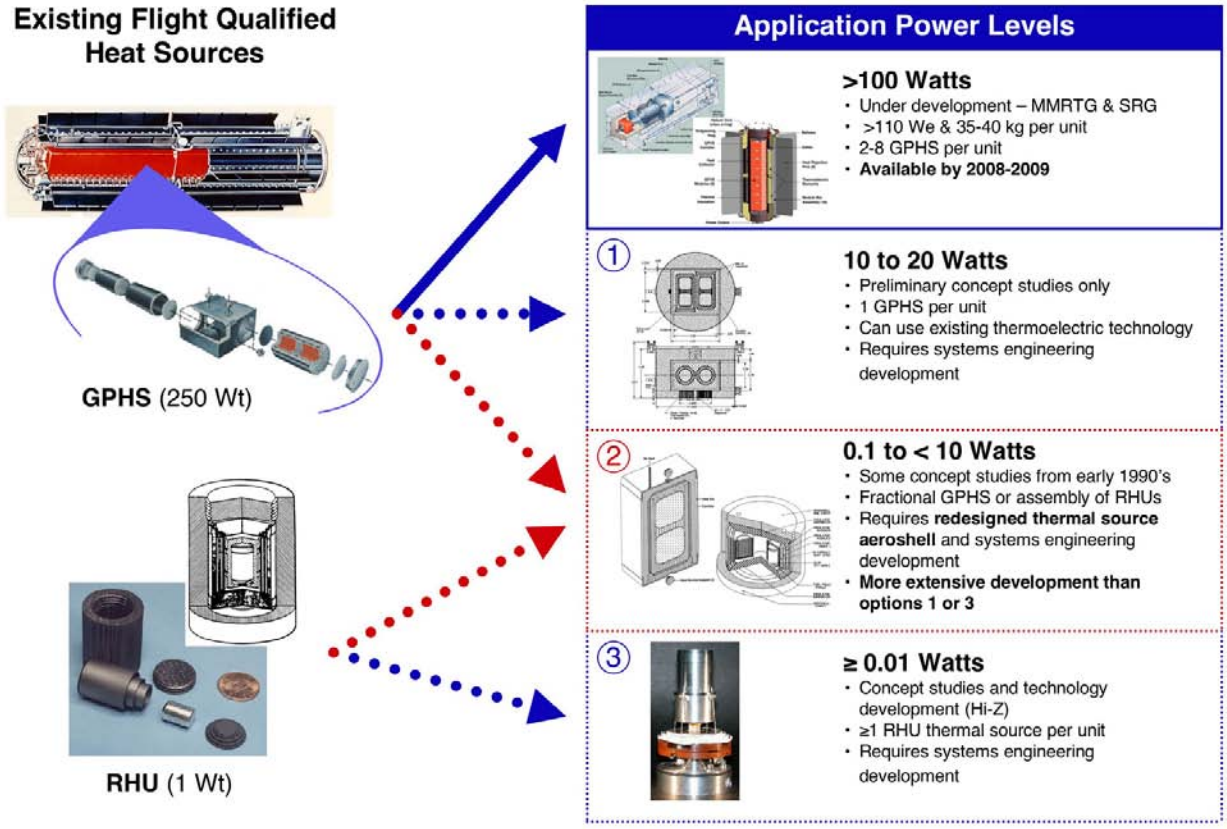

Figure 1-1. Classes of Small-RPS Dictated by Available Pu-238 Heat Sources

A list of all the potential mission applications identified to date is shown in Table 1-2. This list was developed from the survey conducted by ARC and the JPL-led study that addressed Mars and other planetary destinations. This list is by no means complete or final, but it does point to some interesting results and provides a reference for development of requirements.

The ARC survey indicated strong interest in using small-RPS technology on future Mars missions. Eighty percent of the respondents stated that they could use a small-RPS if it were available. This was not surprising since the strongest interest in this technology originally came from

Table 1-2. Mission Concepts and Applications Potentially Enabled by Small-RPS Technology

Mission #	Heat Source	Mission or Application	Power Level (Electrical)	RTG Configuration (Note1)	Spacecraft G-Load	Environmt	Mission Class (Estimated) (Note 2)	Time Frame
1	RHU	Pascal Micro-Lander (Mars)**	27 to 40 mW	1 to 2 RHUs	40 to 600g	Atmosphere	Scout	2009
2	RHU	Pascal-Type Micro-Lander (Other Bodies)*	27 to 40 mW	1 to 2 RHUs	40 to 600g	Vacuum	Scout	2009
3	RHU	Pascal Micro-Lander (Mars)**	100 mW	4 RHUs	40 to 600g	Atmosphere	Scout	2011
4	RHU	Europa Impactor Micro-Lander*	10 to ~100 mW	1 to 4 RHUs	>5000g	Vacuum	Discovery (PB) or Flagship (SA)	2015
5	RHU	Lunar Micro-Lander**	500 mW	~12 RHUs	40 to 600g	Vacuum	Discovery	2009
6	RHU	Prospecting Asteroid Mission (PAM) Micro-Sat***	300 to 400 mW	7-9 RHUs	<40g	Vacuum	New Frontiers	2020-2030
7	RHU	Saturn Autonomous Ring Array Micro-Sat***	300 to 400 mW	7-9 RHUs	<40g	Vacuum	New Frontiers	2025-2035
8	RHU	MUSES-CN Micro-Rover (RPS Derivative)*	10 to ~100 mW	1 to 4 RHUs	40 to 600g	Vacuum	Discovery	2009
9	RHU	Mars Micro-Rover (* and **)	10 to ~100 mW	1 to 4 RHUs	40 to 600g	Atmosphere	Scout	2009
10	RHU	Lunar Micro-Rover*	10 to ~100 mW	1 to 4 RHUs	40 to 600g	Vacuum	Discovery	2009
11	RHU	Titan Micro-Rover*	10 to ~100 mW	1 to 4 RHUs	40 to 600g	Atmosphere	Discovery	2015
12	RHU	Mars Science Micro-Instrument**	5 to 50 mW	1 to 2 RHUs	<40g	Atmosphere	Piggyback (PB) on MSL	2009
13	RHU	Mars Deployable Micro-Seismic Station**	10 to ~100 mW	1 to 4 RHUs	<40g	Atmosphere	Scout	2011
14	RHU	Mars Deployable Micro-Payload**	27-40 mW	1 to 2 RHUs	<40g	Atmosphere	Piggyback (PB) on MSL	2009
15	Fractional-GPHS	Lander Amorphor. Rover Array Mini-Lander***	3 to 9 W	1–3 Capsules	<40g	Vacuum	Scout	2010-2020
16	Fractional-GPHS	Mars Mini-Rover**	3 W	1 Capsule	<40g	Atmosphere	Scout	2011
17	Fractional-GPHS	Mars Deployable Seismic Station**	3 W	1 Capsule	<40g	Atmosphere	Scout	2011
18	Fractional-GPHS	Mars Mini-Rover (* and **)	6 W	2 Capsules	<40g	Atmosphere	Scout	2011
19	Fractional-GPHS	Lunar Mini-Rover*	6 W	2 Capsules	<40g	Vacuum	Discovery (Comsat Extra)	2011
20	Fractional-GPHS	Titan Mini-Rover*	6 W	2 Capsules	<40g	Atmosphere	Discovery (PB) or Flagship (SA)	2015
21	Fractional-GPHS	Mars Moon Mini-Rover*	6 W	2 Capsules	<40g	Vacuum	Scout	2011
22	Fractional-GPHS	Mars Cryobot**	3 to 6 W	1–2 Capsules	<40g	Atmosphere	Scout	2011
23	Fractional-GPHS	Seismic Station Mini-Payload*	3 W	1 Capsule	40 to 600g	Atmosphere	SMEX (PB)	2009
24	Fractional-GPHS	Weather Station Mini-Payload*	3 W	1 Capsule	40 to 600g	Atmosphere	SMEX (PB)	2009
25	Fractional-GPHS	Seismometer Station Mini-Payload*	3 W	1 Capsule	40 to 600g	Vacuum	SMEX (PB)	2009
26	Fractional-GPHS	Mars Mini-satellite**	3 W	1 Capsule	<40g	Vacuum	TBD	2011
27	Fractional-GPHS	Fields and Particles Mini-Payload*	6 W	2 Capsules	40 to 600g	Vacuum	SMEX (PB)	2009
28	GPHS	Lunar Soft Lander*	12.5 W	1 GPHS	< 40g	Vacuum	Discovery	2009
29	GPHS	Europa Lander*	12.5 W	1 GPHS	40 to 600g	Vacuum	Discovery (PB) or Flagship (SA)	2015
30	GPHS	Titan Moon Lander*	12.5 W	1 GPHS	40 to 600g	Atmosphere	Discovery (PB) or Flagship (SA)	2015
31	GPHS	Ganymede Lander*	12.5 W	1 GPHS	40 to 600g	Vacuum	Discovery (PB) or Flagship (SA)	2015
32	GPHS	Callisto Lander*	12.5 W	1 GPHS	40 to 600g	Vacuum	Discovery (PB) or Flagship (SA)	2015
33	GPHS	Lunar Lander*	12.5 W	1 GPHS	40 to 600g	Vacuum	Mid-X	2009
34	GPHS	Landers for other bodies in vacuum*	12.5 W	1 GPHS	40 to 600g	Vacuum	Discovery (PB) or Flagship (SA)	2009
35	GPHS	Landers for other bodies with atmosphere*	12.5 W	1 GPHS	40 to 600g	Atmosphere	Discovery (PB) or Flagship (SA)	2009
36	GPHS	Mars Rough Lander*	12.5 W	1 GPHS	600 to 5000g	Atmosphere	Mid-X	2009
37	GPHS	Mars Network Rough Lander*	12.5 W	1 GPHS	600 to 5000g	Atmosphere	Mid-X	2009
38	GPHS	Titan Rough Lander*	12.5 W	1 GPHS	600 to 5000g	Atmosphere	Discovery (PB) or Flagship (SA)	2015
39	GPHS	Europa Rough Lander*	12.5 W	1 GPHS	600 to 5000g	Vacuum	Discovery (PB) or Flagship (SA)	2015
40	GPHS	Callisto Orbiter Subsatellite*	12.5 W	1 GPHS	< 40g	Vacuum	Mid-X (PB)	2015
41	GPHS	Ganymede Orbiter Subsatellite*	12.5 W	1 GPHS	< 40g	Vacuum	Mid-X (PB)	2015
42	GPHS	Europa Orbiter Subsatellite*	12.5 W	1 GPHS	< 40g	Vacuum	Mid-X (PB)	2015
43	GPHS	Communications Relay Satellite*	12.5 W	1 GPHS	< 40g	Vacuum	Discovery	2009
44	GPHS	Outer Planets Magnetosphere Subsatellite*	12.5 W	1 GPHS	< 40g	Vacuum	Mid-X (PB)	2015
45	GPHS	Mars Rover*	25 to 50 W	2 to 4 GPHSs	< 40g	Atmosphere	New Frontiers	2011
46	GPHS	Lunar Rover*	25 to 50 W	2 to 4 GPHSs	< 40g	Vacuum	New Frontiers (excludes ComSat)	2011
47	GPHS	Titan Rover*	25 to 50 W	2 to 4 GPHSs	< 40g	Atmosphere	New Frontiers	2015
48	GPHS	Titan Amphibious Rover*	12.5 W	1 GPHS	< 40g	Atmosphere	SMEX (PB) or Flagship (SA)	2015
49	GPHS	Mars Moon Rover (Phobos and Deimos)*	25 to 50 W	2 to 4 GPHSs	< 40g	Vacuum	New Frontiers	2011
50	GPHS	Rovers for other bodes in vacuum*	25 W	2 GPHSs	< 40g	Vacuum	New Frontiers	2011
51	GPHS	Venus Aerobot*	12.5 to 25 W	1 to 2 GPHSs	< 40g	Atmosphere	New Frontiers	2011

Legend

* = Mission concept identified or studied by JPL
** = Mission concept identified or studied by NASA ARC (Mars missions identified by Mars MEPAG community)
*** = Mission concept identified or studied by NASA GSFC

PB = Denotes that Indicated mission piggybacks (PB) on another mission, and does not require a separate launch vehicle or communications relay to Earth.
SA = Denotes a standalone mission that requires its own launch vehicle and communications relay to Earth.

All indicated missions are assumed to be stand-alone unless otherwise stated.

Note 1: The RTG configuration assumes a thermoelectric-based system with 5% conversion efficiency.

Note 2: Capped cost limit as a function of mission class as of last announcement of opportunity (AO):

SMEX	$120M
Mid-X	$180M
Discovery	$360M
Scout	$325M
New Frontiers	$700M
Flagship	>$700M

NASA's Mars Exploration Program. The survey identified 12 hypothetical missions, which are noted by "**" in Table 1-2. Two of these applications (ref #'s 12 and 14) would target implementation in 2009 as part of the Mars Science Laboratory (MSL) payload complement. All of the others (ref #'s 1, 3, 9, 13, 16-18, 22, and 26) are aimed at potential application on the 2011 Scout mission opportunity.

The two MSL applications would ride piggyback on the MSL rover: one as an instrument within the rover wheel (5 to 50 mWe), and the other as a deployable science payload (27 to 40 mWe) that would be dropped off by the rover. For the 2011 Scout mission, two investigators indicated that they were planning proposals for a low-power rover (3 We) and multiple science stations (27 to 40 mWe). Five other investigators were considering mission concepts that include a seismic network (10 mWe to 3 We), multiple science stations (100 mWe), a cryobot (3 to 6 We) and a mini-rover (6 We). Lastly, MEPAG scientists stated that they could utilize RPS power for rover concepts (10 mWe to 3 We) and mini-satellites (3 We). In summary, the MEPAG survey identified near-term applications for small-RPS technology in the range of milliwatts to several watts, corresponding to RHU and fractional GPHS-based RPS units.

To understand the potential implications of having small-RPS available for a broader range of applications, JPL conducted an internal survey of its own scientists and identified 36 additional applications involving Mars, the Moon, Titan and other planetary bodies, indicated by a "*" in Table 1-2. Three additional mission applications were identified by NASA GSFC, indicated by "***" in Table 1-2. JPL selected six concepts on which to perform thorough assessments of feasibility and power requirements using the current best estimates of small-RPS performance. The concepts included a Europa lander, Mars and lunar rovers, a Galilean moon orbiter, a seismic monitoring station, and a fields-and-particles monitoring station. Table 1-2 shows that a majority of the missions identified from the JPL study required a GPHS-class RPS, while a smaller number of missions were enabled by a fractional GPHS or RHU-based RPS. As the capability of each mission increased, so generally did the power requirement. Most of the missions required a supplementary battery or super-capacitor to accommodate the peak loads encountered during high-power activities, such as mobility operations, communications, drilling, and certain measurements (e.g., Raman spectroscopy and Laser-Induced Breakdown Spectroscopy, (LIBS)).

Power sources based on a single GPHS module were found to have sufficient power for small landers and subsatellites with relatively sophisticated instrumentation suites, including Raman spectroscopes, LIBS, plasma-wave spectrometers and Doppler extractors. Rovers using 2 to 4 of these RPS units had adequate power to operate Mars Exploration Rover (MER)-class instruments (cameras, APXS, RAT, etc.), and could potentially traverse greater distances than the current MER configuration due to the extended lifetime of the RPS power source. All of the GPHS-class mission concepts assumed a modular RPS design. Thus, multiple RPS modules could be stacked together to achieve greater power levels as needed. The JPL study showed that this building block approach would offer the greatest flexibility to mission designers, while reducing cost and schedule risk through use of a standardized RPS design.

Nearly half of the single GPHS-class RPS missions analyzed by JPL required the capability of surviving acceleration loads greater than 40g (typically due to landing loads). In fact, four mission concepts required acceleration load tolerances as high as 5000g for rough landers. In this study, mission environments included vacuum and atmosphere. Consequently, the ideal multi-mission GPHS-class RPS would be capable of withstanding a maximum spacecraft acceleration of 5000g, while operating in an atmosphere or vacuum.

Fractional GPHS RPSs (based on 1 to 3 GPHS fuel capsules in a reconfigured aeroshell) were found to be sufficient for small standalone seismic and weather monitoring stations, as well as Pathfinder-class mini-rovers. The moderate power output (~3 to 9 We) of such systems lend themselves to deployable mini-payloads with low power instrumentation, short communication distances, and minimal mobility requirements. Rovers using a fractional GPHS-based RPS appear feasible, but would be somewhat limited by the need for longer and more frequent battery chargings to accommodate the relatively large power draws encountered during traverse and communi-

cations. The smaller size of the fractional GPHS-powered rover would also limit the range of terrain over which the rover could navigate due to smaller wheel size and large mobility power requirements.

Nearly a third of the fractional GPHS-based RPS applications identified in this study required the RPS to tolerate spacecraft accelerations up to 600g in either a vacuum or atmospheric environment. Thus, the ideal fractional-GPHS RPS for multi-mission applications would tolerate spacecraft accelerations up to 600g, while operating in either a vacuum or atmosphere.

RHU-based RPSs were found to be sufficient for micro-landers and payloads with extremely low-power electronics and instrumentation. Micro-rovers, such as the Muses-CN [3], are also conceptually feasible, but rely heavily on trickle charging and stored energy to perform basic functions (e.g., recharge durations of 1 hour or more may be necessary to accomplish 1 minute of activity). However, this may be acceptable if the periods of intense activity are infrequent and brief relative to the entire mission. The small size of the micro-rover also constrains the terrain over which it can navigate. Two-thirds of the RHU-class mission concepts were identified as having spacecraft acceleration requirements exceeding 40g, with one concept (impactor) exceeding 5000g. There was an even split between missions conducted in space and those operated within an atmosphere. Consequently, the ideal multi-mission RHU-based RPS would tolerate spacecraft loads >5000g and be able to operate in a vacuum or atmosphere.

The mission studies considered both thermoelectric (TE) and Stirling cycle-based conversion technologies. Thermoelectric converters are static solid-state devices that convert thermal energy into electrical energy with system efficiencies exceeding 6%. Thermoelectric technology is flight proven, highly reliable, easily scalable, and does not produce vibrations during operation. Thermoelectric materials that were considered include silicon-germanium (SiGe), lead telluride (PbTe), tellurides of antimony, germanium and silver (TAGS), and bismuth-telluride (BiTe). Thermoelectrics made from SiGe and PbTe-TAGS use a GPHS heat source, whereas TEs made from BiTe used an RHU heat source. Existing RPSs using SiGe thermoelectrics are designed to operate only in vacuum, and thus their capability is constrained to in-space missions and operations on planetary bodies without atmospheres. RPSs using PbTe-TAGS or BiTe can be designed to operate in either vacuum or atmosphere, providing greater flexibility and the ability to support more mission concepts.

The Stirling convertor is a highly efficient dynamic power conversion technology that is currently under development. Only one Stirling design was considered to have the potential to support a 2011 mission - it is a prototype 10 We converter designed for terrestrial use. Although the high efficiency (18.5%) appeared very attractive, none of the mission studies assumed use of Stirling technology in their primary designs. This was due to a limited knowledge base regarding the performance, mass, and reliability of a flight-qualified model.

1.4 CONCLUSIONS

The results of initial surveys and studies point to many scientifically valuable mission concepts that could benefit from or be enabled by small, reliable, long-lived RPSs. Based on this initial work, there do not appear to be any significant technological or design issues that would prevent developing such units for missions by the end of the decade. However, there are several important considerations that must be addressed before a decision to proceed with development can be made.

The most obvious consideration is ensuring that key operational and design requirements are sufficiently defined to capture the needs of future potential users. This includes identifying not only plausible mission concepts, but also the power levels, acceleration loads, lifetimes, and operational environments that would be representative of these applications. It would be difficult to design a single unit that could effectively satisfy all needs identified within this report—the power range associated with small-RPS alone covers nearly three orders of magnitude. It would be more reasonable to favor development of a unit in the power regime that captures the greatest number of possible applications. Requirements will also have a significant impact on the cost, schedule and risk in developing the system. The efforts described in this report have provided a good start to this process, but are by no means complete. Additional interaction with the science and potential user community is needed to flesh out details, and ensure that future needs and requirements are defined as comprehensively as possible.

Another important consideration is the Pu-238 heat source options associated with different categories of power. Activities to date have assumed use of the GPHS or RHU fuel capsule designs in different aeroshell configurations. The more the design of the heat source deviates from the existing GPHS module or RHU, the more costly the development will likely be. Furthermore, as with other sensitive nuclear materials, the design, fabrication and testing of Pu-238 heat sources would rely exclusively on the DOE infrastructure and laboratories that specialize in processing of Pu-238 and associated materials. The activities so far have identified the four heat source options shown in Figure. 1-1. The potential milliwatt applications identified in the ARC survey and JPL study use RPS units based on 1 or more RHUs that would operate in a vacuum or atmosphere, and tolerate maximum spacecraft loads that can exceed 5000g. Potential applications involving several watts would use RPSs based on either a derivative of the GPHS module using 1 or 2 GPHS fuel capsules, or a heat source composed of multiple RHU fuel capsules. These would be capable of tolerating maximum spacecraft loads of 600g, and operating in a vacuum or atmosphere. Higher power applications in the 10- to 20-We range would benefit from a single GPHS-based RPS that is modular, operable in a vacuum or atmosphere, and capable of tolerating maximum spacecraft accelerations up to 5000g. Further study is needed to identify other alternatives, and to determine the cost and development requirements for different heat source configurations.

A third consideration is the funding that could be made available to support future development. The most obvious funding source is the RPS Development Program, managed by NASA's Office of Space Science. This program is currently supporting development of the SRG, as well as research and development of several advanced power conversion technologies. The RPS program has also been responsible for sponsoring the small-RPS investigations described in this report. Based on current projections, the earliest at which resources could be made available for flight system development is in late-2005 to early-2006. Prior to that, the RPS program could provide limited funds to support DOE management of competitively selected design assessments with industry and specialized studies with DOE laboratories and NASA field centers. It is also possible that another program could come forward with a need for a small-RPS unit, but this is unlikely to occur before this timeframe.

Finally, it is important to determine how requirements, heat source development and funding availability play together into an overall implementation strategy, which must ultimately target a mission(s) for first use of these units. It is possible that a small-RPS unit could be offered as an option for competitively selected missions, much in the same way that MMRTG and SRG were

made available for the New Frontiers Announcement of Opportunity in 2003. In this case, the flight project pays for the replacement cost of each unit, along with the costs for launch approval engineering, NEPA compliance, etc. If small-RPS units are to be treated as an optional resource, then the implementation strategy must look beyond a single application and consider a broad range of potential missions that could make use of this capability. It is also reasonable to consider, as part of the overall acquisition strategy, the development of more than one type of unit if the potential applications have a large disparity in power requirements.

Activities to date have identified two applications for milliwatt-class units on the Mars Science Laboratory (MSL) 2009 mission. There were several other milliwatt and multiwatt applications identified for the 2009 timeframe, but the cost caps for some of these missions (i.e., Mid-X or SMEX) may be too low to accommodate inclusion of RPS hardware and NEPA/Launch Approval activities. Furthermore, other applications (i.e., Discovery) have not officially embraced use of radioisotopes for power generation. In any case, it would be difficult to develop a completely new RPS unit by 2009, even if such an effort were started as early as late-2005.

The Scout mission opportunity in 2011 appears to be a reasonable near-term candidate for first application of small-RPS. The Scout program has expressed a strong interest in this capability, and the $350 million cost cap for its missions could likely accommodate the inclusion of small-RPS units, NEPA and launch approval activities. Furthermore, a 5-year development program initiated in late-2005 would be quite practicable, especially if development focused on a milliwatt-scale unit. For now, the 2011 Scout mission opportunity will serve as the reference for first implementation of small-RPS. However, this could change as requirements and implementation strategy evolve through interchange with the science community.

Over the next one to two years, activities will concentrate on laying the foundation to support a possible flight system development starting as early as late-2005. This will include performing concept trade studies and evaluations needed to determine whether to proceed with such a project. During this time, NASA and DOE will continue outreach activities with various science groups in order to refine requirements and to maintain ongoing studies across a spectrum of power and operational requirements. These efforts will address mission and system issues, and delve into the detailed aspects of heat source and power conversion subsystem design. NASA and DOE are also considering the initiation of competitively selected design studies with industry in late-2004 to early-2005. These studies and the interactions with the science and user community will assist in the formulation of system requirements and will provide a basis for initiating a development effort. In parallel, DOE will evaluate heat sources that could be used over the power ranges of interest.

2. MISSION CONCEPTS AND APPLICATIONS

2.1 PURPOSE AND OBJECTIVES

NASA's Office of Space Science requested the Jet Propulsion Laboratory (JPL) to lead a study to identify and assess mission concepts that could be enabled as early as 2011 by small Radioisotope Power Systems (RPSs) with electrical power outputs in the range of milliwatts to tens of watts. The goal was to identify high-value missions and applications that could be enabled by RPS technology, and to define the top-level requirements for small-RPS units. Study participants included NASA Ames Research Center (ARC), NASA Goddard Space Flight Center (GSFC), NASA Glenn Research Center (GRC) and the Department of Energy (DOE). The RPS heat sources that were considered included the existing Radioisotope Heater Unit (RHU), its derivatives using RHU fuel capsules in a redesigned aeroshell, the GPHS module, and its derivatives using fewer GPHS fuel capsules in a redesigned aeroshell. The choice of power converter was constrained to those technologies already flight-proven (i.e., thermoelectrics) or expected to be flight-qualified within the next 5 to 7 years (i.e., Stirling conversion). NASA also requested that the Level-1 requirements of the small-RPS be defined and prioritized based on their ability to enable high-value missions and their capability in satisfying the power requirements of near-term missions with identified users. This section documents the Level-1 RPS requirements based on six detailed mission studies obtained from the 51 mission concepts potentially enabled by small-RPS power sources in Table 1-2.

2.2 INTRODUCTION AND DESCRIPTION OF THE MISSION CATEGORIES

An exciting new class of solar system exploration missions and applications could be enabled by small-RPSs with power levels of milliwatts to tens of watts. Studies were performed to identify and assess the range of missions that would be enabled by small-RPS technology for four classes of deep space vehicles comprised of landers, rovers, subsatellites, and mini-deployable payloads. Integrated mission design teams were created that included scientists, RPS technologists, and mission design architects. The scientists assisted in defining the science goals of each mission based on the Vision for Space Exploration [4] and on NASA and National Research Council (NRC) roadmaps [5]. The RPS technologists provided performance data on existing RPS components (including heat sources and power converters), and provided conceptual designs for small-RPS systems that could potentially be built within 5 to 7 years. Lastly, mission architects worked with the scientists, RPS technologists, and often a host of subsystem experts (e.g., communications, instruments and environments) to weave together the mission and define the associated RPS requirements.

Detailed design studies were performed for six missions including a Europa lander, Mars rover, Lunar rover, Galilean satellite orbiter, seismic monitoring station, and fields-and-particles monitoring station. Additional small-RPS-enabled missions were identified based on modifications and extrapolations of the point designs and from mission studies performed by other design teams (e.g., JPL's Team In-Situ and Team X), and other NASA centers (ARC and GSFC). Each of the missions belongs to one of four categories as defined by their function, operating location and mobility. The categories are Landers, Subsatellites, Rovers and Deployable Mini-Payloads. Landers include all vehicles that land on another interplanetary body, including planets, moons, asteroids or comets, to perform their mission from a fixed location (e.g., Europa Lander, Viking, Ranger). Subsatellites are small orbiting spacecraft that perform standalone scientific measurements, but rely upon a mother spacecraft for transportation to their target destination and for relaying their data back to Earth (e.g., Galilean satellite orbiter). The category of Rovers includes all mobile vehicles that operate on the surface (e.g., Pathfinder and MER), above the surface (e.g., aerobots) and below the surface (e.g., cryobots and submarines). Deployable mini-payloads are small, simple, standalone instruments that are carried on and deployed by a mother vehicle, such as a rover or JIMO spacecraft, to key points of interest. The instruments could be science driven

(such as long-duration seismic stations or fields-and-particles stations), or application-driven (such as positional beacons to mark points of interest for future study by other rovers or spacecraft).

Lastly, the top-level RPS requirements have been documented and are presented for each identified mission. The four classes of requirements are power level, heat source type, operational environment, and maximum acceleration level. The RPS power level is subclassified into three ranges: 10 to ~100 mWe, ~3 to 9 We, and 12.5 to 50 We. The heat source type includes the RHU and its derivative, fractional (1 to 3 fuel capsules) GPHS, and full (4 fuel capsules) GPHS. The RPS operating environment is either vacuum or atmosphere, and the maximum spacecraft acceleration level is subcategorized into the following four ranges: <40g, 40 to 600g, 600 to 5000g, and >5000g. Additionally the mission class has been estimated (e.g., SMEX, Scout, Discovery, New Frontiers, or Flagship) for each concept, and the launch timeframe identified.

2.3 LANDER MISSIONS

2.3.1 Europa Lander Mission

This section describes a conceptual landed mission to the Jovian satellite Europa using a small-RPS powered lander that would ride piggyback on the proposed Jupiter Icy Moons Orbiter (JIMO).

2.3.1.1 *Science Goals*

Europa is recognized as a high-priority target for future exploration because of the possibility that it may possess environments suitable for life [5]. The primary science goals for the Europa Lander Mission (ELM), as recommended by the JIMO Science Definition Team [6], would be to perform investigations of the *astrobiology*, *geophysics and geological-composition* of Europa.

The *astrobiology* goal would be to search for signs of past or present life, and to characterize the habitability of the Jovian moons. To meet this objective, ELM instruments would be designed to search for organic materials and to determine their composition. In-situ experiments would be conducted to reveal chemical patterns that might be indicative of biological origin, and measurements would be taken of the local temperature and radiation intensity. The *geophysics* goal would be to determine the local thickness and characteristics of the icy crust, and determine the location of liquid water beneath Europa's icy crust (Fig. 2.3.1-1). This knowledge would lead to a better understanding of the interior structure and crustal dynamics of Europa. ELM would perform in-situ seismometry experiments to achieve this objective. The *geological-composition* goal would be to determine the evolution and present state of the Galilean satellite surface and subsurface, and to determine the processes affecting them. Lander experiments would be performed to determine the elemental and mineralogical composition of surface ice and non-ice materials. Imaging, radiation and temperature measurements would also contribute to achieving the *geological-composition* goal. The ELM mission would, in addition, provide ground truth for remote measurements of temperature, composition, and radiation levels obtained by the JIMO spacecraft.

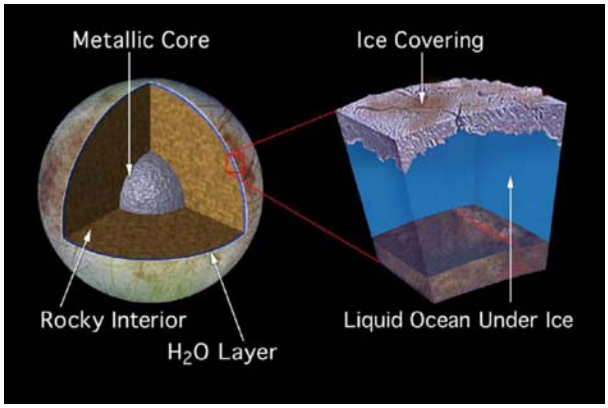

Figure 2.3.1-1. Europa's Predicted Internal Structure and Composition

2.3.1.2 *Mission Goals*

The mission goals of the ELM would be to land on Europa and take in-situ measurements for a nominal duration of 30 Earth days, corresponding to ~8.5 Europa days (limited by JIMO timeline), in order to meet the scientific objectives.

2.3.1.3 *Mission Architecture Overview*

The ELM concept is derived from the Europa Pathfinder (EPF) study [7] and takes advantage of RPS technology to enable a 30-day surface mission (the duration of the EPF mission was battery-limited to 3.5 days). ELM (Fig. 2.3.1-2) would ride as payload on the aft section of JIMO as shown in Figure 2.3.1-3. The launch date of the JIMO spacecraft is assumed to be 2015 for the purposes of this study. The nominal JIMO transit time to Europa is not yet defined, but is assumed to be ~13 years, with a 65-day spiral-in period, a 30-day science period, and a 6-day spiral out period [8].

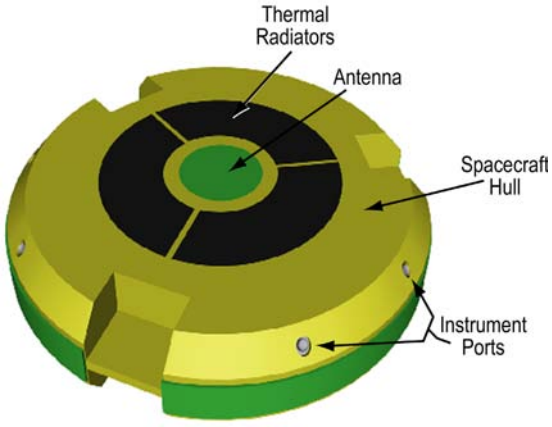

Figure 2.3.1-2. Configuration of the Europa Lander Mission (ELM) Surface Lander [7]

The Europa landing site would be determined during the 65-day JIMO spiral-in phase where detailed Europan surface mapping could be performed by JIMO, assisting the science and engineering communities in choosing the landing location that maximizes science returns and minimizes landing risk.

JIMO would enter a nominal 100 km (altitude) circular orbit about Europa at an inclination of 45°. The JIMO orbital inclination constrains the maximum possible landing latitudes to between ±45° for this mission design. Upon reaching this orbit, the ELM spacecraft would separate from JIMO and would perform a series of maneuvers, known as "Stop and Drop," to prepare for landing.

After separation, the ELM spacecraft would be spun-up using small solid rockets in preparation for two subsequent descent burns. The first descent burn would impart a velocity change (Delta V) of 22 m/s opposite the direction of travel, which would alter the original 100 km circular orbit to an elliptical orbit with a 1.5 km periapse and 100 km apoapse (Fig. 2.3.1-4). The second descent burn would be performed at periapse, and would impart a Delta V of 1458 m/s opposite to the direction of travel. This would null out all forward motion, resulting in the lander "falling" into Europa under the force of gravity. The total Delta V requirement to perform the "Stop and Drop" maneuver would be 1480 m/s.

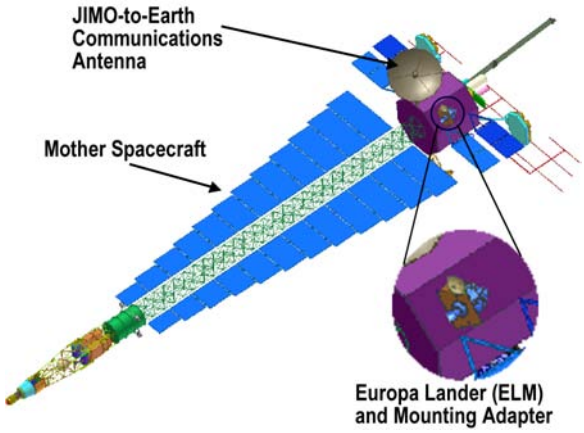

Figure 2.3.1-3. Artist's Concept of the ELM Spacecraft Riding the Aft Section of the JIMO Mothership (Preliminary Version) During the Cruise Phase

Following the second descent burn, the ELM lander would separate from its propulsion stages (Fig. 2.3.1-5) and inflate its airbags in preparation for surface impact. The free-fall time would be ~48 seconds based on a periapse altitude of 1.5 km, and the resulting impact velocity would be 63 m/s. As Europa has a negligible atmosphere, aeroshells and parachutes would be ineffective. Thus, airbags and a low periapse are the key design techniques to control the impact acceleration, with a resulting maximum landing acceleration of <600g. Upon landing, the pressurized airbags would be released and would bounce away, allowing the ELM lander to make direct contact with the Europan surface.

During the surface mission, ELM would communicate with JIMO using omni-directional antennas onboard the lander and a JIMO-mounted parabolic antenna. The JIMO High Gain Antenna (HGA) would be then used to relay the ELM science and engineering data to Earth.

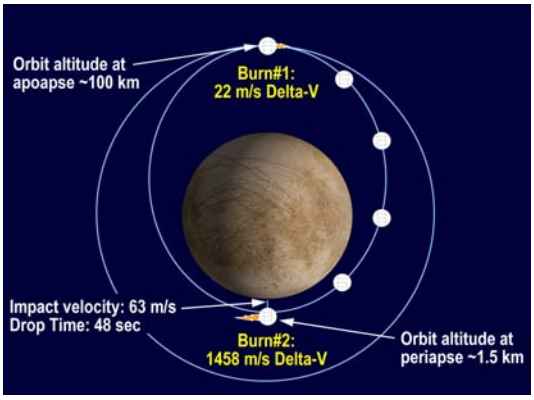

Figure 2.3.1-4. Orbital Maneuvers Performed by the ELM Spacecraft During the Entry and Landing Phases

2.3.1.4 *Power Source Trade Study*

Trade studies were performed on three different potential power systems for the ELM spacecraft, including solar arrays, primary batteries and RPS. The critical driving factors were: 1) the high-latitude landing requirement (±45°); 2) distance of Europa from the Sun (~5 AU) and the resulting low insolation levels; 3) Europa's long rotation period (85.2 hrs); and 4) the extremely low surface temperatures. Europa receives only 3.7% of Earth's insolation, corresponding to an average solar flux (during daylight hours) of less than 22 W/m^2 at 45° latitude (Fig. 2.3.1-6). The long rotational period means that the ELM lander would see 42.6 hrs of shadow per Europa day. Additionally, the average surface temperature approaches a frigid 103 K, (and the nighttime surface temperature can drop even further to ~85 K. Thus, significant thermal power and energy would be required to maintain operating temperatures during both the proposed multi-

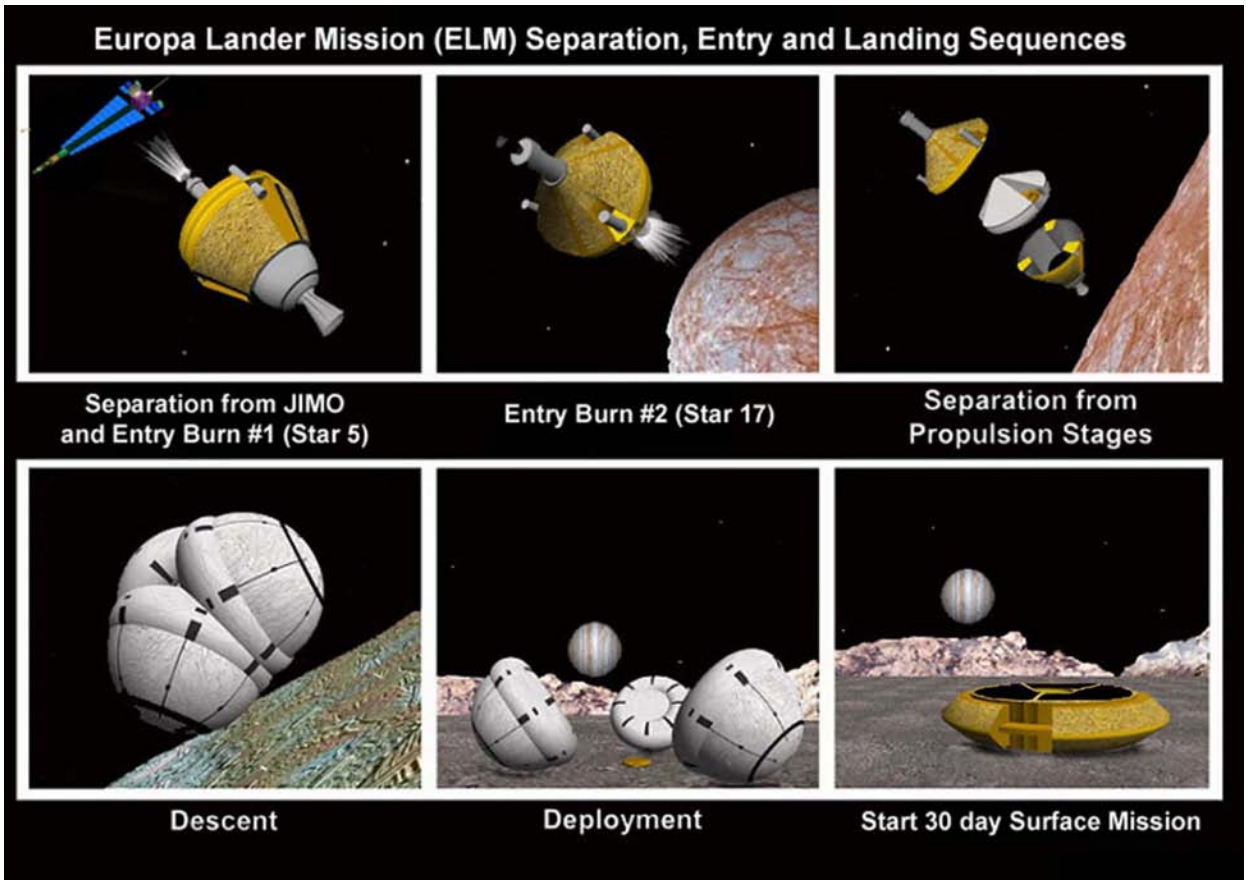

Figure 2.3.1-5. Illustrations of the separation, orbital-insertion, airbag deployment and landing phases of the Europa Lander Mission (ELM) spacecraft [7].

year cruise phase (on JIMO) and during the nominal Europan surface mission. Lastly, due to the rough surface topography, ELM would need to be designed to operate in any landing orientation, (e.g., right-side up and up-side down); thus, power generation would have to be possible in any landing orientation. The baseline total energy requirement for the surface mission was estimated at ~6820 W-hrs including a 5-W heater budget. This is assumed to be the minimum required thermal power necessary to maintain operating temperatures in addition to any RHUs.

For a solar array power system to be employed on ELM, a number of technological challenges would have to be overcome. First of all, as the ELM lander would see 42.6 hrs of shadow per Europan day, a large energy storage system (e.g., rechargeable batteries) would be required to permit operations and maintain operating temperatures during the long periods of eclipse. Secondly, as the specific landing orientation of the spacecraft could not be guaranteed apriori, the solar array system would need to be capable of generating enough power regardless of landing configuration, i.e., it would need solar panels on both the top and bottom surfaces of the lander. Thirdly, the ELM spacecraft would need an additional power system or umbilical to JIMO during the proposed multi-year cruise phase, as the solar arrays would be shrouded within the entry system (i.e., retrorockets and airbags) and would not be capable of generating any power to perform health and status checks and maintain operating temperatures.

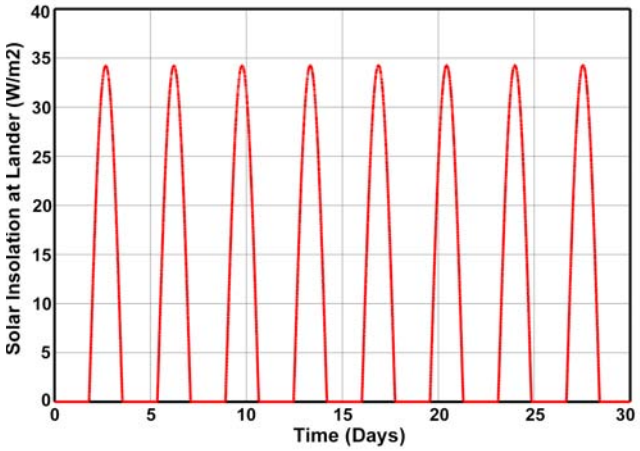

Figure 2.3.1-6. Incident Solar Flux at Surface of Europa at 45° Latitude Over 30 Earth Days

Lastly, solar array technology would need to be developed to operate at the low solar insolation levels specified above, in a high natural radiation environment (multi-Mrads), and in the extreme cold. Analyses were conducted on the solar array size and total mass (array + batteries) required to meet the energy requirements of the surface mission—the effects of radiation and the need for an auxiliary power system during cruise were ignored in this study. The results are presented in Table 2.3.1-1 and indicate that ~14.9 m^2 of solar panels (~7.4 m^2 on each surface) would be needed to meet the total energy requirement for the surface mission. This would correspond to a solar array and battery system mass of ~69 kg (89 kg with 30% margin) in order to permit continuous operations and maintain operational temperature during the long Europan nights. Considering that the conceptual ELM spacecraft would have a diameter of ~1 m, and a mass of ~30 kg (without power system), it is clear that the solar option is not practical from either a size or mass perspective.

Table 2.3.1-1. Solar Array Trade Study Parameters for the ELM Mission

Parameter	Value
Avg ELM Power Reqt's w/o Heating (W)	4.5
Estimated ELM Heating Power Reqt (W)	5.0
ELM Batt Power for Nighttime Ops (W)	9.5
Total ELM Power Req'd During Insolation w/ 30% Margin (W)	**24.7**
Avg Solar Power Rec'd During Daylight (W/m^2)	21.7
Estimated SA Conversion Efficiency (EOM) (%)	17%
Avg SA Electrical Output During Daylight (W^2)	3.3
Required Solar Array Area (m^2)—Single Side	**7.4**
Required Solar Array Area (m^2)—Both Sides	**14.9**
Required Solar Array mass (kg)	52.1
Avg Power Used during Nighttime (W)	9.5
Energy Used during Nighttime Cycle (W-Hr)	406
Battery Energy Requirement, (W-Hr)	1231
Req'd Batt Mass to Run through Nighttime (kg)	10.3
Mass of SA Cables, Hinges, Supports, etc. (kg)	6.2
Total Mass without Margin (kg)	**69**
Total Mass with 30% Margin (kg)	**89**

The use of primary batteries was also analyzed, and issues similar to those for solar arrays were discovered. Namely, in order to maintain the batteries at their operational temperature (typically above -40°C), a significant amount of thermal power would be required to heat them as well as sensitive key electronics and systems. The resulting power requirement would result in a battery mass and volume significantly larger than that required for an equivalent RPS. Additionally, an auxiliary power source or umbilical to JIMO would be required to power the lander and keep it warm during its cruise phase.

The use of a small-RPS was analyzed and found to have significant advantages that would enable the ELM mission from a power system perspective. These advantages include long-life (the small-RPS could operate for decades), generation of excess heat that could be used to maintain operating temperatures, and a relatively high specific power. This study assumed the RPS was based on using one GPHS module and thermoelectric power conversion. The associated RPS trade study assumptions are provided in Table 2.3.1-2 [9, 10]. Due to the excess heat generated by the GPHS module, the total energy requirement for the 30-day mission would be less than that for solar or batteries, and was estimated at ~3200 W-hr (Section 2.3.1-10). The total RPS electrical output for the surface mission would be 7300 W-hr (based on 13-year EOM performance), resulting in the RPS system having a total energy margin exceeding 100%. To meet the peak power demands of all the instruments and communications equipment, a small rechargeable battery would be utilized. An additional advantage of RPS is that it would permit the ELM spacecraft to be a self-contained system, eliminating the need for external recharging or alternate power connectivity with the JIMO spacecraft during the cruise phase. In summary, RPS technology would enable the ELM mission by providing a small, long-lived, low mass power source that would produce valuable excess heat to keep the spacecraft.

Table 2.3.1-2. RPS Trade Study Assumptions for the ELM Mission

Parameters	Value
RPS Heat Source Type	GPHS
Thermal Power Ouput @ BOL, (W)	250
Mission Duration (Years)	13
Pu^{238} Decay Rate / year (%)	0.8%
Thermal Power Output @ EOM, (W)	225.2
Thermoelectric Degradation Rate / year	0.8%
Power Conversion Efficiency	5%
Electrical Power Output @ EOM, (W)	**10.1**

2.3.1.5 *Small-RPS Characteristics*

The small-RPS power system utilized for the ELM mission is a conceptual design based on a single GPHS module utilizing TE conversion, and assumed to possess a total system efficiency of ~5% at Beginning of Life (BOL). This RPS system is based on individual components (heat source, TEs and insulation) that all currently exist and have been flight proven. Conservative estimates of power system performance were assumed in the RPS (Table 2.3.1-2) and battery sizing calculations. The existing GPHS module produces a nominal 250 Wt at BOL, and its thermal output is reduced by ~0.8%/year due to the radioactive decay of the Pu^{238} fuel ($T_{1/2}$ = 87.8 years). Degradation of the TE material would result in an additional ~0.8%/year reduction in electrical output. Thus, the power output from the small-RPS is estimated as 225 Wt and 10.1 We at EOM (13 years).

This RPS thermoelectric converter is assumed to be comprised of PbTe–TAGS, operating with a cold shoe temperature of ~155°C. The TEs are oriented normal to each of the four sides of the GPHS module (Fig. 2.3.1-7a), and Min-K thermal insulation would provide the structural support for the TEs and heat source. The RPS assembly would be packaged in a cylindrical container that allows venting of the Pu^{238} decay products (helium) to the ambient environment through vents penetrating the Min-K and external RPS canister. The RPS would be centrally located within the body of the ELM spacecraft (Fig. 2.3.1-7b), permitting efficient channeling of the excess GPHS heat to the surrounding electronics, subsystems and radiators via conduction straps. The RPS is assumed to be capable of surviving the 600-g maximum spacecraft landing loads without damage.

The maximum extrapolated mass of the RPS is 10 kg based on existing detailed RPS designs (Section 4) reinforced to handle the increased acceleration environment.

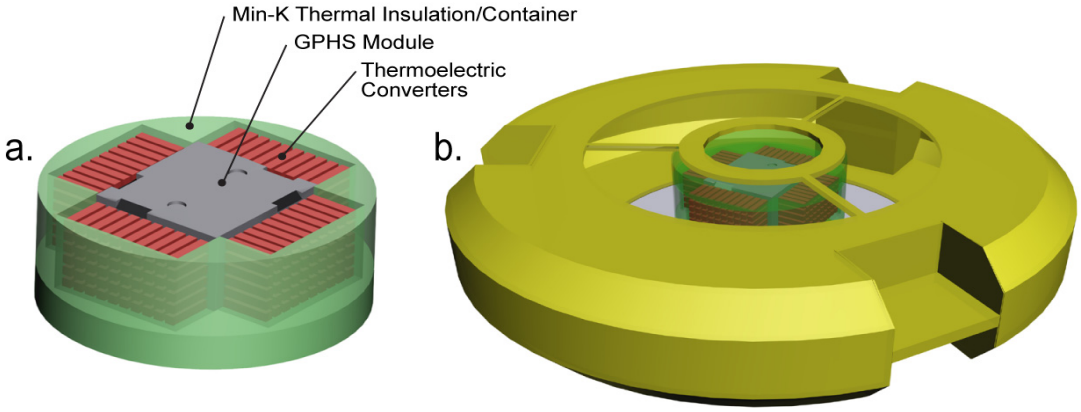

Figure 2.3.1-7. (a) Small-RPS (with Top Removed) and (b) ELM Spacecraft with Small-RPS Installed (Radiator panels and internal systems removed for clarity.)

2.3.1.6 *Science Instruments*

The proposed ELM spacecraft would carry a complement of six science instruments specifically-chosen to meet the science objectives of the mission (Table 2.3.1-3). Of these, the temperature and radiation sensors would provide information on surface conditions relevant to the *Astrobiology* goal (determining the habitability of the subsurface) and to the *Geological-Composition* goal of determining the physical state and mechanical properties of the surface. These relatively simple sensors would be installed on the top and bottom surfaces of the lander.

The imaging system would view the surface through a set of transparent ports that are distributed over the outer surface of the lander. All of the ports would convey their information to a centralized imaging system via fiber optic leads. Some ports would be optimized for far-field views to image the surroundings, while others would be optimized for near field views to resolve small-scale features of surface ice that may be in close proximity to the port. The imaging system addresses the *Geological-Composition* goal.

The Raman spectroscope and the Laser Induced Breakdown Spectroscope (LIBS) are sophisticated instruments that would obtain information on surface compositions in complementary ways. Both would utilize laser light to stimulate a target and both would employ fiber optic leads to measure the resulting emissions. The Raman spectroscope would nondestructively excite the molecules of the target surface, with the resulting emissions being diagnostic of mineralogical composition. The LIBS would break down the molecules of the surface materials, and wouild determine the elemental compositions by recording and analyzing the emission lines of the resulting short-lived plasma. Both organic and inorganic materials are characterized by each of these instruments, making them directly relevant to the *Astrobiology* goal and the *Geological-Composition* goal.

The microseismometer would directly address the *Geophysics* goal, as this instrument would be designed to enable researchers to determine both the mechanical properties of the icy crust and its thickness. This would be crucial information with respect to the question of whether or not Europa possesses an ocean beneath its icy crust.

Table 2.3.1-3. Science Payload and Instrument Description for the Proposed ELM Spacecraft

Instrument	What it does	Science Objective Addressed
1. Imager	Obtains near-field and far-field images through viewports.	Characterizes the surface characteristics and surface geology of the landing site.
2. Microseismometer	Detects and records ground motions (icequakes).	Determines the internal structure of Europa.
3. Raman Spectroscope	Measures backscattered laser light to determine composition and concentration of minerals and chemical species present, including organics.	Searches for signatures of biological activity. Characterizes the chemical and physical habitability. Describes the composition of non-ice materials.
4. Laser Induced Breakdown Spectroscope (LIBS)	Pulsed laser focused on surface ice produces an ionized plasma whose emissions are indicative of the elemental composition of surface materials (Complementary to the Raman instrument).	Searches for signatures of biological activity. Characterizes the chemical and physical habitability. Describes the composition of non-ice materials.
5. Temperature Sensor	Measures ambient temperature at the landing site.	Provides ground truth for remote observations. Characterizes the thermal properties of the surface through measurements over the diurnal cycle.
6. Radiation Sensor	Measures levels of ion and electron irradiation at the landing site.	Characterizes surface habitability. Provides ground truth for models of surface radiation levels based on orbiter data.

2.3.1.7 *Data*

Mission data would be generated from the six scientific instruments and other sensors designed to assess the health and status of the spacecraft. Each science instrument would operate at its own data rate and data-taking frequency that would be dependent upon the phenomena or object being measured, the desired temporal resolution, and how often the measurement would be expected to vary (Table 2.3.1-4). All lander data would be uplinked to the JIMO mothership during the communications events described in Section 2.3.1.8 for transmission to Earth.

The total volume of data obtained over the course of a Europa day is estimated at ~1150 Mbits, with the data stream comprised primarily of microseismometer data (79%) and high-resolution images (19%). Communication from ELM to JIMO would occur only during limited windows of opportunity; thus, a solid-state data recorder (SSR) with ~1400-Mbit capacity would be used to store all measurement data until the next communication cycle. Due to the quantity of stored data and short duration communication windows, a 1.4 Mbit/s bandwidth would be used to transmit all stored data and any newly generated data to JIMO during each window. To allow for uncertainties and limited future growth, both the SSR storage requirement and communications bandwidth requirement include ample margin (20% and ~200%, respectively). Additionally, data compression algorithms could be used to significantly decrease the accumulated data volume, especially from the microseismometer, by 4:1 or greater. The resulting data margin could then be allocated to new higher-bandwidth instruments (e.g., increased imaging resolution and sampling frequency, etc.) or used to simplify the communications and data storage systems by permitting the use of smaller antennas, transmitter and SSR.

Table 2.3.1-4. Data Rates, Uplink Rates and Data Storage Requirements for the ELM Spacecraft.

Instruments	Data Rate (kbits/ msmt)	# of Instruments	#Measure measurements per Europa Day	Measuremt Frequency (#/Earth Hr)	Accumulated Data Volume per Europa Day (kbits)	Accumulated Data Volume per Europa Day (Mbits)
Imager	2600	16	85	1	219762	220
Microseismometer	1	3	304286	3600	912858	913
Raman Spectroscope	10	1	85	1	845	0.85
LIBS	10	1	42	1	423	0.42
Temperature Sensors	0.016	16	169	2	43	0.04
Radiation Sensors	0.016	4	304286	3600	19474	19
Engineering Data	0.100	1	5071	60	507	0.51
			Total Accumulated Data Volume / Europa Day (Mbits)			1154
			Design Uplink Capability / Europa Day (Mbits)			3407
			Required Uplink Rate (Mbit/s)			0.47
			Design Uplink Rate (Mbit/s)			1.40
			Margin in Uplink			195%
			Data Storage Requirement (Mbits)			1154
			Design Data Storage (includes 20% Margin) (Mbits)			1385

2.3.1.8 *Communications*

The ELM communications architecture would be designed to allow the lander to transmit all of its science and engineering data to JIMO for any landing latitude between ±45° (Fig. 2.3.1-8) and in any landing orientation (right-side-up, upside-down, and in-between). The lander would utilize a pair of omni-directional antennas (one on each surface), to communicate with JIMO, and an SSR to buffer all data when JIMO is out of sight of the lander.

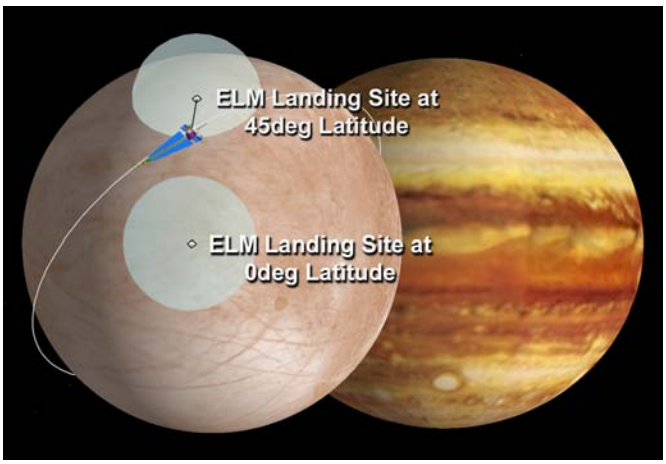

Figure 2.3.1-8. Communications Event Between ELM (at 45° latitude) and JIMO

Due to the orbital and geometric parameters of the mission, ELM-JIMO communication events would occur in groups (called cycles) of 5 to 14 (dependent upon landing latitude) and would take place over a relatively short duration (hours) as illustrated in Figure 2.3.1-9. These cycles would repeat with a period that is determined by the landing latitude, and range from 0.5 to 1 Europa day. The communications architecture would be designed such that all data generated between successive cycles would be uplinked to JIMO prior to the next interval.

The frequency and duration of communications events would be highly dependent upon the ELM landing latitude. As the latitude is decreased (towards the equator), the total number of JIMO over-flights of the landing vicinity would decrease, as illustrated in Figure 2.3.1-9. Quantitatively, there would be 10 possible ELM-JIMO communication opportunities per Europan day at 0° landing latitude, whereas there would be 14 possible opportunities at 45° latitude assuming a mini

mum 5° line-of-sight (LOS) angle is required to close the link (Table 2.3.1-5 and Fig. 2.3.1-9). Additionally, as the landing latitude is decreased (towards the equator), the average duration of the communications window would also decrease. The result is that the total amount of communications time during the surface mission would be lowest at the equator (710 minutes), and highest at 45° (1050 minutes). As the rate of data generation would be independent of latitude, the 0° latitude case represents the most stressing case from a data uplink perspective, and drives the minimum bandwidth requirement for the lander.

Table 2.3.1-5. Frequency and Duration of Comm. Events Versus Landing Latitude for the ELM Mission

Communication Parameter	Lander Latitude	
	0 deg	45 deg
# Comm. Cycles (Total Mission)	~17	~8
# Comm. Periods / Europa Day	10	14
# Comm. Periods (Total)	83	111
Comm. Duration (Total)	710 min.	1050 min.
Comm. Duration per Cycle (Avg)	43 min.	130 min.
Eclipse Period between Cycles (hr)	43	84

Conversely, as the landing latitude is increased (to a maximum of 45°), the duration between successive communications cycles (called the eclipse period) would increase significantly (Fig. 2.3.1-9). Analyses show that a lander at 0° latitude would experience ~43 hours of eclipse, whereas 84 hours would be observed at 45° latitude. The 45°latitude case is the most stressing in terms of the volume of generated data, and thus would drive the solid-state recorder memory requirement.

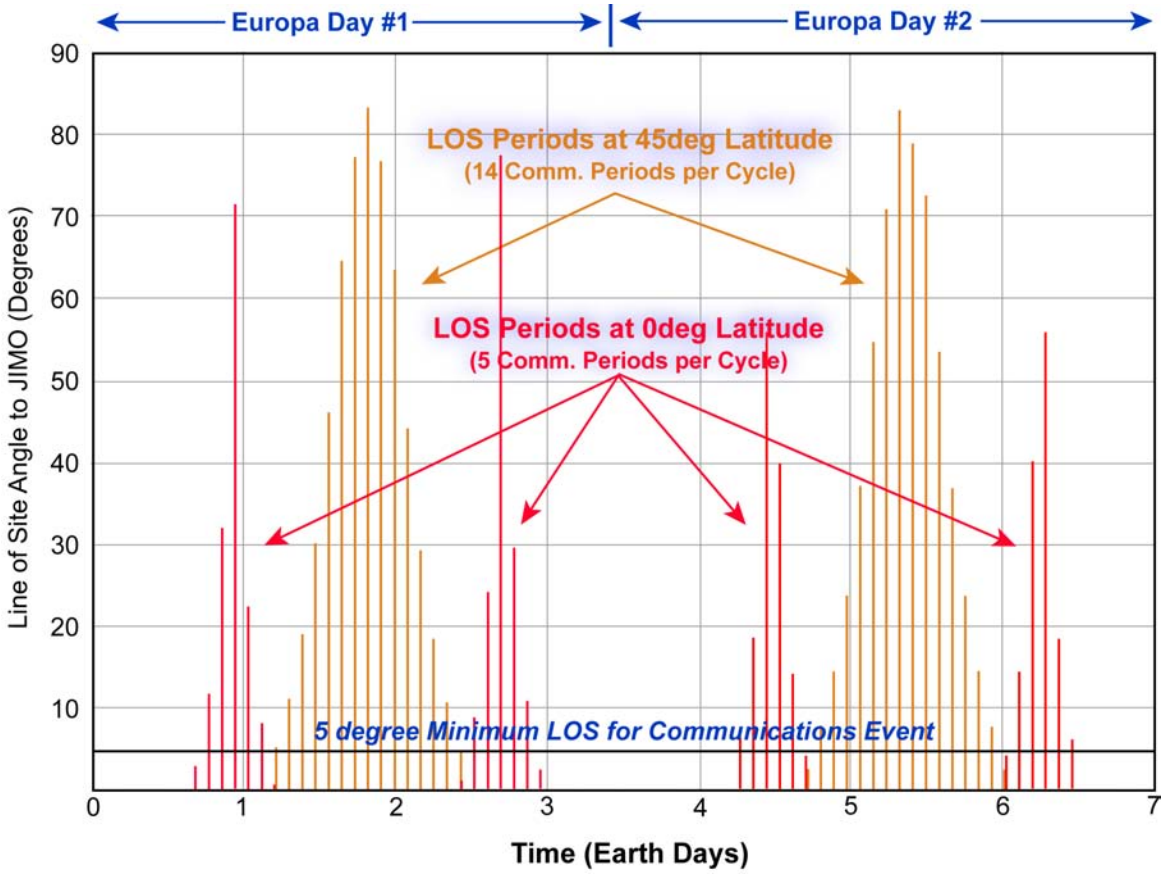

Figure 2.3.1-9. Elevation Line of Site (LOS) Angle between ELM and JIMO as a Function of Latitude and Time

2.3.1.9 *Thermal*

A significant amount of thermal power would be required to maintain operational and survival temperatures during the cruise phase and on the surface of Europa where the nighttime temperatures can drop to 85 K. The source of this thermal power would be the RPS unit that would produce ~225 Wt at EOM, and would have a thermoelectric cold-shoe temperature of 155°C. Thermal control would be accomplished via a combination of conduction straps and thermal switches designed to keep critical electronics, batteries and subsystems warm. Heat rejection from the spacecraft would be performed via variable-emissivity radiators [11–13] whose emissivity could be actively varied between ~0.3 and 0.7 to maintain the desired temperature profile. The radiators would be mounted on both surfaces of the lander to ensure functionality regardless of landing orientation (Fig. 2.3.1-2). Heat rejection to the Europan surface would be made via conduction between the surface and lander structure, and thermal switches would manage the heat flow.

2.3.1.10 *Power*

The proposed ELM would use a combination of RPS power and secondary (rechargeable) batteries to supply power to the spacecraft during the mission. The power requirements, duty cycle, and operating duration of each system is presented in Table 2.3.1-6. To manage the spacecraft power draw, five distinct operating modes would be used that correspond to specific sets of activities. The baseline modes would be *Standby*, *Basic Measurements*, *Raman Measurements*, *LIBS Measurements* and *Communications*. The *Standby* mode would be used only during the launch and cruise phases, and would involve powering the minimum number of spacecraft systems including the Command and Data Handling (C&DH) system, Power Distribution (PD) system, and the data storage system. All other modes would nominally be used only during the surface science mission. In the *Basic Measurement* mode, the imager, microseismometer, temperature sensors and radiation sensors would be operated in addition to the basic spacecraft systems (C&DH, PD and data storage). In *Raman Measurement* mode, the only instrument operating would be the Raman spectroscope. Likewise, in *LIBS Measurement* mode, the LIBS insturment would be operated. Lastly, in *Communications* mode, all available power would be directed to the communications system (all instruments would be powered down in this mode) to uplink science and engineering data to the mothership. Each mode would have its own average and peak power draw and operating duration (Table 2.3.1-7 and Fig. 2.3.1-10).

Table 2.3.1-6. Proposed ELM System Power Levels, Duty Cycles and Operating Durations

System	Quantity	Power Draw (W/unit)	Power Draw All Units (W)	Duty Cycle	Avg Power Draw per Europa Day (W)	Operating Time per Europa Day (hrs)
Command and Data Handling						
System Flight computer	1	2.60	2.60	0.30	0.78	85.20
Peripheral Subsystem Interface	1	1.00	1.00	0.30	0.30	85.20
Power Distribution						
DC/DC Converter Card	1	3.00	3.00	0.30	0.90	85.20
Power Distribution Slice	1	2.20	2.20	0.30	0.66	85.20
Science Instruments						
Imager	1	0.20	0.20	1.00	0.20	0.23
Microseismometer	3	0.14	0.42	1.00	0.42	84.52
Raman Spectrometer	1	5.00	5.00	1.00	5.00	2.82
LIBS	1	5.00	5.00	1.00	5.00	2.82
Temperature Sensors	16	0.10	1.60	1.00	1.60	0.47
Radiation Sensors	4	0.10	0.40	1.00	0.40	84.52
Comm. Subsystem (JIMO Link)						
Transceiver (33% Efficient)	1	6.00	6.00	1.00	6.00	0.68
Data Storage						
Data Storage (SSR)	1	3.00	3.00	0.30	0.90	85.20

The spacecraft power system would be sized to meet the demands of all modes, and would be driven by peak power requirements of the *Communications* mode (17.8 We), *Raman Measurement* mode (17.3 We) and *LIBS Measurement* mode (17.3 We). Because peak power utilization occurs infrequently, the total energy usage would be very modest and is estimated at ~3200 W-hr for the surface mission (Table 2.3.1-7). This corresponds to an average power level of 4.5 We that would be adequately supplied by a single GPHS-module RPS with 10.1 We (EOM) output.

To handle the peak power demands, a small lithium-ion battery with a minimum of 63 W-hr capacity would be used. The battery would discharge only during the transient periods where total load exceeded the RPS output; otherwise, the battery would be continually recharged by the RPS. The total energy margin using a single GPHS RPS would be 126%, which allows for uncertainty and limited future enhancements.

Table 2.3.1-7. ELM Operating Modes and Total Energy Requirement

Mode	Peak Power Draw (W)	Avg Power Draw (W)	RPS Output Power at EOM (W)	Duration of Mode / Europa Day (hr)	Total Energy Used During Mode (W-hr)
1: Standby	11.80	1.50	10.14	N/A	N/A
2: Basic Measurements	12.34	4.12	10.14	78.89	325.02
3: Raman Measurements	17.34	9.12	10.14	2.82	25.7
4. LIBS Measurements	17.34	9.12	10.14	2.82	25.7
5: Communications	17.80	7.50	10.14	0.68	5.07
Max (Peak Power Draw) (W) =	**17.80**	**Energy Req'd/Europa Day (W-hr)=**			**381**
Avg Power Draw (W) =	**4.5**	**Generated RPS Energy/Europa Day (W-hr)=**			**864**
RPS Power Output at EOM (W) =	**10.14**	**Total RPS Energy Margin (%)=**			**126%**

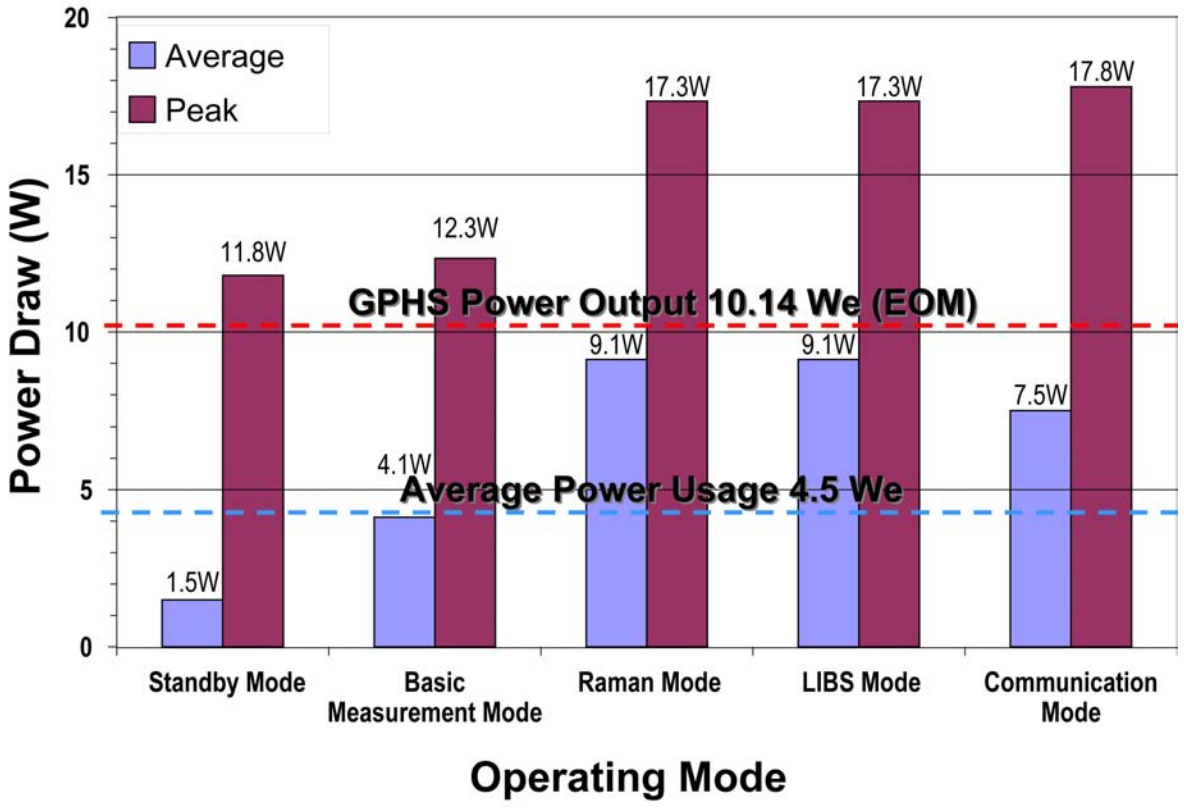

Figure 2.3.1-10. ELM Power Requirements (Peak and Average) for Each Operating Mode

2.3.1.11 *Mass*

The total mass of the ELM spacecraft would be ~233 kg, and includes the lander, dual propulsion stages, landing system (airbags, etc.), JIMO attachment system, and JIMO-mounted communications equipment (Table 2.3.1-8). The mass of the lander would be ~39 kg, constituting 17% of the total spacecraft weight. The RPS power system is assumed to weigh 10 kg, and is extrapolated from conceptual RPS designs (Section 4.5.1) upgraded to handle the expected landing loads. The total instrument mass allocation is 9.3 kg, and the heaviest instruments are the imagers, Raman spectroscope and LIBS.

Table 2.3.1-8. Mass Breakout of the ELM Spacecraft Systems and Subsystems

Item	Qty	Mass (kg)	Margin (kg)	Mass with Margin (kg)*
Lander Payload				**38.7**
Command Data and Handling				**1.84**
System Flight Computer	1	0.50	0.08	0.58
Peripheral Subsystem Interface (PSI)	1	0.10	0.02	0.12
Bus	1	1.00	0.15	1.15
Power Distribution				**1.64**
Power Distribution Slice	1	0.49	0.05	0.54
DC/DC Converter Card	1	1.00	0.10	1.10
Power Generation and Storage				**11.16**
GPHS RPS	1	5.00	5.00	10.00
Batteries	1	0.33	0.17	0.5
Packaging	1	0.63	0.03	0.66
Pyro and Valve Control				**0.87**
Battery Charge Control	1	0.30	0.03	0.33
Prop Drive	1	0.49	0.05	0.54
Science Instruments				**9.30**
Seismometer	3	0.05	0.01	0.18
Imagers	16	0.20	0.04	3.84
Raman Spectroscope	1	2.00	0.40	2.40
LIBS	1	2.00	0.40	2.40
Radiation Sensor	4	0.10	0.02	0.48
Temp sensors	16	0.01	0.00	0.17
Telecom Subsystem				**3.30**
Transceiver	1	0.30	0.03	0.33
S-Band Antenna	6	0.25	0.03	1.65
Packaging	1	0.30	0.03	0.33
Coax Cables to antennas	6	0.15	0.02	0.99
G & C Sensors				**0.21**
Accelerometers	3	0.05	0.00	0.16
3-axis gyroscope	1	0.05	0.00	0.05
Thermal				**1.26**
Heater Elements	10	0.02	0.00	0.21
Insulation	1	1.00	0.05	1.05
Mechanical Systems				**10.00**
Structure	1	3.60	0.36	3.96
Covers	6	0.10	0.01	0.66
Misc (fasteners)	1	0.72	0.03	0.75
Cabling	1	0.60	0.03	0.63
Radiation Shielding	1	2.00	2.00	4.00

Item	Qty	Mass (kg)	Margin (kg)	Mass with Margin (kg)*
Propulsion				**111.4**
Upper Desent Stage				13.7
Support and Separation Mechanism	3	1.00	0.05	3.15
Support structure	1	2.54	0.25	2.79
ARC Solid KS40B Thrusters (spin-up)	2	0.38	0.02	0.80
ARC Solid PAC-3 Thrusters (spin-down)	2	0.16	0.01	0.34
Hydrazine trim system	1	1.80	0.09	1.89
Star 5 rocket motor	1	4.50	0.23	4.73
Lower Desent Stage				97.7
Support and Separation Mechanism	3	1.00	0.05	3.15
Support Structure	1	5.70	0.57	6.27
Star 17 Motor	1	84.10	4.21	88.31
Thermal				**2.2**
Thermal Blankets	1	1.00	0.05	1.05
Temp sensors	10	0.01	0.00	0.11
Misc	1	1.00	0.05	1.05
Mechanical Systems				**13.9**
JIMO Attachment System	1	5.00	3.00	8.00
Ballest	1	5.00	0.50	5.50
Fasteners	1	0.40	0.01	0.41
Landing System				**61.0**
NSI - Gas Generator	3	1.00	0.05	3.15
Airbags	3	16.06	3.21	57.82
JIMO-Based Comm.system				**5.5**
Antenna	1	3.00	1.00	4.00
Gimbal	1	1.00	0.50	1.50
Net Spacecraft (EPF)*				**232.7**
Lander Mass (Total)				**38.7**
Propulsion Mass (Total)				**111.4**
Thermal Mass (Total)				**2.2**
Mechanical Systems Mass (Total)				**13.9**
Landing System Mass (Total)				**61.0**
JIMO-Based Comm. System				**5.5**

* The total spacecraft mass includes an effective 30% margin. This is because the mass estimates of the rocket motors and airbags used herein are for the previous heavier models of these two systems, whereas the new lighter models (using composite casings, etc.) would be used in an actual flight system [14]. The resultant mass savings could then be reallocated to increase the mass margins of the remaining subsystems.

The dual propulsion stages (upper descent and lower descent) make up the bulk of the spacecraft mass at 111.4 kg, or 48%. The Star 17 solid rocket motor within the lower descent stage has the single greatest component mass at 88.3 kg due to the large delta V (1458 m/s) required at periapse (Section 2.3.1.3). The landing system, comprised of airbags and gas generators, has a total mass of 61 kg (26% of total). The three air bags dominate the landing system mass, cumulatively weighing 57.8 kg.

The JIMO attachment system would include the struts and structure used to mount the ELM spacecraft to the JIMO mothership during the cruise phase. The mass of this system is estimated at approximately 14 kg. A supplemental JIMO-mounted communications system would be used to allow JIMO to exchange commands and data with the lander during descent orbital insertion and during the surface science mission. This communications system would include a gimbaled parabolic antenna, transceiver electronics, mounting brackets, and all necessary power and data interfaces to the JIMO spacecraft. The mass of this communications system is estimated at 5.5 kg.

2.3.1.12 *Radiation*

The ELM spacecraft would be required to operate in a range of extreme radiation environments that include externally produced (natural) and internally produced gammas, neutrons, and other high-energy particles (alphas, betas, etc.). Key sources of natural radiation include the Van Allen radiation belts traversed during the Earth spiral-out phase, cosmic radiation received during the multi-year cruise phase, radiation generated by the JIMO reactor, and the intense radiation environment around Jupiter's inner moons. Internal radiation would be generated from the decay of the plutonium fuel within the RPS's GPHS module and from resulting secondary fission reactions that would occur due to fuel impurities. The lifetime dose of the ELM spacecraft from natural radiation would be ~6 Mrad, and assumes 100 mils of aluminum shielding [15]. The majority of this radiation would be received in proximity to Jupiter's moons, particularly during Europa spiral-in, where Jupiter's radiation field is very strong (Fig. 2.3.1-11). Once landed on Europa, ELM would benefit from the shielding properties of this moon and would receive a marginal ~400 krad during the surface mission. To mitigate the effects of natural radiation, potential strategies include housing ELM in a JIMO-mounted radiation shelter (thus reducing the received natural dose), using localized spot shielding around critical components, and employing radiation hardened electronics that could tolerate doses up to 1 Mrad. The use of a radiation shelter and spot shielding could potentially reduce the ELM lifetime external dose to <1 Mrad, making the mission potentially feasible with radiation-hardened parts. ELM would capitalize on the JIMO radiation-tolerant

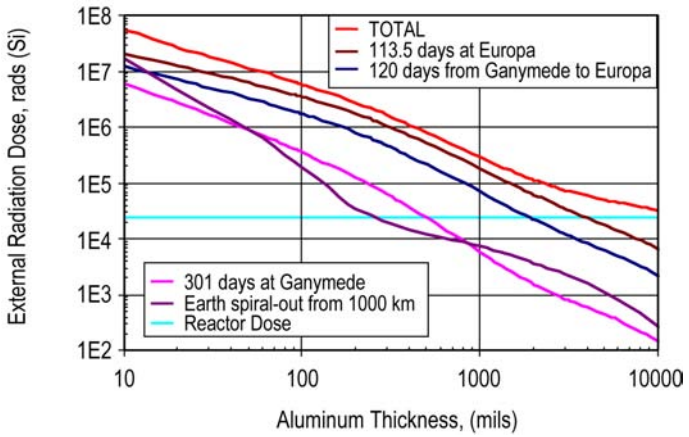

Figure 2.3.1-11. Natural Radiation Dose (4-Pi) Received by the JIMO Spacecraft Versus Shielding Thickness [15]

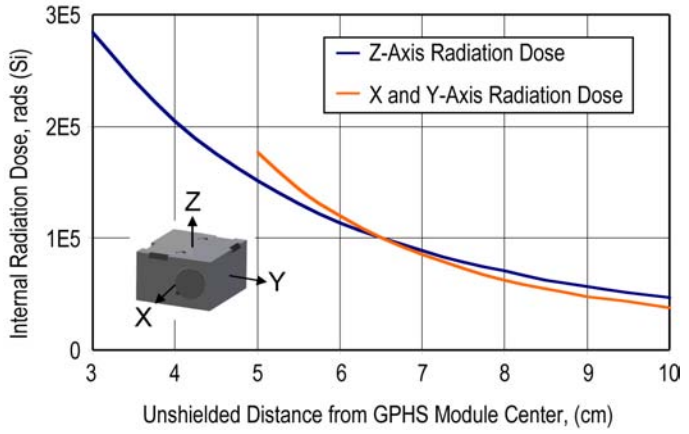

Figure 2.3.1-12. Lifetime (13-year) Radiation Dose Generated by a GPHS Module Versus Distance [16]

technology currently being studied, and would utilize similar or identical mitigation schemes as appropriate.

The magnitude of the internally generated GPHS radiation dose would be significantly lower than that received from natural sources (by more than an order of magnitude), and would be highly dependent upon the distance between the GPHS and the "target" component [16]. The intensity of the dose falls off quickly with distance from the GPHS module due to geometric attenuation (Fig. 2.3.1-12) and structural attenuation through the spacecraft. With judicious placement of sensitive subsystems and components, the total lifetime internal dose could be reduced to <100 krad

2.3.1.13 *Alternate RPS Power Systems*

The baseline ELM design would be powered by a single GPHS-based RPS using PbTe–TAGS thermoelectric conversion, which is assumed capable of generating 10.1 We at EOM. A small supplemental battery would be used to meet peak power demands (maximum of 17.8 We) during LIBS, Raman spectroscopy and communication events. In addition to this baseline design, three alternate RPS concepts were considered that could generate enough power to eliminate the need for a battery.

The first concept would use two GPHS-based RPSs with PbTe–TAGS thermoelectrics, and would generate 20.2 We at EOM. This RPS configuration would meet all ELM power requirements without the need for a supplementary battery; however, this larger RPS system would require a redesigned spacecraft that is larger both in size and mass. Additionally, the ability to reject the increased amount of waste heat could pose a significant challenge to the ELM thermal control system.

The second concept would use a single GPHS-based RPS with higher-efficiency (9%) thermoelectric converters (e.g., segmented PbTe–TAGS/BiTe). This RPS configuration could generate ~18 We (EOM), which would be sufficient to meet all power requirements without a battery. Studies have been performed by the DOE (Section 4.5) that suggest this RPS configuration may be attainable in the near future.

The third concept uses a fractional GPHS-based RPS with a conceptual high-efficiency Stirling convertor (20%). This RPS could produce 18 We (EOM) using half the fuel of the baslined RPS concept (two fuel capsules instead of the normal four). However, the Stirling convertor would need to be sufficiently vibration-free to prevent interference with microseismometer measurements, and the fractional GPHS (with a redesigned aeroshell) would need to be developed.

2.3.2 Additional RPS-Enabled Lander Missions

The design of the ELM spacecraft and its small-RPS power source is somewhat generic and could potentially be utilized for missions to other planetary bodies with minimal modification. Examples inlcude missions to the outer Galilean satellites Callisto and Ganymede, using either the JIMO spacecraft as transport and communications relay to Earth, or a dedicated orbiting satellite that would perform an analogous function. One preliminary version of the JIMO mission includes a nominal 60 day science orbit around Callisto and a 120 day science orbit around Ganymede [8]. A variant of the ELM spacecraft, with its long-lived small-RPS power source, would be sufficiently capable of performing the analogous surface science mission on either of these moons, both of which are of high scientific interest.

Other lander-class missions potentially enabled by small-RPS technology include landers for outer solar system planetary bodies, including moons, Pluto, asteroids and comets. These missions could have different science payloads using similar power requirements as the ELM mission. Lunar human-precursor missions could also be enabled by a small-RPS, with its ability to operate continuously, independent of solar insolation, at the lunar poles and in craters that are permanently shadowed. Mars network landers, Scout-class rough landers, and Mars human precursor landers are additional missions that could potentially benefit from small-RPS technology.

2.3.3 Summary and Conclusions

Europa is a high-priority target for future space exploration, as it may possess a subsurface liquid ocean that could sustain life. The ELM mission is designed to land on Europa and take in-situ measurements for a nominal period of 30 Earth days in order to meet the science objectives defined by the JIMO Science Definition Team [6]. Due to Europa's vast distance from the Sun, long cruise phase, and surface mission duration, small-RPS would provide unique capabilities not possible with conventional power sources.

The small-RPS used in the ELM concept is a conceptual design based on a single GPHS module using thermoelectric conversion with 5% system efficiency to produce 10.1 We at EOM. This RPS configuration would provide a 126% energy margin, and would employ a small Li-Ion battery to carry the peak loads during high-power operations, i.e., communications events, Raman spectroscopy and LIBS. The small-RPS would need to be designed to withstand the 600-g acceleration load incurred by the spacecraft during landing.

In conclusion, ELM is a high-value mission that could potentially be enabled by small-RPS technology.

2.4 ROVER MISSIONS

2.4.1 Mars Rover Mission

After the great success of the Mars Exploration Rovers, Spirit and Opportunity [17], NASA continues working on future mission concepts in support of the Mars Exploration Program. Some of these missions include rovers to achieve surface mobility, others concentrate on subsurface access, and some on sample return. This section focuses on surface mobility, and describes a point design that demonstrates the feasibility of a MER-class Mars rover powered by a small-RPS unit.

2.4.1.1 *Science Goals*

The Vision for Space Exploration [4] recognizes Mars (Fig. 2.4.1-1) and the Moon as prime destinations for both robotic and human exploration. Additionally, NASA's Mars Exploration Program Assessment Group (MEPAG) [18] identifies the high-priority science and technology issues relevant to the program. The four highest-priority objectives identified by MEPAG are, in descending priority: (1) the search for life; (2) understanding the Martian climate, (3) assessing Martian geology; and (4) preparing for human exploration. Consequently, the conceptual mission design described in this study builds on heritage from the MER missions [19], while specifically addressing astrobiology-driven science goals. This systematic approach places this rover mission in line with other planned Mars exploration missions, while helping to establish an exploration path that leads towards the ultimate goal of human presence on Mars.

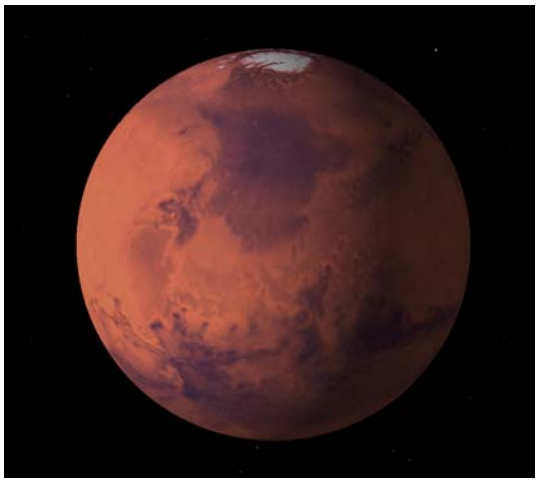

Figure 2.4.1-1. Mars: Future Destination for Manned Space Exploration

2.4.1.2 *Mission Goals*

Both MER and Mars Pathfinder [20] operated on Mars in an energy-limited mode, since the solar panels generated power during daylight hours only. At other times, the rovers relied on power stored in batteries. Radioisotope power systems offer a power-enabled paradigm, where power is generated for long mission durations (measured in years), independently from the Sun, and on a continuous basis. To take advantage of these benefits, the goal of this mission study concept is to demonstrate the feasibility of a small-RPS enabled generic MER-class rover, and to assess the relative advantages of such a mission. Although the power level for this point design is sized to match MER-class rover mission requirements, additional rover designs, scaled to various power levels, are identified in Section 2.4.3.

2.4.1.3 *Mission Architecture Overview*

In order to conduct high priority science in line with MEPAG goals, the science community needs a mobile platform to perform astrobiology, geology and climate experiments at locations potentially inaccessible to solar powered rovers (e.g., poles, shadows, caves, areas of low insolation). This rover concept extends the capability and longevity of the power source, using RPSs, to further increase the science return. For the present astrobiology-oriented mission concept, the Mars Exploration Rovers presented a suitable starting point. Consequently, a significant portion of this mission is based on the original MER mission architecture and hardware configuration.

The launch and arrival characteristics are determined for two launch periods, one that allows access to maximum northern latitudes and one to maximum southern latitudes. The latitudes bridged by the two trajectories range from 70° S to 70° N. A Type II trajectory is used for either latitude regime. The permissible range of latitudes is limited by the launch configuration and not by the power system—RPS enabled rovers are operational at any given Martian location.

To land between 70° S and 40° N, the launch window is from October 27 through November 16, 2009. This corresponds to a cruise phase of 334 to 354 days and an arrival date of October 16, 2010. The heliocentric longitude of the Sun (Ls) at arrival is 165°. The C_3 for this launch period is 20 km^2/s^2. The corresponding injected mass is 3100 kg on an Atlas 521 launch vehicle (LV) or 2897 kg on a Delta 4450-14 LV.

To reach the maximum northern latitude of 70° N (and ranging down to 50° S), the launch window is set between October 6 and 26, 2009. The cruise phase is ~300 days with an arrival date between July 23 and August 22, 2010. The longitude of the Sun at arrival ranges from 120° to 133°. The C_3 is 15 km^2/s^2, which allows for injecting a mass of 2923 kg on the Delta 4240-14 LV or 2806 kg on an Atlas 511 LV.

Figure 2.4.1-2. MER-type Airbag without the Aeroshell

Entry, descent, and landing (EDL) is assumed using either MER-type airbags or a Viking/Phoenix-type powered descent stage. Using an airbag configuration (Fig. 2.4.1-2), the rover can be accommodated in a 2.57 m aeroshell, with a total launch mass of ~1070 kg. The Viking-type powered landing configuration with a larger 3.65-m aeroshell has a launch mass of ~1620 kg. For both cases, the launch mass is less than half of the available LV capacity. Therefore, further optimization can be made by choosing a smaller LV, for example Atlas IIIB [with a single-engine Centaur (SEC) stage] (1995 kg) or Delta IV 4040-12 (1565 kg) for C_3 of 20 km^2/s^2 [21].

Figure 2.4.1-3 shows a Viking-type aeroshell and lander with the rover. The choice of airbag landing versus powered landing results in different landing accuracies and acceleration load environments. The landing ellipse for airbags with no entry guidance (attitude hold only) and optical navigation is ~96 km (e.g., as calculated for MER). For powered descent, the landing ellipse can be as small as ~10 km, but at a significantly increased propellant penalty. An airbag landing requires ~40g acceleration tolerance, while a powered landing requires only ~20 g. Both configurations would employ a single parachute.

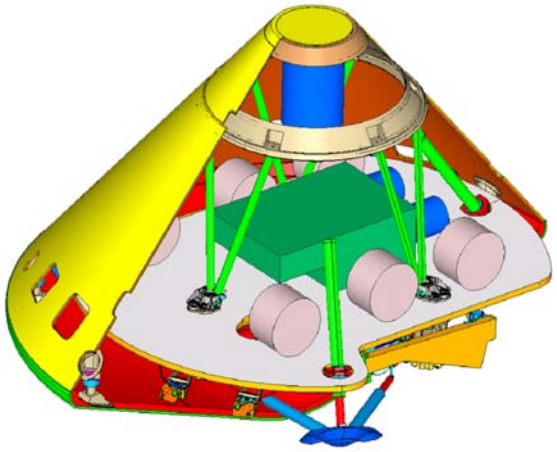

Figure 2.4.1-3. Viking-type Aeroshell, Lander, and Rover

Upon landing, the rover would decouple from the lander, perform initial health checks and environment assessment, egress from the lander and initiate the surface operation phase. Active measurements would be planned for a 3-year mission duration, resulting in a total mission time of ~1400 days. It should be noted that the power system would be capable of providing continuous power for an extended mission phase. The actual mission duration is theoretically limited only by the failure of a key sub-system; most likely an actuator or other moving component, and is accelerated by uncontrolled thermal cycling. Component failures can be reduced by tight thermal control. When a mission extends over several years, additional development work is required to improve the reliability of the moving parts, including motors, actuators, wheels and robotic arm joints. The present rover configuration is shown in Figure 2.4.1-4. The top and mast of the rover are identical to those installed on MER, and are not included in the figures to allow for better illustration of the internal components. The two small-RPSs would be placed at the end of the

rover. Modular design of the RPSs would allow for much flexibility in placing them at the most suitable locations. In turn, the configuration (e.g., side-by-side, back-to-back) impacts the thermal and the radiation environments inside and around the rover. The thermal design is further discussed in Section 2.4.1.9, while the radiation dose from RPSs on the instruments and electronics is addressed in Section 2.4.1.13.

During the surface operation phase of the mission, the rover would perform scientific measurements and relay the data back to Earth. Details of these are given in Sections 2.4.1.6 and 2.4.1.8.

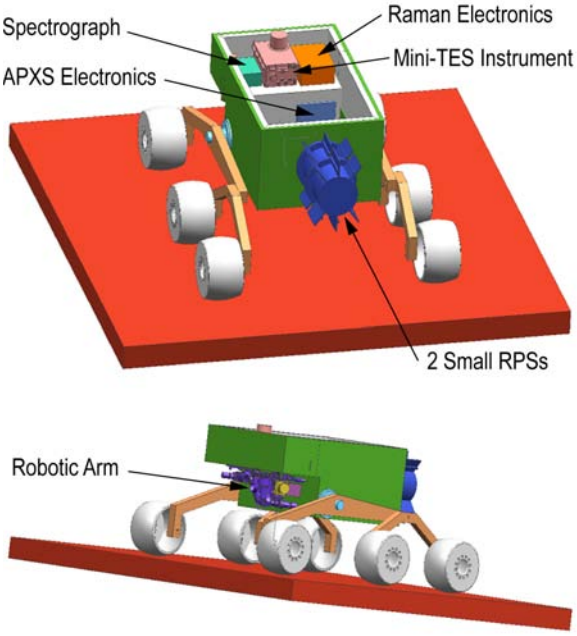

Figure 2.4.1-4. Mars Rover Configuration (top removed to show internal systems)

2.4.1.4 *Power Source Trade Study*

The Mars Exploration Rovers employed solar panels for power generation. The unfolded 1.3 m^2 GaInP/GaAs/Ge triple-junction solar panels were capable of generating ~140 We (electrical) peak power for up to 4 hours per sol, depending upon the season. Although solar power generation has many advantages out to 3.5 to 4.5 AU from the Sun, this section discusses the advantages of RPS power on the surface of Mars.

Solar insolation varies inversely with the square of distance from the Sun (i.e., $1/R^2$). Thus, the solar flux at Mars (~1.5 AU) is only 43% of that at Earth [22]. In addition, solar power generation on Mars is further impacted by atmospheric conditions, sand storms, operating latitude, seasons, terrain shadowing, and solar panel degradation (due to dust accumulation and thermal cycling from diurnal temperature variations) [23]. This can reduce the received solar flux on the surface to 6.5% of that at Earth. Continuous year-round solar insolation is limited to the equatorial region and middle latitudes (from 60° N to 60° S). At high latitudes (above 60° N and below 60° S), long-term continuous operation is not feasible due to seasonal variations, including low solar insolation during polar winters (Fig. 2.4.1-5).

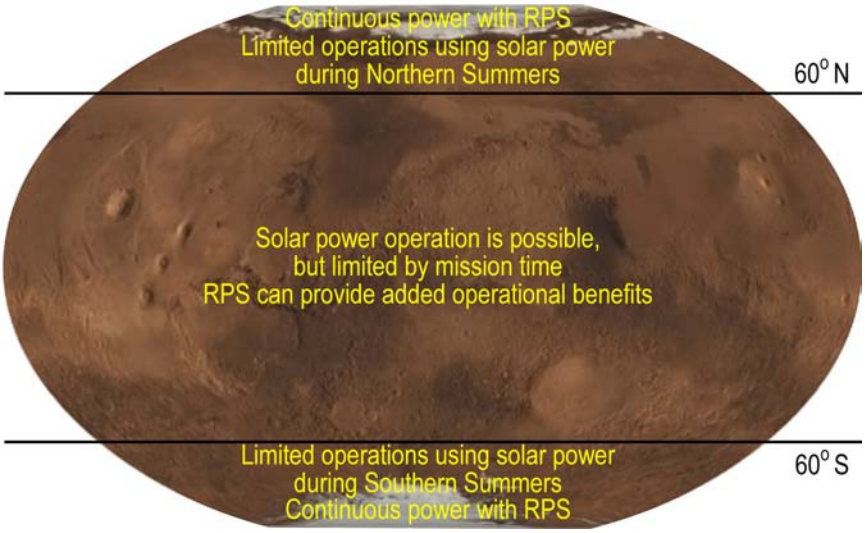

Figure 2.4.1-5. Operating Performance of a Mars Rover as a Function of Landing Location

For some operating conditions and mission requirements, RPS presents distinct advantages over solar powered systems. RPS-based power generation is independent of solar insolation and atmospheric effects. It also enables a significantly greater lifetime (potentially measured in years), which translates into a greater mobility range that could afford greater scientific discovery and data accumulation. RPSs would be advantageous for rovers operating at high latitude regions, especially the poles during winters, enabling operations in partially or permanently shadowed regions such as valleys, canyons and caves. Radioactive decay from the fuel generates a significant amount of thermal power, of which only a small percentage is converted into electricity. The rest is excess heat and nominally rejected to the environment. However, this waste heat can be used to achieve tight temperature control of subsystems inside the rover. This would reduce thermal cycling of the components, potentially decreasing component failures and extending operability. Additionally, batteries have tight temperature windows, and maintaining them at a constant temperature (~0°C) helps preserve battery performance, and extend battery life. This characteristic advantage of RPSs is beneficial not only for operations in polar regions, but at any given location on Mars. In comparison, solar powered systems rely on batteries to heat components overnight using high-powered resistance heating. This impacts the lifetime of the batteries, uses valuable resources and may result in a power system that is larger than an equivalent RPS system and that is driven by system survivability requirements.

2.4.1.5 *Small-RPS Characteristics*

The conceptual power source for this rover study consists of two individual small-RPSs, each configured with a single GPHS module. Each module contains 4 plutonium dioxide fuel capsules, and the total fuel and module mass would be 0.5 kg and 1.445 kg, respectively. The thermal power output for each module would be 250 Wt (thermal) at BOL. This heat output decreases by ~0.8% per year [9] due to radioactive decay of the plutonium fuel.

The heat generated by the RPS would be converted to electric power using thermoelectric (TE) conversion. As discussed in Section 3, the selection of material used for TE conversion depends on the operating environment. For use in the Martian atmosphere, PbTe–TAGS multicouples are proposed, using a close-packed array (CPA) configuration (Section 4.5). There is a 0.8% loss associated with TEs per year, resulting in a total power system degradation of ~1.6% per year.

Based on these assumptions, two small (single GPHS module-based) RPSs could generate 25 We of power (or 620 W-hr energy per sol) at BOL and 23.44 We (or 580 W-hr/sol) at end of mission (EOM). The EOM values correspond to a 1 year cruise phase plus 3 years of surface operation. In addition, the design also accounts for an appropriate heat rejection system for the 475 Wt waste heat. The total mass of the two RPSs is ~12 kg, with approximate bounding dimensions of 320 mm by 230 mm by 140 mm. This is significantly smaller than a solar array system with similar power output (e.g., a 1.3 m^2 solar panel generates ~600 W-hr/sol at EOM and weighs 16.5 kg.) A conceptual drawing of a single GPHS module-based RPS is presented in Figure 2.4.1-6, and is based on the work conducted by the DOE [24].

2.4.1.6 *Science Instruments*

The present rover design concept is based on the initial MER configuration [17] to provide design heritage, but incorporates two significant enhancements. The solar panels are replaced with two small-RPSs, and the Mossbauer spectroscope is replaced with a laser Raman spectroscope to meet the astrobiology-driven science goals. The instruments on the rover would be categorized into to two groups: remote sensing and contact instruments. Remote sensing instruments would be located on a mast placed on the top of the rover (not shown). Contact instruments would be positioned on a robotic arm as shown in Figure 2.4.1-7.

In this design concept, remote sensing instruments are configured identically to those on MER, and include a Mini-Thermal Emission Spectrometer (Mini-TES) and a Panoramic Camera (Pancam). Mini-TES takes measurements of emitted thermal infrared radiation. It is used to characterize the mineralogy of rocks and soil, and to determine the thermo-physical properties of selected soil patches. In addition, the Mini-TES can be used to determine the temperature profile, dust/

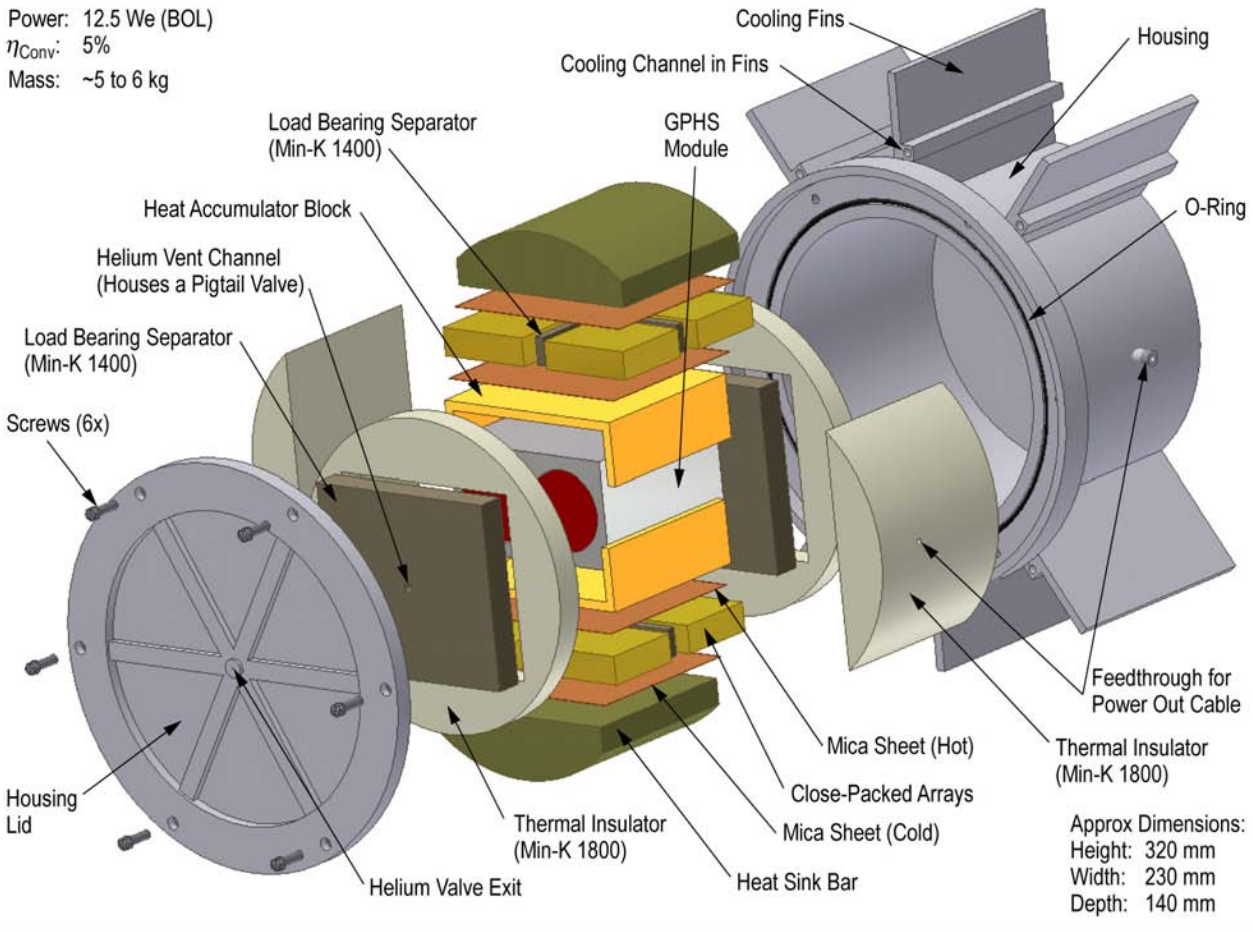

Figure 2.4.1-6. Conceptual Small-RPS for the Mars Rover Using a Single GPHS Module

water-ice opacity, and water vapor abundance in the lower atmosphere. The collected data helps to understand the climate and geology of Mars (MEPAG Goals 2 and 3). The Pancam is used to generate 360° panoramas and multi-spectral images of the surface. This high-resolution stereoscopic imaging camera complements the rover's navigation cameras and aids in characterizing the geomorphology of the surface through the generation of terrain maps, slope maps and ranging. The Pancam works in conjunction with the Mini-TES to describe the Martian environment, thus providing a foundation for subsequent human missions (MEPAG Goals 3 & 4).

Contact measurements are performed with instruments positioned on the robotic arm. These instruments include a contact microscopic imager, an Alpha Particle X-ray Spectrometer (APXS), and a Mars Microbeam Raman Spectroscope (MMRS). These instruments are supported by a Rock Abrasion Tool (RAT). The microscopic imager is the combination of a microscope and a camera, and is designed to measure fine scale morphology, texture and reflectance of natural surfaces. This contributes to the petrologic and geologic interpretation of rocks and soil in support of MEPAG Goal 3. Small-scale imaging may help identify tiny veins of minerals, which potentially contain microfossils (MEPAG Goal 1). It also provides context imaging for collaborative measurements with other contact and remote sensing instruments.

The MMRS performs mineral characterization and assists in the detection of water, organic and inorganic forms of carbon (MEPAG Goal 1). It identifies many major, minor and trace minerals and their relative proportions (i.e., Mg/Fe ratio), and carbon ratios. Sharp Raman spectral features and statistical point counting help identify minerals in complex mixtures and morphologies (MEPAG Goal 3). The APXS instrument uses alpha particles and X-rays to accurately determine the elemental chemistry of rocks and soils in order to complement and constrain the mineralogical analyses of other instruments. APXS can quantify the abundances of all rock forming elements, except hydrogen. It performs elemental analyses of Martian surface materials by direct contact with rocks or soil, and helps to understand weathering processes and water activity on Mars (MEPAG Goals 3 & 4). In order to expose the interior of rocks, a grinding wheel (RAT) is used to remove dust and upper surface layers. Rock abrasion is used as a precursor step before measurements are performed with the instruments listed above. It can also be used to measure rock hardness during RAT penetration. The performances of the above instruments are considered identical to those on MER (with the exception of the MMRS). [17, 20]

While the remote and contact sensors would be located external to the rover, the delicate instrument electronics would be placed inside the rover's warm electronics box (WEB) for protection against the harsh Martian environment.

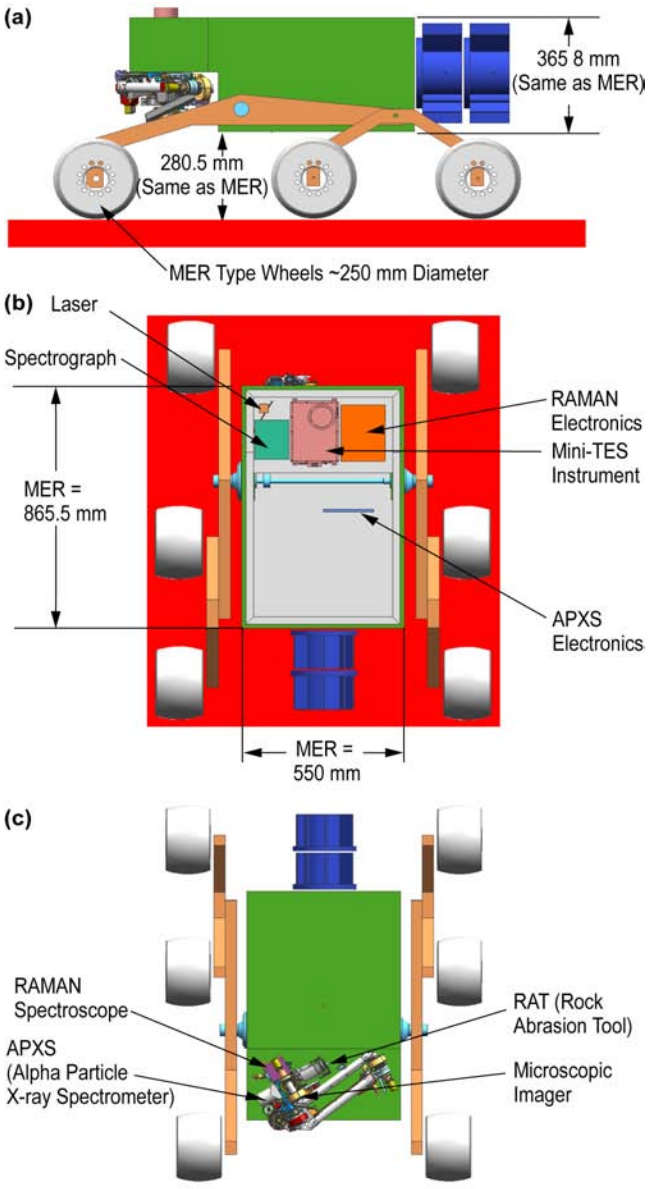

Figure 2.4.1-7

Figure 2.4.1-7. Mars Rover Instrumentation Configuration and Layout

2.4.1.7 *Data*

All instruments described in Section 2.4.1.6 generate scientific data that needs to be stored and returned to Earth. Engineering data is also collected and returned. A bounding estimate is given for the present rover configuration, as conceived. Assuming a more aggressive use of the rover instruments relative to MER and by replacing the Mossbauer spectroscope with a Raman spectroscope, the rover would be expected to collect, on average, between 50 to 100 Mbits of data per sol (Spirit and Opportunity each generated and collected up to 50 Mbits of data per sol). The actual data accumulation rate would be driven by the science needs. For example, taking high-resolution stereoscopic Pancam images or using the microscopic imager would result in raw data up 12.5 Mbits per image. All collected data would be stored on a 256 MByte flash memory card. If required, this storage capacity could be increased without significant impact on the rover design.

It is concluded that, with the availability of high uplink data rate to the planned Mars Telecom Orbiter (MTO), significantly more data could be collected and relayed to Earth than the specified 50 to 100 Mbits per sol, allowing for increased operational flexibility throughout the mission.

2.4.1.8 *Communications*

The rover would generate a significant amount of data (scientific and engineering) that would need to be transferred back to Earth. The telecom design for the rover is similar to that used on MER. Communication between the rover and Earth would rely on the Mars Telecom Orbiter, which is assumed to arrive at Mars before the rover's arrival. MTO is planned to orbit Mars at an altitude of 4450 km with a 13.5° inclination. The rover would also utilize the Mars Global Surveyor, and/or the Mars Odyssey, and potentially any other orbiting assets available at the time of the mission.

The rover would use X-band and UHF electronics. Antennas would include a 0.28-m X-band high gain antenna (HGA), an X-band low gain antenna (LGA), and a UHF monopole antenna. This configuration is identical to the MER design, except MER's CE 505 UHF transceiver would be replaced with the new ElectraLite transceiver.

The rover would transmit up to MTO in the X-band at a rate of ~1 Mbits/s. The UHF downlink from MTO to the rover would be available at a rate of 8 kbits/s. From MTO, the rover data would be sent to the Deep Space Network (DSN) in X-band at 400 kbits/s or Ka-band at 500 kbits/s. Direct to Earth (DTE) communication from the rover is available from the rover's X-band HGA to the 34-m DSN antenna at a rate of 1 kbits/s. The uplink from DSN (34-m) to the rover's X-band HGA could reach a maximum data rate of 2 kbits/s.

The multiple orbital assets around Mars and the capability of DTE communication would provide a well-supported mission environment for the rover to transfer all collected science and engineering data to Earth.

2.4.1.9 *Thermal*

Radioisotope power systems generate continuous heat through radioactive decay of $Pu^{238,}$ which has an 87.75-year atomic half-life. The amount of generated heat only reduces by ~0.8% per year, making Pu^{238} a good candidate for powering long duration missions [9].

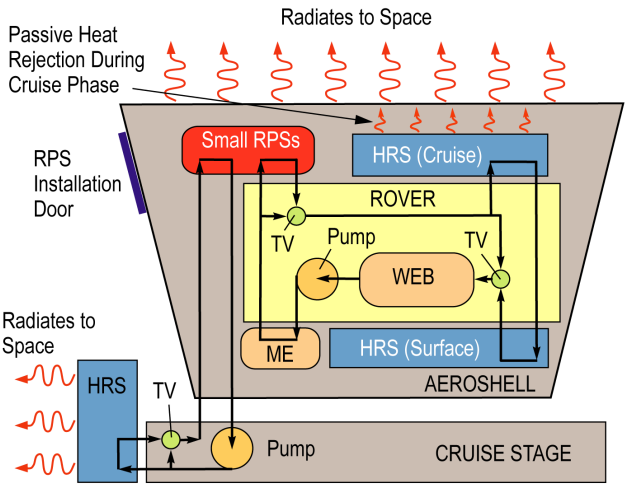

Figure 2.4.1-8. Thermal Design Concept for an RPS-enabled Mars Rover

Throughout all mission phases, including RPS integration with the spacecraft, launch, cruise, EDL and surface operation, the waste heat must be removed from the power source. Two GPHS modules generate ~500 Wt of thermal power at BOL. For the present design concept, fluid thermal loops would be used for both the cruise and surface operation phases. During cruise phase, heat would be generated by electrical systems (CPU, avionics, etc.) in the warm electronics box (WEB) that must be removed to prevent overheating (Fig. 2.4.1-8). Thermal valves (TV) would direct the coolant from the WEB to the heat rejection system (HRS) at a flow rate of 0.5 l/min, driven by a 5-W pump. From there, the heat would be rejected to the aeroshell and then radiated to space. An additional loop would remove heat through the cruise stage to radiators, rejecting the remaining waste heat into space. Before EDL, the aeroshell would separate from the cruise stage and disconnect the fluid loop from the aeroshell. For the short EDL phase, the heat generated by the RPS is absorbed by the aeroshell. A successful landing initiates the surface operation phase, during which heat would be removed by the rover's HRS, consisting of two fluid

loops connected to radiators and routed through the WEB. Thermal control valves inside the rover WEB, along with aerogel thermal insulation, maintain the internal temperature within a set range. This thermal control would help minimize thermal cycling of critical rover subsystems during the diurnal period, thereby increasing the mission lifetime. A primary loop would service equipment both inside and outside of the rover's thermal enclosure. Fluid lines, installed external to the thermal enclosure, provide thermal management to the mobility electronics (ME). The backup loop would service only the equipment inside the WEB and has no lines external to the thermal enclosure. Heat exchangers outside the rover could be sized to remove waste heat during daytime, when the WEB does not require heating. This thermal design is similar to that suggested for the Mars Science Laboratory (MSL). Other heat rejection systems can also be considered, for example removing excess heat from the RPSs with heatpipes (Section 2.4.2.9) [19].

2.4.1.10 *Mobility*

Figure 2.4.1-9. Sojourner and the Rock Named Yogi

Two important mobility requirements are addressed in this section, namely traversing and hazard/obstacle avoidance. It has been shown in previous and current landed missions [20] that the Martian terrain varies significantly with location. Experience from the Mars Pathfinder mission showed that landing site determination is important relative to the size of the rover. The highest resolution Mars orbital cameras provide only 1.5-m/pixel resolution. The Sojourner Rover, with a length of 0.6 m, had to land in an area where rock size, distribution and abundance would not significantly affect its operation [25]. Figure 2.4.1-9 shows Sojourner in-situ, illustrating the relationship between rover size and environment [20]. Similarly, boulder fields at Olympus Mons Caldera include terrains with 12-m diameter rocks. Such fields with over 20% rock abundance might be difficult or even impossible to traverse using any of the conceived rovers. Other areas such as the Gusev Crater and the Meridiani Planum presented a suitable environment in comparison to the size of MER.

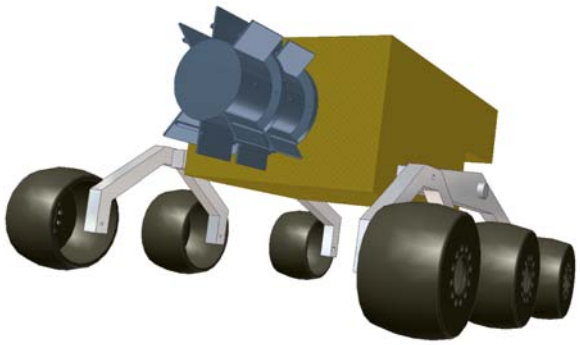

Figure 2.4.1-10. Design Concept View of the Mars Rover Wheels and the RPSs

The present design concept uses MER heritage for mobility. The diameter of each of the 6 wheels is 25 cm (Fig. 2.4.1-10), identical to those on MER. Larger wheels can assist with negotiating tougher terrains, but require more torque and, consequently, larger wheel actuators. In fact, the cascade effect from an enlarged wheel size can result in a significantly greater total mass.

The terrain also influences rover traversability and associated power requirements. Driving on rocky, sandy or hilly topography requires more power than driving on flat hard surfaces. To account for these diverse conditions, the traversing analysis for this rover concept divided driving into a number of operating modes, such as complex or normal driving. These modes are further explained in Section 2.4.1.11 dealing with power requirements. MER-class rovers are capable of traversing at speeds ~35 to 72 m/hr depending on the terrain. A solar powered rover can nominally cover distances up to a few kilometers due to its limited mission duration. In comparison, the small-RPS-enabled rover could traverse distances up to 20–25 km over its nominal lifetime—assuming 2 drive-days per week, 1 hour drive per day, and 3 years of operation on the surface. It can be concluded that small-RPS enabled rovers could potentially cover an order of

magnitude more terrain than solar powered rovers, due primarily to the significantly longer mission time. This allows more opportunity for traversing, exploration, and data collection than a solar powered equivalent.

2.4.1.11 *Power*

This section describes power-sizing considerations, including power allocation to science instruments and assumed activity modes. Being a MER derivative, the power requirements for this rover concept are similar to that of MER, where the solar panels generate 900 W-hr/sol energy at BOL, and 600 W-hr/sol at EOM. For a successful substitution of the power source, the RPSs on the rover should provide as much energy as similarly sized solar panels. Thus, for this design concept, the RPS-enabled rover would require a minimum of two GPHS modules, supplying a total of 620 W-hr/sol, based on continuous power generation of 25 We at BOL. Figure 2.4.1-10 shows the position of the two RPSs at the back of the rover.

On solar powered rovers, high load activities are performed around Martian noon to maximize the use of the peak solar flux. Since the peak power from the two RPSs would be lower than that of the solar variant, a hybrid power system would be used. This system would combine two small-RPSs and two 8 Ah 28 V Li-Ion batteries to obtain MER-type capability. The total energy stored in the fully charged batteries would be 448 W-hr.

Table 2.4.1-1. Mars Rover Instrument Power Requirements

Instrument	Power (W)
Remote sensing instruments	
Pancam on mast	4.3
Mini-TES	5.6
Contact instruments	
Microscopic Imager	2.1
Raman Spectroscope	18
APXS	0.7
Support Instrument	
Rock Abrasion Tool (RAT)	11
Support Equipment	
Hazcam/Navcam (Context)	5
Mast Actuator	0.1

The power system is sized by assessing the power requirements for typical activity days, based on instrumentation, operating procedures and assumed measurement sequences. The power requirements for the proposed rover's instruments are given in Table 2.4.1-1. Additional systems that require power include command and data handling, power distribution, attitude determination and control (for mobility), and telecommunications.

Five distinct activity modes are identified within the power analysis, with each representing a single activity day. The *Panorama Mode* defines the use of the panoramic camera (~11 W-hr). The *Mini-TES Mode* represents the use of the Mini-Thermal Emission Spectrometer (~40 W-hr). Three drive modes are considered. During *Simple Drive* (low impact) the terrain is characterized by low hazard levels and low rock abundance (~85 W-hr). During *Complex Drive* the terrain has large rocks, deep sand or steeper hills drawing higher power than simple drive (~125 W-hr). *Approach Drive* precedes the use of contact instruments and is characterized by slow motion over short (<10 m) distances while drawing ~100 W-hr of energy. *Contact Measurement* activities with the microscope or Raman use ~40 W-hr. When using the RAT, the energy requirement for this mode of operation increases to ~55 W-hr. The last activity is defined as a *Charge Day*, which usually follows a high-energy activity day to recharge the depleted batteries.

In addition to the energy requirements for any of these activity days, a housekeeping overhead and two 80 W-hr telecom loads are also added. Detailed analysis of the activities indicated that the highest power usage occurs during complex drive days, and the highest operating modes are mobility and telecom. For these operations, batteries would complement RPS power. Assuming 1 hour of intense drive and two one-hour telecom windows, the battery charge would end in a power negative mode, which means that the charge level at the end of sol is below that at start. This can be resolved by following on with a charge day. Continuous driving represents the bounding case for traversing, when the system would use all of the RPS-generated power and simultaneously draw power from the batteries. Driving could be made more efficient by either increasing the battery size (impacting rover mass and size) or by changing from continuous drive to stop-and-go operation, where after a short drive the rover would stop, charge back the batteries and then go again.

In summary, the power analysis indicates that two GPHS modules would provide enough power and energy to enable a MER-class rover design, with a similar instrument complement and power profile, including a 30% margin.

2.4.1.12 *Mass*

As conceived, the spacecraft, including the rover, would be launched to Mars with a positive C_3 on a Type II trajectory. The rover mass would be 181 kg, but the launch mass would differ depending on the landing approach. For an airbag landing, the launch mass is 1070 kg and the final landed mass (rover, landing platform and airbags) is 410 kg. Using a powered lander the launch mass is 1620 kg, and the landed mass is 700 kg. The higher landed mass is attributed to the powered descent stage.

A breakdown of the rover's proposed mass allocation is shown in Table 2.4.1-2, detailing both the instrument mass and the support system mass allocation. The rover would carry 9.5 kg of payload. The support system would include components for telecommunication, attitude control, thermal management, power, mechanical and avionics. Telecom covers electronics and antennas. The thermal system accounts for the heat rejection system (radiators), thermal valves, pipes and pumps. The power system would include the small-RPSs (12 kg), batteries (7.5 kg) and power electronics. Avionics accounts for electronics and interface boards to the various systems and sub-systems. The largest mass would be assigned to the mechanical components, including the rover's body (with thermal insulation), the drive mechanisms, drive train, and wheels.

Table 2.4.1-2. Mars Rover Mass Allocation

Instrument	Mass (kg)
Remote sensing instruments	
Pancam on mast	0.7
Mini-TES	2.7
Contact instruments	
Microscopic Imager	0.3
Raman Spectroscope	2.5
APXS	0.5
Support Instrument	
Rock Abrasion Tool (RAT)	0.9
Calibration Target; Magnets etc.	1.9
Total Instrument Mass	**9.5**
Rover Support Systems	
Telecom	16.6
ACS	2.6
Thermal	2.7
Power	23
Mechanical	97
Avionics	30
Total Rover System with Instruments	**181.4**

The dimensions, instrumentation and total mass of this rover concept are comparable to that of MER.

2.4.1.13 *Radiation*

Electronic components are affected by radiation and can tolerate ionizing radiation doses only up to a certain limit. Space based instruments counteract the damaging effects by using radiation hardened components. Today's state-of-the-art radiation hardened electronics can tolerate doses up to 300–500 krad and there are discussions about increasing this tolerance in the near future to as high as 1 Mrad. For RPS-enabled missions, ionizing radiation is attributed to natural (cosmic) radiation sources and to radiation from radioisotope decay of the Pu^{238} fuel. Decay radiation primarily consists of alpha particles, which are essentially helium nuclei. These high mass particles can be blocked easily even with a sheet of paper. However, a small amount of secondary radiation is also present in the form of gamma rays and neutrons. Neutron shielding would not be effective with the available wall thicknesses for this rover concept. Hence it is necessary to address the impact of the above-mentioned ionizing radiation environment on the mission hardware.

The two small-RPSs considered in the present design concept would be installed at the back of the rover. Two configurations are considered—side-by-side and back-to-back (Fig. 2.4.1-11). The radiation environment was scaled from preliminary data for a single GPHS module [16], and presented in Figure 2.4.1-11 for both studied configurations. The calculated total ionizing dose (TID) radiation levels are based on a generic mission with a conservative 1-year cruise phase and 3 years of surface operation. It is found that the radiation dose for the back-to-back configuration is marginally higher. For this case, natural radiation accounts for 1.43 krad during cruise, and 0.52 krad on the surface. The total radiation dose, including the RPSs, is 16 krad, as calculated at the

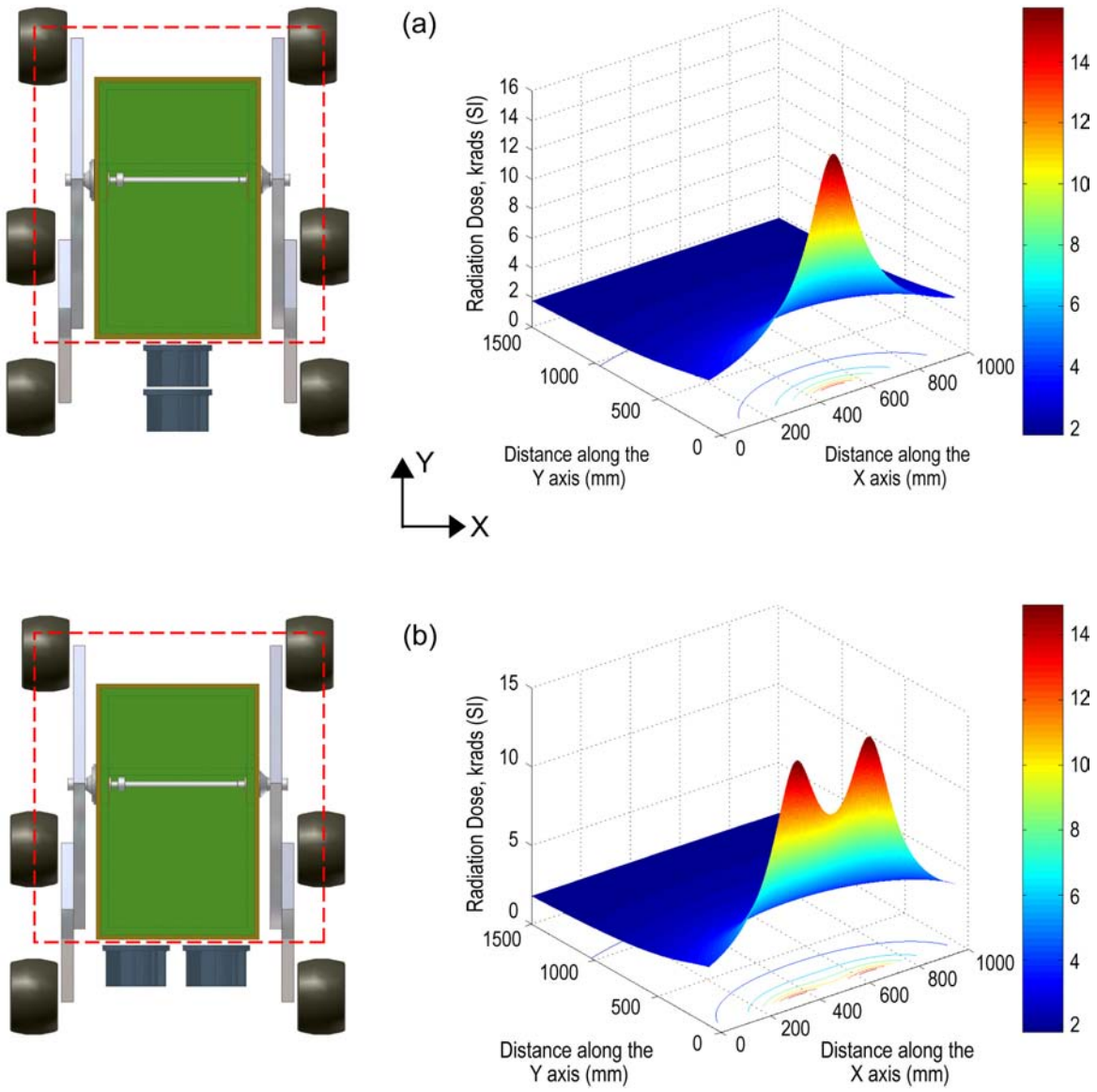

Figure 2.4.1-11. Radiation environment for two RPS mission concept configurations of the Mars Rover: (a) end-to-end configuration and (b) side-by-side configuration; dotted line represents area in radiation plots.

location of the RPS. However, due to distance and radiation shielding by the structure, the internal radiation dose within the rover is ~2 krad. The results are similar for a side-by-side configuration, where the maximum radiation dose is ~14.5 krad at the location of the RPSs.

As a result, it is concluded that radiation would not present any difficulties for MER-type instruments designed to tolerate at least 150 krad (i.e., 300 krad with a radiation design factor of 2).

2.4.1.14 *Alternate RPS Power System*

For an alternate concept, segmented PbTe–TAGS/BiTe multicouples could be used in a CPA configuration, replacing the PbTe–TAGS thermoelectric converters. The CPA arrangement could provide greater structural support during acceleration loading (e.g., landing or roving) than the larger unicouples. This configuration could potentially increase the TE conversion efficiency from the conservatively assumed 5% to 9-9.7% in the future [24]. Beside static conversion technologies, dynamic power conversion can also be considered. A Stirling system would require less radioisotropic material, while achieving higher power conversion efficiency. This technology, however, has

not been tested; thus its acceleration load tolerance and lifetime must be demonstrated before use in future space missions.

2.4.1.15 *Mars Rover Summary and Conclusions*

The study described here demonstrates the feasibility of a MER-class rover using two small-RPSs. Each of the power systems would utilize a single GPHS module, generating 12.5 We of power (BOL). Since RPSs operate continuously, the 25 We power from the two GPHS modules could produce up to 620 W-hr of energy per sol. Assuming 3 years of surface operation and a 1-year cruise phase, the power would drop by the end of the mission to 23.4 We (corresponding to 580 W-hr/sol), due to degradation of the fuel and the thermoelectric converter. This is the same magnitude of energy per sol as that for MER. However, the RPS-enabled rover would have a lifetime potentially much greater than the nominal MER mission.

The rover's power system would be sized to handle peak power demands and to maintain a positive energy balance, based on typical daily surface activities. The highest power usage would be contributed to mobility and telecom for this configuration. To perform these activities, a hybrid power system was adopted for this concept using the combination of RPSs and batteries. RPS-enabled rovers could surpass solar powered systems in mission duration, location accessibility, and mobility over lifetime. Besides rejecting the excess heat generated by radioisotope decay, a portion of it could be utilized by routing through the rover's warm electronic box, controlled by thermal valves. This would provide further advantages for RPS-enabled systems even at locations where solar power is feasible, due to tighter temperature control with waste heat utilization. It is also found that radiation from the RPSs would not present problems to the rover's electronics and instruments.

While this point design focuses on a rover with two small-RPSs, the conclusions are applicable to other scaled up rovers as well. Therefore, a new set of RPS-enabled rover missions can be envisioned for Mars exploration, targeting astrobiology related science objectives and powered by 2 to 4 GPHS modules.

2.4.2 Lunar Rover Mission

This study demonstrates that a conceptual lunar science and exploration mission could be enabled by a small-RPS power source. The goal of the mission would be to explore the floor of a permanently shadowed crater near the north pole of the Moon (Fig. 2.4.2-1) looking for surface and subsurface deposits of water ice. A science payload would be carried on the rover to search for and characterize hydrogen-bearing materials in the crater floor. Both remote and in-situ spectroscopy would be used in the exploration and would be augmented by optical instrument systems that contain illumination sources for imaging in the visible spectrum in this dark crater.

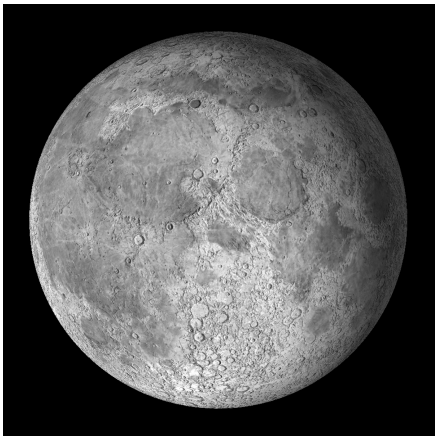

Figure 2.4.2-1. The Moon—Possible Source of Water Ice for Support of a Permanent Human Presence.

Two rover concepts were considered in the studies. The baseline rover would have 4 single-GPHS module RPS systems and is reported herein. A second concept would have 2 GPHS module RPS systems and is only summarized here. Because the Earth would not be visible from the crater floor, an orbiting relay satellite would be used for data return to the Earth.

2.4.2.1 *Lunar Rover Science Goals*

The science goals for this lunar rover are to determine the chemical composition(s) of the hydrogen-bearing materials in the near-surface layers of the polar regions of the Moon, to determine the abundances of those materials, and to describe the geologic context in which they are found.

Evidence of the presence of substantial quantities of hydrogen-bearing materials in lunar polar regions was obtained from the Clementine and Lunar Prospector missions [27, 28]. Theoretical studies suggest that water ice could be present and could be responsible for the observed hydrogen "signal." This is an hypothesis with significant scientific and practical implications; water is one of the most important resources necessary for sustaining a human presence on the surface of the Moon. Because the remote observations cannot tell us whether or not water is in fact present, it is necessary to perform in-situ science measurements to answer this pressing question. Thus the primary science goal for this mission concept is to answer the question of whether or not significant quantities of water ice or water-bearing materials are present in the near-surface layers of the polar regions of the Moon.

The need for a *quantitative* description of the abundance of the hydrogen-bearing materials implies knowledge of the geological context of the areas surveyed. Measurements to determine the depth and thickness of these deposits and their areal extent within the confines of the crater selected for our landing site are required. Obtaining this geological context is a secondary science goal.

Knowledge of the lithologies associated with the "hydrogen deposits" would constrain theories of the origins of those deposits [29]. One hypothesis is that thin water-rich stratigraphic layers might be found, each potentially associated with a single large cometary impact event. Another hypothesis has the hydrogen-bearing deposits originating due to loss of primordial water from the interior. Thicker but more localized deposits should result if this hypothesis is correct. Addressing questions such as these aligns the goals of this mission study with key questions articulated in the Solar System Exploration Decadal Survey [5]. This mission would help in understanding how the processes that shaped the contemporary character of planetary bodies (such as cometary impacts) operate and interact.

The science objectives for the this proposed lunar rover mission concept can be summarized as follows:

- Objective 1 (O1): Determine the composition and the spatial distribution (area, thickness, and depth of the polar hydrogen-bearing deposits).

- Objective 2 (O2): Describe the geologic context of the hydrogen-bearing materials deposits.
  - O2a. Characterize the geomorphology of each sample site.
  - O2b. Determine the composition, texture, structure, and thickness of proximate (adjacent) surface and subsurface deposits (rock and regolith layers).

The science goal of understanding the nature and distribution of lunar polar hydrogen deposits constrains the choice of proposed landing sites. The first criterion is that the selected site must have a strong epithermal neutron scattering signature as determined by orbiting spacecraft [27]. Remarkably, large areas in the lunar polar regions meet this requirement. To maximize the probability of finding water ice deposits, another requirement would be to land within a permanently-shadowed crater. Permanent shadow produces the lowest temperatures and thereby the greatest stability (and longevity) of ice deposits [28].

There are hundreds of craters in both polar regions that are permanently shadowed [29]. Thus, to further restrict the possible choices, additional criteria can be considered. A key feature of lunar water resources will be their proximity to locations that could be selected for permanent outposts. Work by Bussey et al. [30] has identified a number of sites near the lunar north pole that represent ideal locations for human outposts. There are high-standing areas on the north rim of Peary crater that are in permanent sunlight. This would provide a constant source of solar power for a permanent human outpost, together with a relatively benign environment; temperatures there are nearly constant at ~223 ±10 K. (Midday temperatures at the lunar equator approach 400 K, falling to ~120 K during the night). In addition, the north pole is an excellent location for astronomical observatories.

Two permanently-shadowed craters are found along the north rim of the Peary crater system, in proximity to the permanently-sunlit highlands. The larger of these, with a diameter of 12 km, is designated "Peary B." Its center is at approximately 89.3° N, 105° E. The floor of this crater has an area > 100 km^2. This crater has been chosen as the preferred landing site for this study because of its potential importance as a source of water for future installations located on the permanently-sunlit highlands nearby. Typical depths (measured from the rim) for 12-km-deep craters on the Moon are on the order of 2.4 km [31]. However, the Peary complex is recognized to have a subdued, presumably ancient topography, and its depth is considerably less than this; even though its diameter is ~50 km [32]. Thus, the depth of Peary B is unlikely to exceed 2.4 km, and is probably significantly less than this.

Once landed in the crater bottom, the Earth would never be in view. Thus, a telemetry relay capability [33] must be provided by an orbiting relay satellite system (which is assumed to be in place prior to this mission).

2.4.2.2 *Proposed Lunar Rover Mission Goals*

The lunar rover mission goal is to land within a permanently-shadowed crater near the lunar north pole and to perform in-situ geological investigations of the crater during the rover's expected lifetime of 4 years.

2.4.2.3 *Mission Architecture Overview*

This mission would employ previously flown systems to reduce cost and development schedule issues. Thus, a landed system consisting of a modified MER [34] and a modified Phoenix [35] lander would be mated with a large propulsion module to accomplish the landed mission.

The flight system could be launched using a "heavy" class vehicle (e.g. Atlas 511) on a trajectory to the Moon allowing a direct lunar descent to the crater floor. The delivery system would include the propulsion module to slow the vehicle during the approach to the Moon. A terminal deceleration capability in the lander would provide the final velocity reduction and hazard avoidance during the touchdown phase. The rover would then be deployed from the lander for its surface exploration objectives.

The mission has been designed to land in a potentially hazardous region inside the permanently shaded crater. The Phoenix lander would be modified to allow a landing in an unknown topography in the crater bottom. A hazard avoidance system [36] was proposed for Phoenix using a Laser Detection and Ranging (LADAR) system. This will be required to provide active illumination of the scene on the dark crater floor.

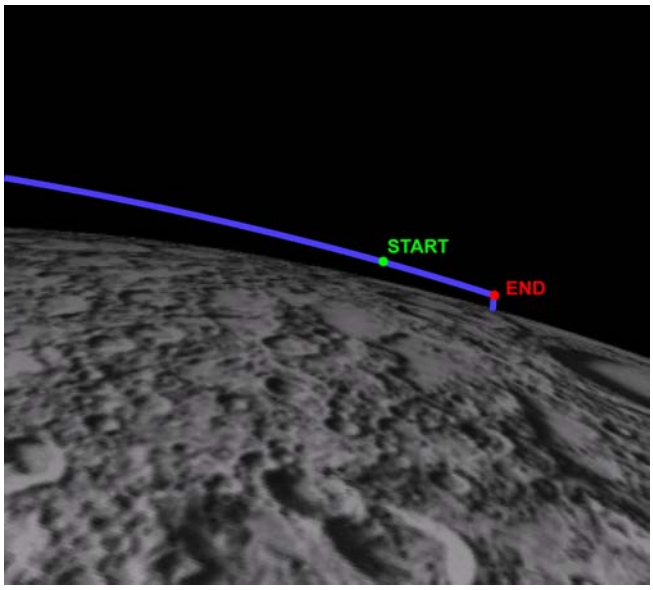

Figure 2.4.2-2. Lunar Rover Descent Trajectory

The approach, descent, and landing trajectory design for the lunar rover mission would use a large approach burn (LAB) of about 2.5 km/s as the first deceleration maneuver near the Moon, followed by a smaller propulsive maneuver phase to establish the final descent trajectory as shown in Figure 2.4.2-2. The figure illustrates the abrupt change in the vehicle's direction as a result of the LAB burn. The burn would basically cancel the forward velocity of the vehicle allowing it to enter a freefall from an altitude of ~10 km. The lander propulsion system would then be used to perform a soft landing. Analysis has shown that the major axis of the landing error ellipse would be less than 1.8 km (3σ). Thus, the floor of the Peary B crater (diameter = 12 km) would be easily targeted within the orbit determination accuracy. The events from approach to landing are given in Table 2.4.2-1, including the duration of the event and the magnitude of the ΔV required for maneuvers. The LAB maneuver would be augmented by the propulsion system on the Phoenix lander, which would also include a hazard avoidance system. The Phoenix avionics would control the transit and descent phases of the mission.

Table 2.4.2-1. Mission Events for the Proposed Lunar Rover Descent Phase (from [34])

Event	Duration (s)	Delta V (m/s)(3σ)	Source Vehicle	Comments
Cruise TCMs	10	30	Lander	Phoenix System
Large Approach Burn (LAB)	80	~2500	Propulsion Module	Star 48V Propulsion Module
Post Burn Coast	6	—	Propulsion Module	Ends with Prop Mod separation
LAB Velocity Clean-up	30	25	Lander	Phoenix System
LAB Position Clean-up	30	28	Lander	Phoenix System
Final Descent Burn	30	170	Lander	Phoenix System
Hazard Avoidance Maneuvers	20	10	Lander	Phoenix System
Totals				
Propulsion Module		2500		
Lander		263		Phoenix Capability = 300 m/s

Because no previous observations exist of the Peary B crater floor, the landing hazards within the crater are basically unknown. Thus, it seems prudent to baseline a hazard avoidance capability for the final touchdown phase. Without light in the crater, the observations for hazard avoidance must use active illumination from the lander. Research in Laser Detection and Ranging (LADAR) and Autonomous Target Recognition (ATR) has been underway for many years [36]. Using this laser imaging system, observations begin at an altitude of about 1500 m and can identify a landing region of 20 m in diameter with obstacles less than 35 cm in diameter. During the LADAR operations, the scene images will be recorded and transmitted in real time to the Earth to identify for the first time the characteristics of the landing site on the crater floor.

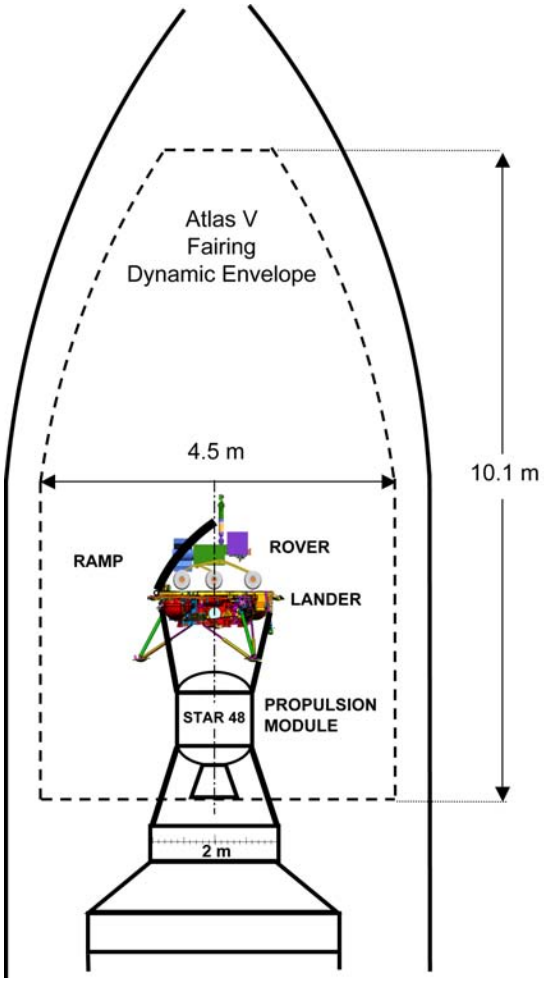

Figure 2.4.2-3. Proposed Lunar Rover Launch Configuration

The baseline rover concept for this study is derived from the MER design to maximize flight heritage and decrease development risk and cost. Changes to the MER configuration would include RPS power provided by four GPHS-class heat sources using thermoelectric conversion, and enhanced elements of the rover to increase its design lifetime to 4 years. In addition, the Mars surface scientific instruments would be changed to accommodate a payload more relevant to searching for water and to perform lunar surface science. For example, the Mossbauer Spectrometer would be replaced by a Laser Raman Spectroscope. The rover power system would include both the RPS sources as well as rechargeable batteries (see 2.4.2.11) for operations requiring peak power levels beyond what the RPS sources can provide (e.g., mobility, data return, and surface penetration activities).

Figure 2.4.2-3 illustrates the launch configuration showing the propulsion module and the modified Phoenix lander with the baseline rover located on the lander deck. No appendage deployment (such as lander legs, rover mast, or rover suspension) would be necessary allowing easier accommodation and more volume available on the lander deck. As shown in the figure, the large Atlas fairing would allow the Phoenix lander legs to be fully deployed before launch (unlike the restricted volume of the Phoenix Mars aeroshell). Also, the rover could be standing at launch (as shown) so that the suspension does not have to be stowed as in the MER mission.

The deployed baseline rover concept is illustrated in Figures 2.4.2-4 and 2.4.2-5. The first figure shows the deployed rover as it would appear on the crater floor. A ramp system, shown schematically in Figure 2.4.2-3, would be used to drive the rover from the deck to the surface. The vertical mast is shown that houses the panoramic and navigation cameras. For the lunar rover application, dual strobe lights would be added to the mast for camera operations in the darkness of the crater floor (Section 2.4.2.10). Also, the bare upper deck (where the MER solar arrays were located) suggests more external surfaces available for payload accommodation and thermal radiators. Note

Figure 2.4.2-4. Lunar Rover in its Fully Deployed Configuration

also that the RPS power sources would be mounted on the "rear" of the rover to allow a maximum distance between the RPS and the instruments mounted on the front of the rover. Because of the delicate balance required by the rocker-bogie suspension system, this would allow the science payload in the front of the lunar rover to be heavier than the MER payload; retaining this balance requirement. This balance relationship can be seen more clearly in Figure 2.4.2-5 that illustrates the rover top view (with the top plate removed) showing the instrument electronics bay in the forward part of the WEB of the rover. The aft bay or Rover Electronics Module (REM) would contain the avionics (mobility guidance subsystem, telecom subsystem, etc.) and would remain virtually unchanged from the MER system configuration. The power system elements would be located behind the avionics bay.

The proposed network architecture of the flight vehicle is shown in Figure 2.4.2-6 and is intended to visualize primarily the power as well as telemetry and command (TLM/CMD) relationships for each of the vehicle systems. The propulsion module would derive its power during cruise from a solar array, which would also maintain the battery charging, through the power bus, of the Li-Ion batteries on the lander (and the rover). The propulsion module would have no telecommunications capability and would depend on the lander's X-band system for return of its telemetry during the cruise and approach phases. Also, the propulsion module depends on the avionics of the lander to support the vehicle's guidance and control during the LAB maneuver. The gimbaled nozzle on the STAR 48V would be sufficient to control the pitch and yaw force instabilities during the burn but the lander's roll thrusters would be used to control the roll instabilities during the burn. Note that after the separation occurs between the propulsion module and the lander, the only power sources on the lander would be its large Li-Ion batteries (that are in the existing Phoenix lander), which would provide sufficient power for the propulsion, hazard avoidance and touchdown activities during the descent phase.

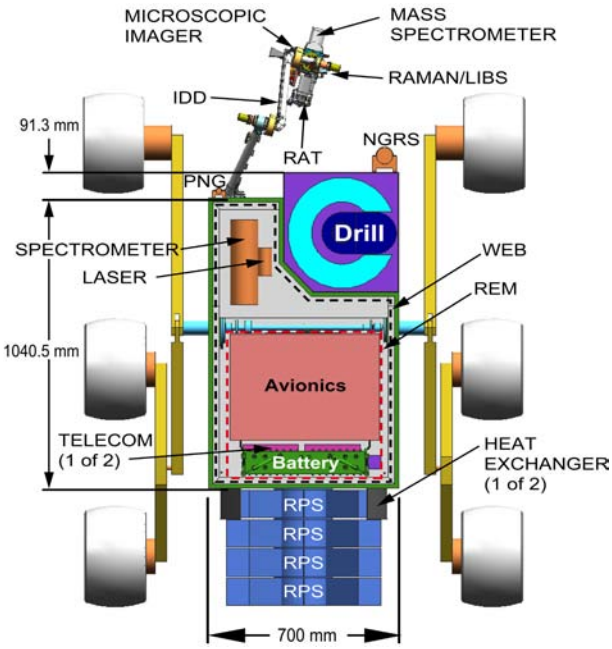

Figure 2.4.2-5. Baseline Lunar Rover—Top View

The lander would maintain an X-band telecommunications link to the Earth at the beginning of the descent phase while the rover's Ultra High Frequency (UHF) link would be communicating with the lunar orbiter (LO) overhead. Once the lander passed below the Moon's horizon as seen from Earth (the crater rim), the only link to Earth would be through the lunar orbiter overhead via the Rover's UHF link. Following the landing, the power bus and the TLM/CMD network between

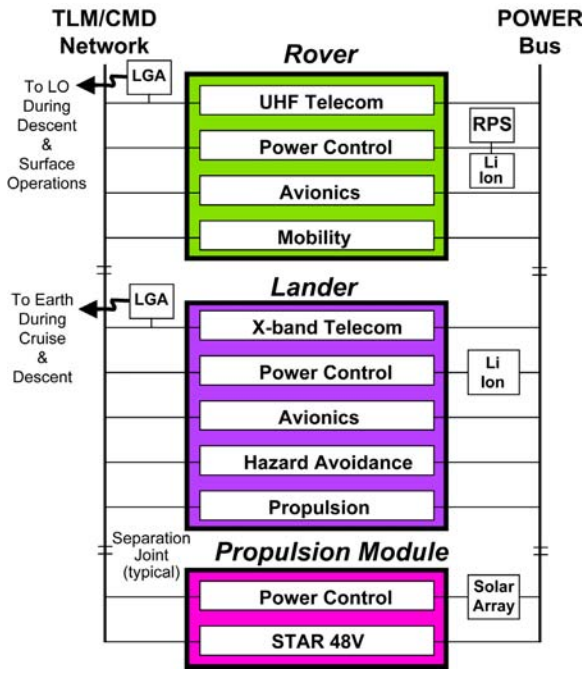

Figure 2.4.2-6. Proposed Lunar Rover Flight System Architecture

the lander and the rover would be separated. The spacecraft network and power bus would require sophisticated control software to assure that these data and power transitions would occur in an orderly way as the systems are reconfigured. Power for each phase of the mission would be provided by different sources for each configuration. The cruise configuration would have its own solar array in operation from the Earth until the propulsion module separation. The lander batteries would provide power during the descent phase. The rover would be powered by its RPS sources augmented by the rechargeable batteries that would be used for its surface operations during peak power operations.

2.4.2.4 *Lunar Rover Power Source Trade Study*

The destination of the rover is a lunar crater floor that is permanently in darkness. Thus, solar power is not an option. In addition, batteries with sufficient energy to be the sole source of rover power for the duration of the mission would be prohibitively large. It is therefore clear that an RPS power source is truly enabling for this unique mission.

2.4.2.5 *Small-RPS Characteristics*

The baseline rover concept uses four GPHS-based RPSs (shown in Fig. 2.4.2-7), each with PbTe-TAGS unicouples arranged with a geometry similar to those in the MMRTG. Assuming a 5% efficient system, the 50-We BOL system would have ~46.88 We of power after 4 years.

In addition to being the primary power source for the lunar rover mission, the RPS would also act as a heat source to maintain operating temperatures in the lunar rover components. The loop heat pipe design for the thermal control system (Section 2.4.2.9) would rely on the RPS as the heat source for the working fluid. A preliminary design concept for the evaporator end of the loop heat pipe is shown in the figure and consists of cylindrical shells around the hot fins of the RPS. The fluid would circulate through the shells to raise its temperature for heat dissipation within the loop heat pipe of the rover elements. The shell design would minimally restrict the thermal radiation from the fins, thereby allowing the RPS to function efficiently as a power source.

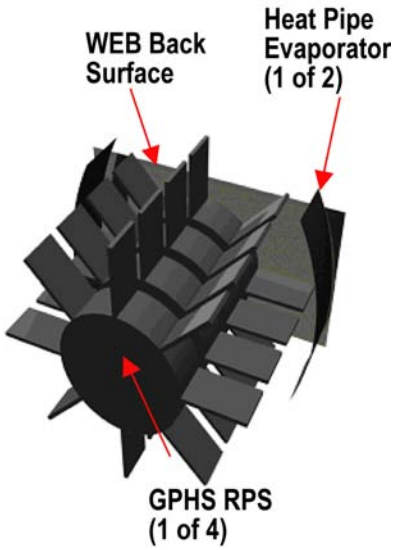

Figure 2.4.2-7. Conceptual Lunar Rover RPS Configuration

2.4.2.6 *Science Instruments*

The lunar rover would carry eight science instruments. Together these would provide a highly reliable and complete description of the materials sampled to meet the objectives of the mission (Table 2.4.2-2).

The Pancam and microscopic imager (MI) instruments would return panoramic and microscopic images to characterize the geomorphology and geologic structures and features of the areas sampled. If surface deposits of water frosts or ices are present, these instruments would identify and describe them. These address the goal of describing the geologic context of the materials of interest.

Table 2.4.2-2. Lunar Rover Science Instruments and Science Objectives

Instrument	Observation	Science Objectives
Pancam	Panoramic Images	O2, O2a
Coring Drill	1-m penetration for core	O1, O2, O2b
GPR	RF Sounder	O1, O2, O2b
GRNS	Emissions from H_2 bearing species	O1, O2, O2b
Microscopic Imager	Mineralogical images	O2, O2b
LIBS-Raman Spectroscope	Elemental & Mineralogical composition	O1, O2, O2b
TOF-MS	Elemental & Isotopic Composition	O1, O2, O2b
NIR/VIS	Mineralogical Composition	O1, O2, O2b

The ground penetrating radar (GPR), the Gamma Ray/Neutron Spectrometer (GRNS), and the 1-m drill each would access or characterize the subsurface. The GRNS is the primary science instrument for detecting hydrogen-bearing deposits within the upper meter or so. However this instrument cannot resolve the subsurface thickness of layers; the GPR is employed for that task. Surveys made with these instruments can characterize the spatial extent and geologic context of the hydrogen-bearing materials, but cannot reliably determine their composition. The 1-m drill would be employed to retrieve core samples from promising layers beneath the surface, for direct analysis by the other instruments.

The lunar rover would carry five different instruments for determining the composition of samples obtained. Each of these has certain strengths and weaknesses, but together they would provide a tightly constrained description of the chemical makeup of the samples analyzed. Elemental compositions are measured by 3 instruments, the LIBS/Raman, the Time-of-Flight Mass Spectrometer (TOF-MS), and the GRNS. The GRNS would provide bulk measurements within a volume of perhaps a meter cubed. The LIBS and the TOF-MS would employ laser energy to disrupt target materials, but use different physical phenomena (plasma emission versus ion travel time) to characterize the compositions in complementary ways. The Raman spectroscope would nondestructively excite the molecular structure of samples, and provides information on mineralogy rather than elemental composition. The Pancam with its multispectral filters and the Near-IR/VIS instrument both would provide information on compositions of samples based on absorption and reflectance as a function of wavelength.

Working together, these instruments would be able to unequivocally answer the key question of the presence or absence of water ice in subsurface layers of the permanently shadowed polar craters of the Moon.

The mass and power of each instrument on the rover is presented in Table 2.4.2-3. Also given in the table is the duration of a typical observation or operation for that instrument and the data volume that would be produced.

Table 2.4.2-3. Lunar Rover Science Instruments and Observational Requirements

Instrument	Mass (kg)	Power (W)	Ops/Obs Time (s)	Data (Mb)
Pancam	0.7	6	720	215
Coring Drill	20	<35	10800	0.1
GPR	1.5	5	60	0.016
GRNS	6.5	19	<300	0.1
Microscopic Imager	0.7	5	<4	3
LIBS-Raman Spectroscope	2.5	3	3600	1
TOF-MS	3	5	10	4
NIR/VIS	3.6	12	180	20

2.4.2.7 *Data*

The large memory storage capacity of the lunar rover (~2 Gbits) and data return capability through the lunar orbiter relay would allow a very intense data acquisition sequence while returning all of the data collected every 12 hours. For example, the most stressing data day would include a core sample obtained with the drill. That core would be analyzed with the microscopic imager and the LIBS/Raman spectroscope. The total data from this day would be: 100 Mbits for the microscopic imager (3 Mbits per picture, ~32 pictures consisting of 8 pictures using 4 dif-

ferent filters and different magnifications) and ~100 kbits for the LIBS/Raman. This does not include the engineering data overhead. These data could easily be returned daily assuming 520 Mbits per day playback from the orbiter. The data return link from the rover to the lunar orbiter (8 kbits/s) and lunar orbiter tracking duration allows over ~520 Mbits/day (See Section 2.4.2.8). Another large data activity would be the 12 Pancam images (215 Mbits total) that would be taken periodically. Those images would be returned to Earth every 12 hours.

2.4.2.8 *Telecommunications*

A fundamental architectural requirement for this mission would be the need for a supporting lunar communications orbiter for the surface operations. Because of the depth of the crater floor, view of the Earth would be virtually impossible. Thus, for any data return a relay link telecommunications architecture would be required. Recent studies at JPL [33] identified a Molniya-type elliptical polar orbiter about the Moon (shown in Fig. 2.4.2-8) that could provide nearly continuous relay link telemetry from inside the crater. The orbiter would have a highly elliptical orbit with a period of 12 hours allowing rover-to-orbiter contact over 75% of the time or 9 hours per orbit. There would be two "uplink" sessions per day from the rover to the orbiter. The apolune altitude of the orbit would be 8700 km and the rover could transmit a telemetry rate of 8 kbits/s at this most distant range. Thus, the uplink would have a daily telemetry return capability of about 520 Mbits. It is assumed that the lunar orbiter would have an X-band downlink capability to the 34-m DSN network of about 0.8 Mbits/s using a 5-W (RF) power amplifier and a LGA on the orbiter. The lunar orbiter would use a store and forward mode of operation. With the relatively low data volume from the lunar surface, the data could be relayed from the lunar orbiter to the Earth in about 5 minutes.

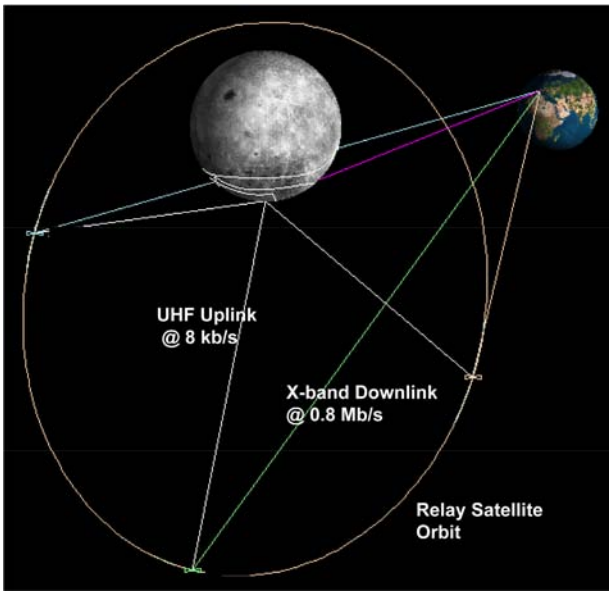

Figure 2.4.2-8. Lunar Rover Telemetry Return Path

The rover communications system would consist of a redundant radio system at UHF frequency utilizing a system such as the ElectraLite transceiver [34]. With a 10-W power amplifier, it would have an uplink telemetry rate to an lunar orbiter of greater the 8 kbits/s through a low gain monopole (whip) antenna on the rover.

2.4.2.9 *Thermal*

The thermal environment of the Moon is extremely harsh, and the low surface temperatures (~100 K) represent a significant challenge unlike that seen on any previous rover mission. As the nominal operating region (Peary B crater) is permanently shadowed, the primary heat loss mechanisms would be conduction to the lunar surface via contact with the rover wheels, and through radiation to space (T~4 K) and the lunar surface. To maintain survival and operating temperatures within the rover, a loop heat pipe system would be used to transfer heat from the warm RPS to the critical subsystems and batteries within the rover's WEB. The loop heat pipe would not require a separate fluid pump, which is important from a power and reliability perspective. The heat pipe would rely upon capillary forces within the wick, and a gas pressure gradient between the evaporator and condenser to circulate the working fluid through the rover subsystems [37, 38]. The evaporator-portion of the loop heat pipe would be coupled through thermal radiation to the RPS (Fig. 2.4.2-9) using a heat exchanger system similar to that proposed for MSL. This concept would not require any additional connections to the RPS system (other than structural and electrical power), and would be designed to accept four single-GPHS RPSs without requiring a redesigned RPS interface. The WEB would be insulated to minimize internal radiative heat losses, and

the external rover surfaces covered with multilayer insulation (MLI) to minimize radiative heat losses to the external environment. Active temperature control of the WEB would be critical in order to maximize reliability and rover life, and would be performed using thermal switches, a bypass loop within the loop heat pipe, and external radiators to ensure a finely regulated temperature profile in the constant 100 K temperature environment.

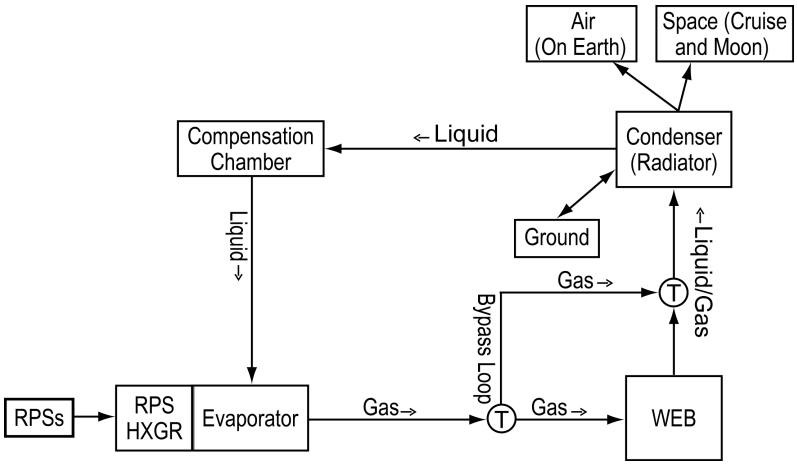

Figure 2.4.2-9. Thermal Management Schematic for the Lunar Rover Concept

Small electric heaters would be required for all external actuators to maintain survival and operating temperatures within the frigid lunar environment. There would be a total of 14 external actuators on the baseline lunar rover: 5 on arm, 3 on the mast (one azimuthal and two pitch) and 6 for the wheels (1 per wheel motor). Each wheel actuator would use a boron epoxy tube (assumed to be 1.5-in long, 0.625-in diameter) in-line with the drive shaft to significantly reduce conduction losses to the ground—this would greatly reduce the required electrical power necessary for the wheel heaters. All actuators would use multilayer insulation (MLI) to minimize radiative heat losses to space and the cold lunar surface. Preliminary analyses indicate that ~0.425 We of heater power would be required to maintain the survival temperature of each actuator. This figure includes radiative and conductive heat losses (as described above), as well conduction through power and data cables attached to each actuator, which could act as heat sinks for the actuator. The total survival heater power for all 14 external actuators is estimated as 5.95 We. For power budgeting purposes, an additional 30% margin is included.

2.4.2.10 *Lunar Rover Mobility*

The baseline lunar rover mobility analysis is similar to that discussed in Section 2.4.1.10 for the Mars rover with the exception that the terrain within the crater floor would be unknown until the rover arrives. Thus, any analysis must assume a worst case scenario, equivalent to the *complex drive* mode, which is defined by large obstacles, deep sand, or steep hills. In addition, the length of an individual traverse would be limited to the range that has been imaged by the rover's lights. Although the Pancam's light range is about 100 m, the Navcam's range would be only 10 m. Thus, it would be prudent to limit a single traverse to <10 m.

One of the key requirements for lunar rover mobility on the dark crater floor would be illumination. A preliminary design concept has been completed and the resulting radiometric calculation parameters are given in Table 2.4.2-4. This set of capabilities would provide approximately 500 electrons of signal in a 5-s integration, which would give a signal-to-noise-ratio of at least 20 with a 20% design margin. Using the commercially available light sources (Luxeon) and the well known Pancam camera capability, this margin would be adequate. To simplify the design calculations, the light source was assumed to be monochromatic.

Because mobility would be an energy limited activity, the combination of RPS power and total battery energy will be considered here and discussed in more detail for all power modes in the next section. Assuming a *complex drive* mode with a traverse length of 10 m, and a traverse duration of 1 hour (in 2, 30-minute increments), the corresponding average speed would be ~10 m/hr. If the rover overhead power is about 76 We and the drive mode takes 124 We for a total of about 200 We, the complex drive traverse consumes 100 W-hr. Power for the two lights would total 10 We (140 lumens) with an exposure duration of 5 s requiring an energy of 0.014 W-hr per event. If the strobe

Table 2.4.2-4. Lunar Rover Illumination System Design Parameters

Parameter	Value
Light source	Luxeon 5-Watt Star, Green: use 2 of these
Source peak wavelength	530 nm
Typical luminous flux from source	120 lumen from each lamp
Source-to-target distance	100 m
Angular size of light beam	45 deg
Target reflectance	0.1
Camera F/# (Pancam)	4.2
Detector pixel size	12 μm
Camera transmittance	0.85
Detector quantum efficiency	0.8 at 530 nm for a focal plane with AR coating optimized for the peak wavelength
Integration time	5 s

were used once for every 10 m traverse (i.e., once per day), then the strobe energy requirement would be negligible compared to the 100 W-hr requirement for the complex drive mode. With the baseline RPS output of 50 We for this 0.5 hr, it provides about 25 W-hr of energy for this mode. Thus, the battery would need to be sized to provide the remaining 75 W-hr of energy (see Section 2.4.2.11).

Another mobility issue unique to the lunar rover mission would be the rover wheel sizing. The MER wheels have a diameter of 25 cm as a compromise between footprint size on the surface and motor torque required. The MER vehicles have experienced some slippage on dusty Martian slopes, but have been capable of recovering from these events. Thus, even if the lunar rover were to encounter a dusty terrain, the larger diameter (35 cm) wheel system should be adequate if we assume that the traction in lunar dust is similar to Martian dust. Without the wind blown effects of Mars, the lunar dust might be more densely packed than on Mars. Also, these wheels can still be used with larger scale obstacles because of the rocker-bogie suspension system that allows a larger effective diameter of the wheels when driving over obstacles. Thus, it is expected that the lunar rover sized wheels and suspension system would be more than adequate for traverses on the crater floor.

2.4.2.11 *Power*

The challenge of the lunar rover mission would be to provide an acceptable science return in a limited energy environment. The science payload has been selected to optimize the science return given the available energy. An energy sequencing simulation tool was used to determine the energy management strategy. The goal of these simulations is to assure a positive energy balance in daily operations that will maintain the charge on the battery for consecutive daily operations. The simulations use an element-by-element power table for each rover activity as shown in Table 2.4.2-5. An operational sequence is then attempted that utilizes a set of power modes by selecting the appropriate modules and their power levels for that mode. The simulation determines the power required as a function of time for these power modes to evaluate if the energy outcome is positive for that operational sequence.

The simulation shown in Table 2.4.2-5 is for the baseline rover with four GPHS RPS sources (50-We total BOL), a 25-Ahr Li-Ion battery and the baseline science payload (see Table 2.4.2-2). Table 2.4.2-5 lists the power for each rover element and the power modes considered for the simulation sequence. Note that a power contingency of 30% applies to all elements. A set of power modes was chosen to consider driving as well as science activities on a single day of operations.

A typical entry is for power sequencing of the Approach/Contact mode is exemplified in the table (see column bounded by a red box). The first activity in this mode is ("ACS_Drive_Approach") that reads (a)1 hr. This character string translates that this is the first activity of the sequence shown by the (a), and that the event lasts for 1 hour. The start time for this event is given in the "Start Times" column: 1000 hours. The Navigation Camera ("Cam_Nav") observations would

Table 2.4.2-5. Lunar Rover Power Loads, Levels, and Operating Modes

Small-RPS-Lunar Rover				Operating Modes [(Order), Total Duration, Breakout Duration]						
Load Names	CBE (W)	Contin-gency	Design (W)	Pan/ Remote	Complex Drive	Easy Drive	Apprch/ Contact	Drill	Battery Charge	Start Times (hr)
CD&H										
CDH_CPU_RAD_750	7.5	0.3	9.75	X	X	X	X	X	X	
CDH_Board_NVM_CAM_+ 2-Gb memory	4.6	0.3	5.98	X	X	X	X	X	X	
CDH_Board_Motor_Control -1_MCB-1	4	0.3	5.2	X	X	X	X	X	X	
CDH_Board_Motor_ Control-2_MCB-2	4	0.3	5.2		X	X	X	X		
CDH_FPGA-SIA	2	03.	2.6	X	X	X	X	X	X	
CDH_Anolog_IO	4	03.	5.2	X	X	X	X	X	X	
CDH_Raman	2.6	0.3	3.38	X						
CDH_Backplane	1.2	0.3	1.56	X	X	X	X	X	X	
Power										
Power_Control_Unit	0	0.3	0	X	X	X	X	X	X	
Power_Distribution_Unit_ PDU	0.56	0.3	0.728	X	X	X	X	X	X	
Battery Control_ BCB	2.8	0.3	3.64	X	X	X	X	X	X	
Rover_Shunt_Limiter_RSL	0.56	0.3	0.728	X	X	X	X	X	X	
ACS										
ACS_Board_IMU_LN200	15	0.3	19.5	X	X	X	X		X	
ACS_Drive_Easy	55	0.3	71.5			(a)2 hr				
ACS_Drive_Approach	65	0.3	84.5				(a)1 hr			1000
ACS_Drive_Complex	80	0.3	104		(a)2 hr, (4×0.5 hr)					
ACS_Wheel_Heater	42	0.3	54.6		(0)0.5 hr, before traverse	(0)0.5 hr, before traverse				
Instruments										
Instruments_Cam_Pan	4.3	0.3	5.59	(a)0.5	(b)0.5	(b)0.5				
Instruments_Cam_Nav	4.3	0.3	5.59		(a)2 hr, (4×0.5 hr)	(a)2 hr, (4×0.5 hr)	(a)1 hr			1000
Instruments_Illuminator	10	0.3	13							1000, 1010, 1020
Instruments_Cam_Haz	4.3	0.3	5.59							
Instruments_Cam_Eng_1	2.15	0.3	2.795							
Instruments_Cam_Eng_2	2.15	0.3	2.795							
Instruments_LIBS_RAMAN	5	0.3	6.5	(b)6 hr, (2×3 hr)			(e)1 hr			1430
Instruments_Radar_GPR	5	0.3	6.5		(a)2 hr, (4×0.5 hr)	(a)2 hr, (4×0.5 hr)				
Instruments_NGRS	19	0.3	24.7		(a)2 hr, (4×0.5 hr)	(a)2 hr, (4×0.5 hr)				
Instruments_Laser_TOF	5	0.3	6.5				(d)1 hr			1330
Instruments_RAT	11	0.3	14.3				(f)1 hr			1530
Instruments_MI	5	0.3	6.5				(c)0.5 hr			1300
Instruments_Arm_IDD	5	0.3	6.5				(b)0.5 hr			1230
Instruments_Drill	35	0.3	45.5					4 hr		
Telecom										
Electra_Light_(XCVR)	50	0.3	65	1.5 hr (3×0.5 hr)	1.5 hr (3×0.5 hr)	1.5 hr (3×0.5 hr)	1.5 hr (3×0.5 hr)	1.5 hr (3×0.5 hr)	1.5 hr (3×0.5 hr)	800, 1200, 1700
Thermal										
Thermal_heaters	5.95	0.3	7.735							

Legend:
- An "X" implies that the specified load is active continuously within the particular operating mode.
- Non-continuous loads are specified by a sequence order (a, b, c,...), an operating duration (1 hr, 2 hr, etc.) and possibly a frequency indicator (3×0.5 hr).

also occur during the driving and the entry has the same character string, (a)1 hr, and start time. The next activity (b) is the Instrument Deployment Device (IDD) mode (i.e., rover arm) that starts at 1230 and lasts for 0.5 hours. There would be four more activities (c), (d), (e), and (f) associated with the approach/contact activities that occur at 1300, 1330, 1430, and 1530 hours respectively. Other activities [Electra_Light (XCVR)] shown in the same column are the telecommunications data return intervals with start times at 0800, 1200, and 1700 hours with a duration of 0.5 hours at each occurrence.

The result of this analysis is shown in Figure 2.4.2-10 where the power level of each activity is shown as a function of time. The blue line illustrates the power for each activity. The activities are labeled corresponding to the example above. The power required is shown above the abscissa in blue and the scale is on the left ordinate. More importantly, the power drain from the battery for each activity is shown below the abscissa in red.

The most important curve here is in green. It is the cumulative state of charge (SOC) of the battery in time and its scale is on the right ordinate. The battery starts the day with a capacity of about 17 Ahr and charging (0.75 A) continues until the beginning of the first activities that draw power from the battery (TELECOM and APPROACH). As the battery supplies power, it is discharged for that interval followed by a recharging interval. The green curve shows the SOC variation during the day. The goal would be to end the day with the battery recharged to its original capacity of 17 Ahr. Rover Operation in this fashion woul maintain a full battery capacity to begin activities on the next day. This analysis confirms that with the 4 GPHS baseline configuration, a productive set of activities would be manageable without any reduction of battery charge by the end of the day.

2.4.2.12 *Mass*

The differences in the two lunar rover options are clearly illustrated in Table 2.4.2-6, which contains the mass estimates for the baseline rover (4 GPHS RPS) and the other smaller rover (2 GPHS RPS). The fundamental difference in the rover masses reflects the 4 RPS versus 2 RPS configurations respectively. Also, the larger science payload on the baseline rover is more than twice the size of the 2 GPHS RPS rover. However, there is virtually no difference in the mass of the supporting vehicles (propulsion module and lander).

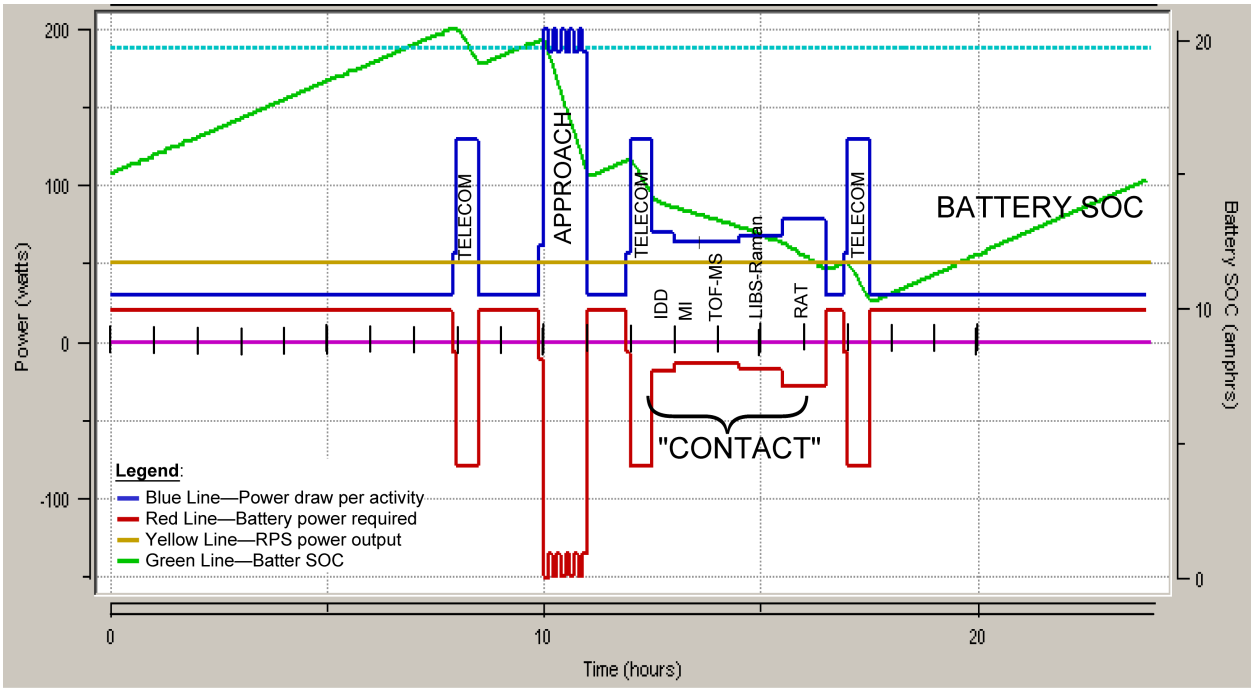

Figure 2.4.2-10. Lunar Rover Power Profile and Activity Sequence for the "Approach/Contact" Mode

Table 2.4.2-6. Mass Estimates for the Lunar Rover Mission

System	Rover Options			
	4-GPHS Baseline		2-GPHS Option	
	Mass (kg)	Mass with 30% Margin (kg)	Mass (kg)	Mass with 30% Margin (kg)
Rover	268.2	348.7	193.5	251.5
Telecom	7.8	10.14	7.8	10.14
ACS	2.6	3.38	2.6	3.38
Thermal	5.4	7.02	5.4	7.02
Power	37.2	48.36	27.2	35.36
Mechanical	131.9	171.47	101.7	132.21
Avionics	33.1	43.03	33.1	43.03
Payload	50.3	65.39	15.7	20.41
RAT	0.9	1.17		
Pancam	0.7	0.91	0.7	0.91
Microscopic Imager	0.7	0.91		
Illumination	3.0	3.9	3.0	3.9
LIBS/RAMAN	5.0	6.5	5.0	6.5
GPR	0.5	0.65	0.5	0.65
Active NGRS	6.5	8.45	6.5	8.45
Robotic Arm	6.0	7.8		
Mass Spectrometer (TOF)	12.0	15.6		
Subsurface Sampling Drill	15.0	19.5		
Lander (Dry)	369.2	479.96	369.2	479.96
Power	49.4	64.22	49.4	64.22
Mechanical	162.8	211.64	162.8	211.64
Propulsion	55.1	71.63	55.1	71.63
Telecom	5.4	7.02	5.4	7.02
Avionics	16.3	21.19	16.3	21.19
ACS	20.8	27.04	20.8	27.04
A&AC	12.8	16.64	12.8	16.64
Hazard Avoidance	8.0	10.4	8.0	10.4
Thermal	11.6	15.08	11.6	15.08
Rover Egress Ramp	30.0	39	30.0	39
Lander (Propellant and Pressurant)	66.1	85.93	66.1	85.93
Propellant	66.0	85.8	66.0	85.8
Pressurant	0.1	0.13	0.1	0.13
Propulsion Module	2340.2	3042.3	2340.2	3042.3
Propulsion	2287.0	2973.1	2287.0	2973.1
Star 48V Motor	2275.0	2957.5	2275.0	2957.5
Star 6B Motors (2)	12.0	15.6	12.0	15.6
Power	12.5	16.25	12.5	16.25
Thermal	1.9	2.47	1.9	2.47
Telecom	0.0	0.0	0.0	0.0
Mechanical	38.8	50.44	38.8	50.44
Total Launch Mass	3043.7	3956.8	2969.0	3859.7

Note that the mass totals include reserves of 30%. The total launch masses for the baseline and the 2 GPHS RPS are about 3953 kg and 3856 kg, respectively. These totals would be consistent with an Atlas 511 launch vehicle that has a capability (at $C_3 = -1.9$ km^2/s^2) of greater than 4000 kg.

2.4.2.13 *Radiation*

For the short flight duration to the Moon, the launch and deep space radiation doses would be negligible. The only significant (yet small) radiation environment on the rover would come from the RPSs. Assuming the 4 GPHS RPS baseline configuration, the radiation can be estimated from the GPHS environment data given in Figure 2.3.1-12, for a 13-year lifetime (the lunar rover mission's lifetime would be < 4 years). A conservative assumption would be that the radiation dose is directly additive from the 4 GPHS sources and that the closest electronics in the Rover Electronics Module (REM) would receive the highest dose. The REM is about 10 cm away from the closest GPHS element (see Fig. 2.4.2-4). With the above conservative assumptions, and referring to Figure 2.3.1-12, the dose would be $0.05 \times 4 = 0.2$ Mrad without any shielding. The shielding of the WEB/REM enclosures and the self-shielding of the stacked GPHS elements would further reduce this. Also, the shorter lifetime would result in a lower total dose. Thus, the radiation issues of the lunar rover are not design drivers.

2.4.2.14 *Alternate RPS Power Architecture*

A lower powered rover option was considered in the study to understand the minimum science and exploration mission possible using small-RPS power sources. The design concept would essentially be a remote measurement platform and use two GPHS RPSs on a smaller rover with a power output of 25 We (BOL). The science payload was identical to the baseline (4 GPHS RPS) lunar rover excluding the drill, arm, microscope imager, and RAT. The configuration for this smaller option is shown in Figure 2.4.2-11 illustrating the remote instruments contained on the vertical mast. A power sequencing analysis (similar that for the baseline in Section 2.4.2.11) was performed that demonstrated reasonable mobility and data return for this smaller rover with reduced instrumentation, while maintaining a positive battery margin each day.

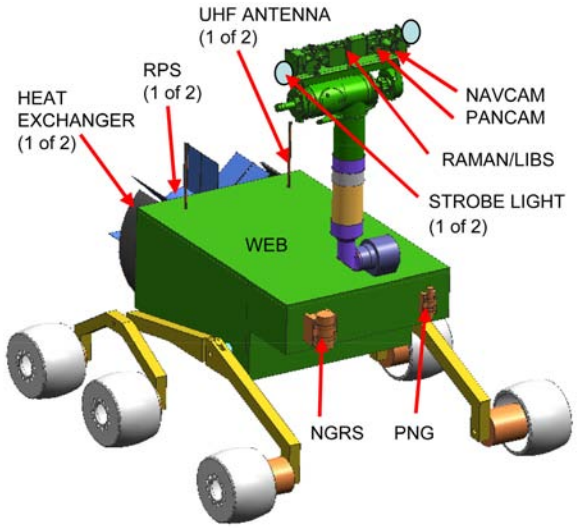

Figure 2.4.2-11. Lunar Rover Option Using 2 GPHS RPSs (25 We BOL)

2.4.2.15 *Lunar Rover Summary and Conclusions*

The goal of this study was to determine if small-RPS power sources could enable a mission to a permanently shadowed crater on the Moon that would return significant scientific data verifying the existence and volumetric extent of hydrogen-bearing deposits on the floor of the crater. A scientific payload was chosen to provide a significant scientific return while having a small enough size to be accommodated on an MER class rover and low-powered enough to be consistent with the total energy that was available. In addition, the instruments were chosen to have total telemetry volume consistent with the rover data storage and the relay telecommunications link from the rover to an orbiting relay satellite.

Motivated by cost, the key elements of the mission were chosen because of the high inheritance of their design. The demonstrated capability of the MER rover made it an obvious candidate that could accommodate the instruments and the RPS systems. The WEB on the MER rover would have sufficient volume to accommodate the payload electronics as well as the secondary battery needed to manage the energy depletion during daily activities. The MER mobility, memory and avionics capabilities would be more than adequate to meet the surface mobility requirements on the crater floor as well as the data handling of the chosen payload. The baseline rover concept and

payload would provide a sufficient science capability to answer the science goals and requirements using 4 small-RPS power sources, each based on a single GPHS module using thermoelectric power conversion. The delivery vehicle would consist of a large propulsion module stage utilizing a commercially available (STAR 48V) motor and a Phoenix lander derivative. A brief study identified the integrated configuration of this stage, the Phoenix lander, and the rover.

A key task in the study identified the daily energy usage during the surface operations of the rover to assure that the combination of the small-RPS and the rechargeable batteries was sufficient to allow a reasonable science data return. This task considered activities such as a complex driving mode over assumed rough terrain, illumination elements necessary for the optical instrument performance supporting the driving, an approach and contact mode with scientific targets (e.g., rocks) of interest, instrument activities necessary to return significant experiment results, and a telecommunications mode to return the data. The results from this task demonstrate that significant mobility and scientific return would be possible while maintaining an overall positive energy margin following daily activities using the small-RPS sources.

In conclusion, this study has demonstrated the viability of using small-RPS power sources to enable a lunar rover mission that could return significant scientific data on a daily basis in the search for hydrogen-bearing materials within a permanently shadowed crater.

2.4.3 Conclusions of Rover Mission Studies

The previous two sections (Section 2.4.1 and 2.4.2) considered RPS-powered rover missions for the surface of Mars and the Moon. Two sizes of small-RPS power sources were assumed and the implications of power levels were discussed relative to mission performance. Figure 2.4.3-1 illustrates some configuration examples of various rovers that have been considered in past and present studies. The blue box below each rover describes the size of the RPS that is appropriate for the particular concept.

The rovers considered within these studies required a hybrid power system, consisting of small-RPSs combined with a secondary battery. This configuration enabled very flexible operations on a daily basis, supporting the high power requirements of science, mobility and telecom, as well as potentially providing a significantly longer lifetime than a rover powered by a conventional power source. A distinct advantage of the RPS-powered rover would be the capability to explore surface regions and latitudes that would be inaccessible by solar powered vehicles due to limited solar insolation. Also, the waste heat generated by the RPSs could potentially provide additional advantages (e.g., longer mission life) by reducing thermal cycling of critical subsystems and components.

The RPSs considered in this study were all built around a single GPHS module, providing 12.5 We of power at BOL. Both the Mars rover concept and a lower-power variant of the lunar rover concept used two of these single-GPHS module RPSs, capable of generating a total power of 25 We at BOL. Using this small-RPS configuration, the MER class Mars rover concept (Section 2.4.1) matched the solar powered MER, with the total energy generated by both power systems equaling approximately 620 Wh/sol. The lower-power variant of the Lunar rover would use two single-GPHS module based RPSs, as described in Section 2.4.2. It has been demonstrated that such a lunar rover could perform high-value remote sensing measurements (in-situ measurements required additional power) within a permanently shadowed crater, and be capable of transmitting all scientific and engineering data back to Earth twice a day using an (assumed) preexisting lunar-polar relay orbiter.

Although not reported here, further studies were performed to scale the Mars rover up from 180 kg to ~230 kg, which would use 50 We of power (or 1250 Wh/sol energy), supplied by 4 GPHS-module RPSs. This larger Mars rover would accommodate additional astrobiology driven instruments, providing enhanced capability and the potential for greater scientific return. The baseline RPS power system for the lunar rover study consisted of a stack of four single-GPHS module RPSs, with a total power output of 50 We (BOL). This quad-module RPS system could potentially enable more energy-intensive and elaborate mechanical operations than would be possible with a 25 We RPS system, including extended mobility, a 1-m drill for subsurface sample analy-

sis, an arm for close-up in-situ measurements, and additional arm-mounted instrumentation. The advantage of the baseline four GPHS RPS rover over the lower-power variant is the increased potential to conclusively detect the presence and quantity of water ice (a primary mission objective) by use of the 1-m long drill.

The above concepts are represented in Figure 2.4.3-1 as the two highlighted rovers in the center (i.e., MER class and lunar rovers). Scaling down from these concept reference points, a Mars Pathfinder-class rover would require around 150 Wh/sol, which corresponds to an RPS using two GPHS fuel capsules (~6.25 We). Micro-rovers could use Radioisotope Heater Unit (RHU)-based power sources with electrical outputs of 40 to ~100 mWe, coupled with a battery or ultracapacitor, to provide enough energy in a trickle charge / burst operating mode to enable a certain amount of functionality. However, the rover's small size relative to the surrounding terrain, and the power required to perform energy-intensive functions (e.g., traversing or telecommunication) could limit the applicability of such mobility devices.

In summary, the above studies demonstrate the potential viability of a new class of RPS-powered rovers that could perform high-priority scientific and human-precursor missions not possible with conventional power sources.

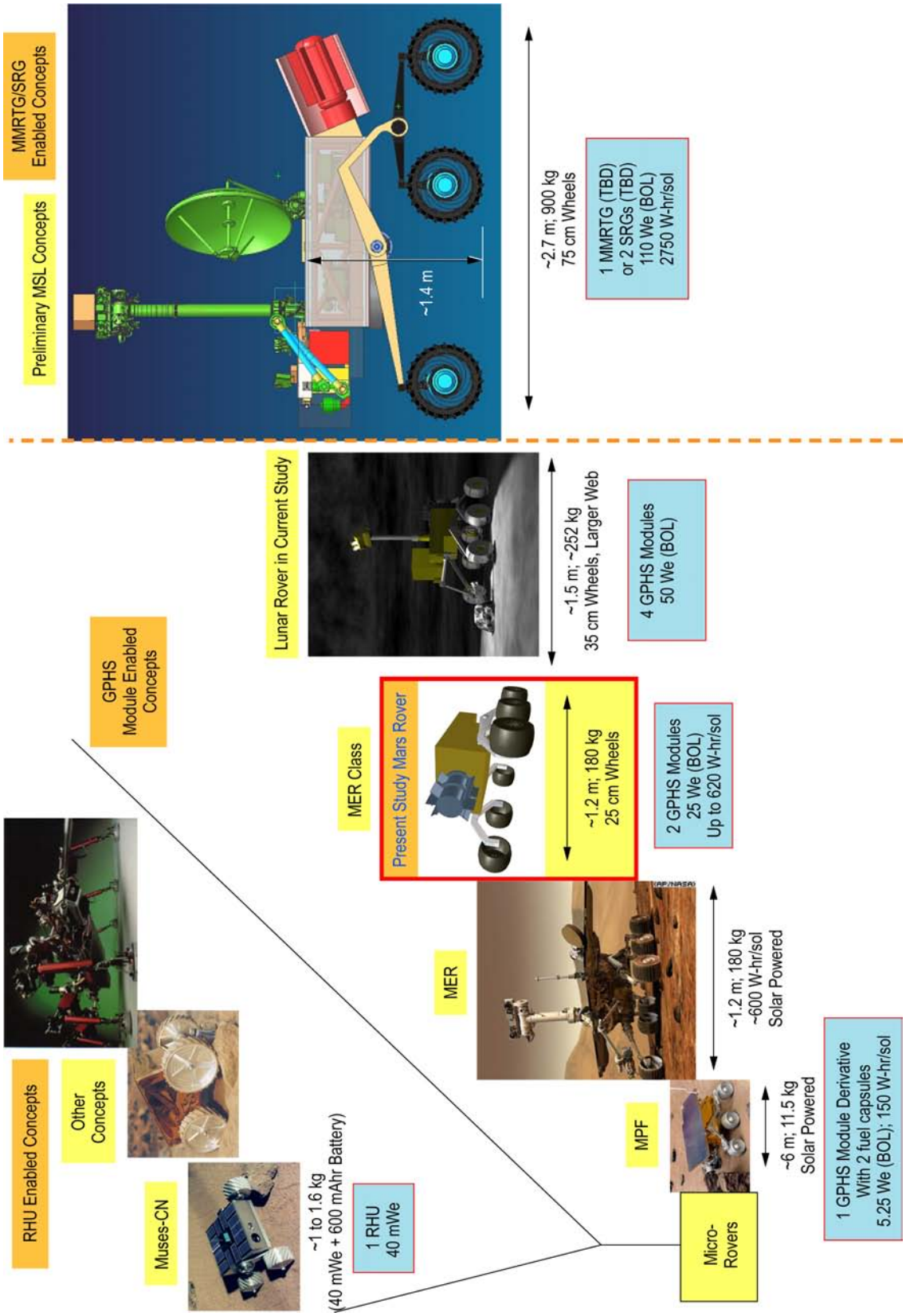

Figure 2.4.3-1. Additional Rover Concepts

2.5 SUBSATELLITE MISSIONS

2.5.1 Galilean Satellite Orbiter Mission

This section outlines a small-RPS enabled scientific mission to a Galilean satellite orbit. The conjunction of small-RPS technology [24], the proposed JIMO spacecraft [39] as a delivery vehicle, and a microspacecraft avionics module (Low Cost Adjunct Microspacecraft, LCAM [40]) would allow a unique mission capability that could return good science at a reasonable cost.

Figure 2.5.1-1. Jupiter and Its Icy Moons

A point design mission, called a Galilean Satellite Orbiter (GSO), has been conceived to demonstrate the existence of a new class of low-powered but scientifically justifiable exploration. The GSO would orbit one or more of the Galilean satellites (Fig. 2.5.1-1) carrying a full fields and particles (F&P) payload to measure the local magnetospheric characteristics of these moons as well as the interaction between the satellite's and Jupiter's magnetospheres. Also, imaging of the satellite's surface would be possible from a small nadir-pointed camera. Finally, measurements of the satellite's gravity field characteristics would be done using the Doppler variations in the communications link with the JIMO spacecraft.

2.5.1.1 *Science Goals*

The science goals of the GSO are to conduct F&P experiments observing the plasma environment in the magnetosphere of a Galilean satellite, determine the gravity field of the satellite using the radio signal from the JIMO spacecraft, and to provide an imaging capability to monitor global processes using a wide angle camera. The scientific goals for such experiments were discussed at a JIMO forum in 2003 [39] where the fundamental requirements for a Galilean satellite orbiter were identified as an electromagnetically clean measurement platform, with full sky coverage for particle detectors, and knowledge of pointing for magnetometry reconstruction.

Specific science goals include the search for evidence of subsurface liquid water or other conductive fluids using magnetic field measurements, determination of the interaction of satellites with Jovian magnetosphere, determination of the radiation environment of the icy satellites, understanding the structure of the satellite magnetospheres and ionospheres, determination of plasma pick-up, wake particle interactions, and particle acceleration processes, measuring the secular variation in satellite magnetic fields over extended period (3 months), characterization of the non-hydrostatic gravity field at regional to global scales, and mapping global surface processes.

These goals and the instruments that satisfy them are listed in Table 2.5.1-1. Further description of the instruments can be found in Section 2.5.1.6.

Table 2.5.1-1. GSO Science Goals and Applicable Instruments

Science Goal	Instrument
Detect Evidence of Subsurface Water	Magnetometer (MAG)
Determine Satellite Interaction with Jovian Magnetosphere	MAG, Plasma Spectrometer (PLS), Plasma Wave Detector (PWD), Particle Detector
Determine Local Radiation Environment	Particle Detector
Quantify Satellite Magnetosphere	MAG, PLS, PWD, Particle Detector
Identify Plasma/Particle Interaction	MAG, PLS, PWD, Particle Detector
Determine Variations in Magnetic Field	Magnetometer
Map Gravity Field and Mascons	Doppler Extractor
Monitor Global Surface Processes	Imaging

The JIMO spacecraft would have significant capabilities for power or data relay that the GSO could utilize. Also, the long duration (few months) GSO mission at each satellite would provide a new and scientifically important set of data about the Galilean satellites and their environment.

2.5.1.2 *Mission Goals*

There is a scientifically exciting mission using a small-RPS power source and employing resources from a larger nearby spacecraft such as JIMO. The mission would use the JIMO resources for all telecommunications to Earth as well as for orbital placement with no additional propulsion required. The mission goals include demonstrating that a mother-daughter spacecraft relationship in the Jovian system is indeed possible with a small power source. Other mission goals include demonstrating viable science return with small, low powered scientific instruments consistent with the low power of a small-RPS unit. Eliminating active attitude control is also important for this mission, as it minimizes power and propulsion requirements. These goals could be met with a mission within a planetary satellite system and would return exciting science results using the advanced technologies and resources discussed herein.

2.5.1.3 *Mission Architecture Overview*

The principal constraint on the mission and system design is the power limitation of the RPS source which drives the configuration and operations of the spacecraft. Small, low power electronics modules and instruments would provide a scientifically rich mission data return. A derived requirement to minimize real time power needs is to have no active attitude control system. This would reduce power requirements on avionics operation and eliminate the need for an attitude control propulsion system. Attitude knowledge from a star camera would be used for reconstruction of the data.

The mission would rely on the mother spacecraft (i.e., JIMO) for orbit insertion about a Galilean satellite. Once the GSO leaves JIMO, the GSO would have no means to correct for orbital perturbations that could change its orbit and potentially limit its utility. Thus, the GSO orbit must be carefully chosen to remain stable for many years in order to be consistent with planetary protection requirements. Although no separate analysis has been performed for the GSO orbits, analysis conducted for JIMO suggests that low inclination orbits ($i \leq 45°$) would be stable indefinitely.

Another consideration affecting the GSO design is the large communication range that is a result of the worst case distance between a GSO in a Callisto orbit and the JIMO spacecraft in a Europa orbit. This range could be as great as 3×10^6 km. With this large range, the small transceiver / amplifier system within the LCAM (see discussion below) is not adequate for communications to JIMO. Thus, the GSO spacecraft system would have a dedicated X-band telecommunications system as a relay capability to JIMO with a relatively high power amplifier combined with a high gain antenna as discussed in Section 2.5.1.8.

A typical JIMO trajectory is shown in Figure 2.5.1-2, where the low thrust trajectory path from Ganymede to Europa is illustrated. The GSO would be left in orbit about Ganymede while the JIMO spacecraft proceeded to Europa. As the GSO spacecraft acquired its scientific data, it would periodically transmit this stored data to JIMO for relay to Earth.

The spacecraft configuration shown in Figure 2.5.1-3 would be consistent with the accommodation of a small-RPS power source. The heat from the RPS would be conducted to the boom which would act as a radiator for rejecting the heat to space. This is a unique design concept made possible by the end-mounted RPS thermocouple configuration (see Section 2.5.1.5), allowing heat transfer only from that end into the boom/radiator. Given the relatively large area required for the radiator, the boom would be lengthened accordingly. An advantage of this design is that the long boom can carry the LCAM and other elements at each end, suggesting the possibility of a passive yet stable attitude utilizing the gravity gradient technique. Another advantage of the long boom is the separation of the science payload at the nadir-end of the boom from the RPS at the zenith-end of the boom. This would minimize the electromagnetic and nuclear interference from the RPS with the science instruments. A heat pipe would allow the necessary heat conductance and would

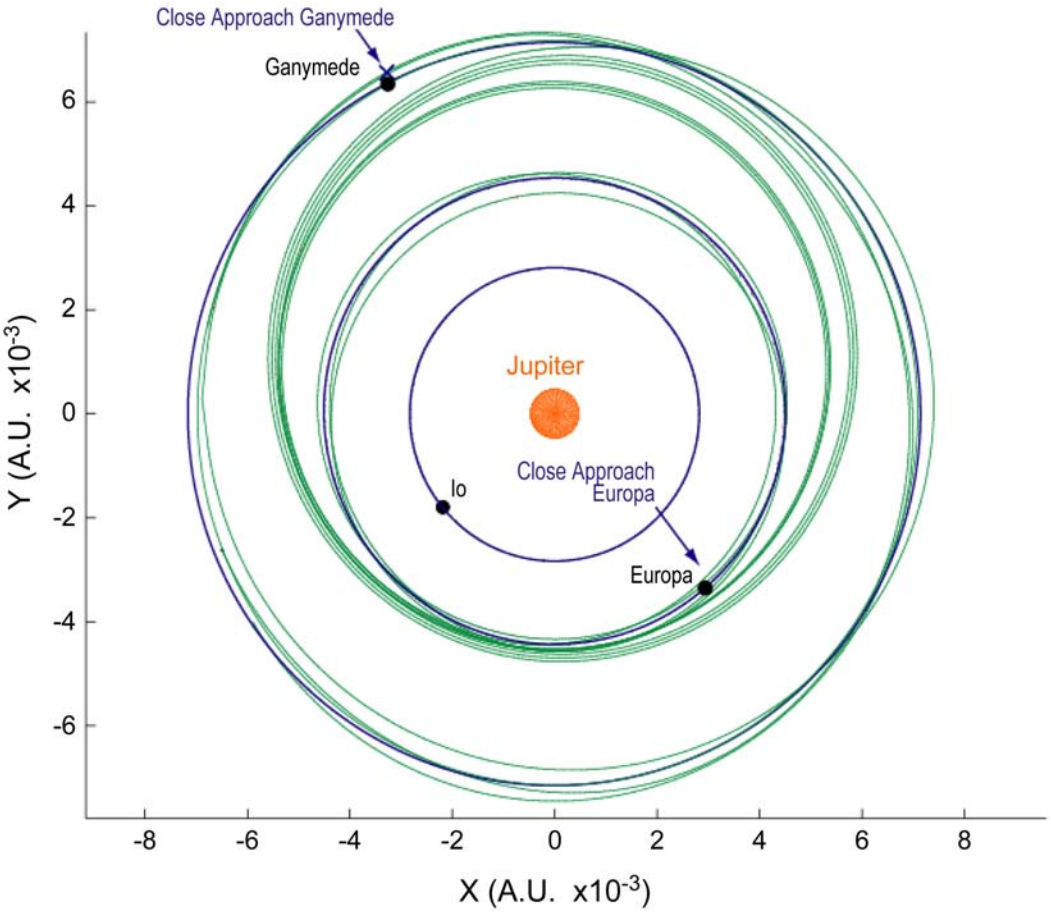

Figure 2.5.1-2. Typical JIMO Trajectory from Ganymede to Europa

spread the heat for radiation along the length of the boom. In addition, the fluid in the pipe would dampen any oscillations that might occur during the gravity gradient attitude variations.

A key element of the spacecraft is an avionics module under development at JPL [40] known as the LCAM. This module contains computational, attitude sensing, and a small propulsion capability in its current design. Two LCAM modules would be used to support two different functions on the GSO spacecraft as shown in Figure 2.5.1-3. The "zenith" end of the boom would contain an LCAM that would provide an avionics capability and a structural support for the RF module and the RPS. At the "nadir" end of the boom, another LCAM would act as a support for the science instruments. A single LCAM would have capability far beyond what is required for all avionics functions allowing the two modules to be functionally redundant and would be cross-strapped for redundancy.

The small LCAM propulsion systems would provide a total impulse of about 36.4 kg-m/s. For the GSO spacecraft, this suggests a total ΔV capability of about 0.6 m/s which could be used for early attitude control or very small translational maneuvers.

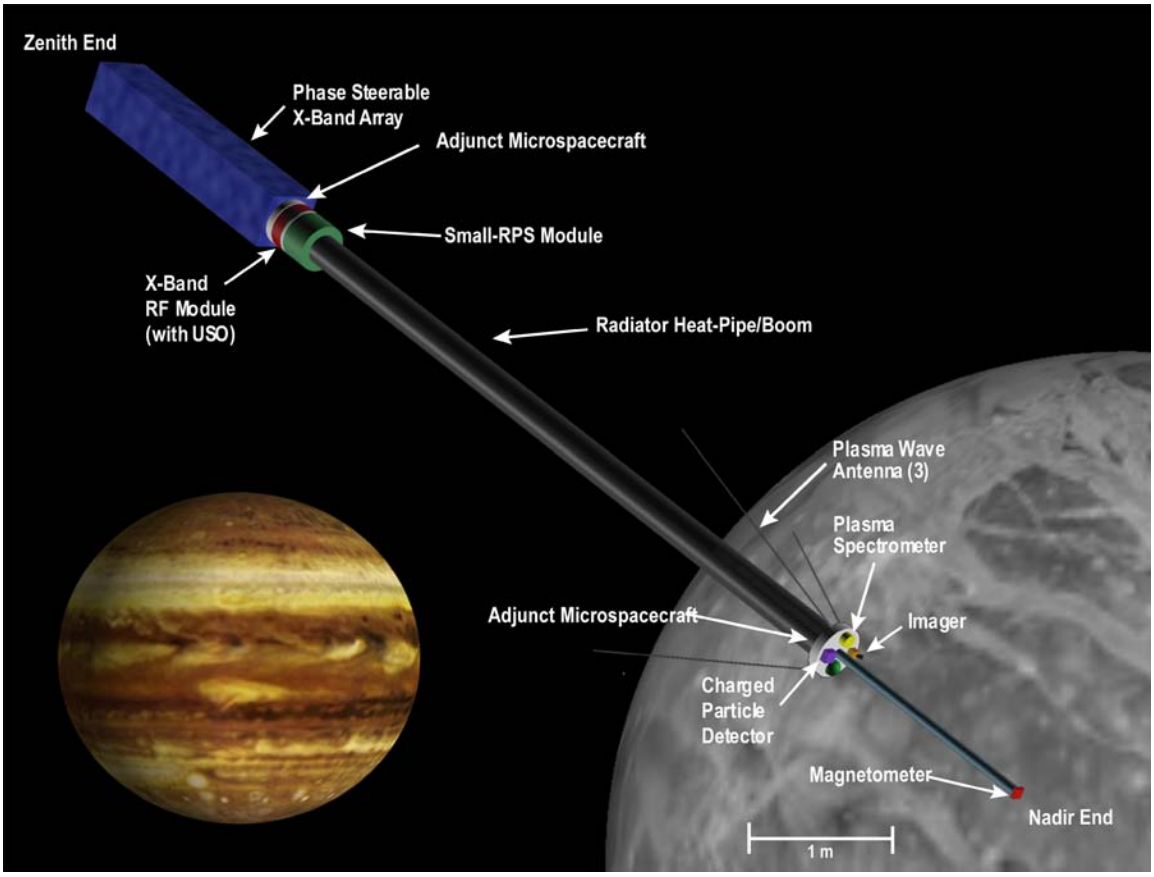

Figure 2.5.1-3. GSO Spacecraft Configuration

Figure 2.5.1-4 illustrates a high level block diagram of the GSO spacecraft system. The vertical lines at each side represent the two key connectivity elements of the spacecraft: the power bus and the telemetry/command network. The RPS would be continually connected to the power bus whereas the battery would augment the RPS as needed for peak power activities. When the battery requires charging, the switch to the RPS would be closed providing the power. The redundancy of the LCAM modules is shown in the diagram. The nominal role of the zenith LCAM is to control the power, attitude knowledge, and telecommunications functions as well as providing the interface for the telecommunications module and the high gain antenna. The nadir LCAM would provide the data handling for the science payload as well as the structural support for the science instruments. The LCAM capability is great enough that the avionics roles of the LCAMs would be interchangeable and they are cross strapped for this redundant capability.

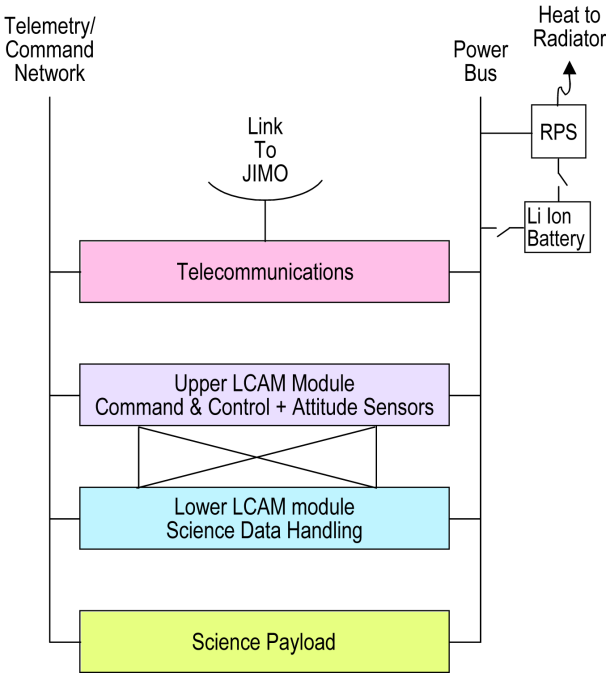

Figure 2.5.1-4. GSO Spacecraft Block Diagram

The LCAM (Fig. 2.5.1-5) is the basic avionics element in the GSO architecture and has been developed in a NASA Code T Program [40]. This module provides avionics capabilities (and a small propulsion capability) for the proposed GSO spacecraft. Although each module was developed as a free-flying concept for Earth orbiting application, each has sufficient avionics capabilities to support the GSO activities. One of the issues in the GSO application is the radiation environment. Shielding must be added to the LCAM module to allow operation in the near Jupiter environment (see Section 2.5.1.12). In the mass estimates, the LCAM component masses have been tripled to accommodate the spot shielding required.

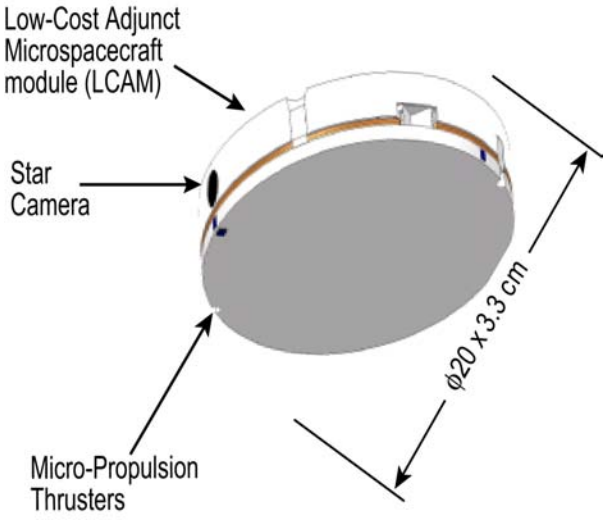

Figure 2.5.1-5. Low Cost Adjunct Microspacecraft Configuration Concept

The central processing capability in the current LCAM design is a Power PC 405 operating in conjunction with a very capable Field Programmable Gate Array (FPGA). The RAM memory has over 64 MBytes which is more than sufficient for the attitude determination and other spacecraft activities.

A key element of the LCAM module would be the star camera that is used to determine attitude knowledge during the mission. With no attitude control and passive gravity gradient stabilization, it is important to know where the cameras, instruments and antenna are pointed for data reconstruction.

The JIMO spacecraft would act as a delivery and support vehicle for the GSO spacecraft. The JIMO configuration shown in Figure 2.5.1-6 illustrates a preliminary version of JIMO showing the GSO spacecraft integrated to one of the JIMO spacecraft bays. This location could easily accommodate the GSOs on the JIMO spacecraft and would allow a straightforward deployment of each GSO into its satellite orbit and initial attitude.

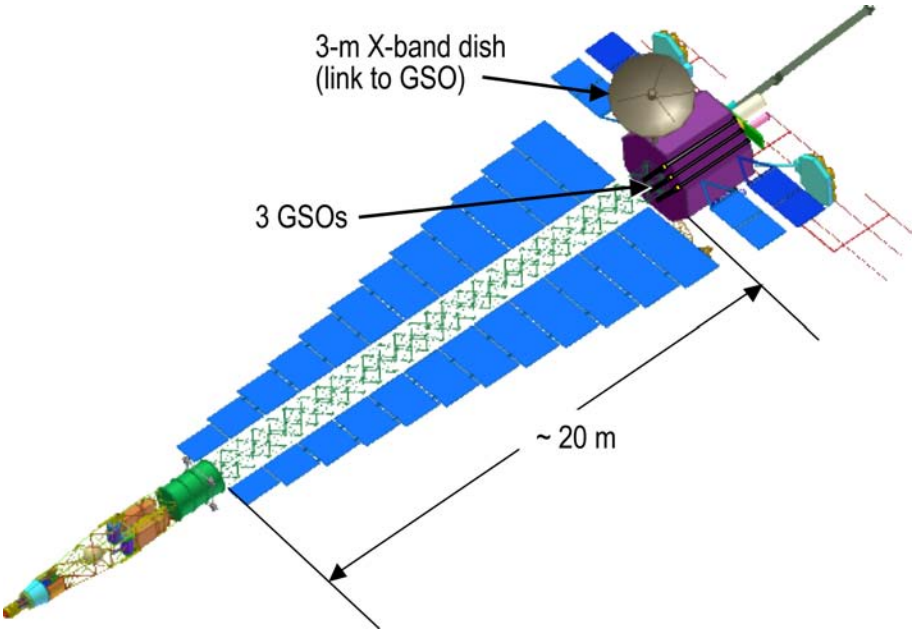

Figure 2.5.1-6. Preliminary JIMO Configuration with Three GSO Spacecraft Attached

2.5.1.4 *Power Source Trade Study*

The alternative power sources considered for the GSO mission included chemical and solar sources but these sources were determined to be impractical. Any solitary chemical source (i.e., battery) would have an obvious life limitation for any reasonable sized battery. Even with the expected life limitation at Europa of about 30 days caused by the radiation, a battery would have a mass and volume that would be larger than the entire GSO spacecraft as currently conceived. Solar power arrays were considered but in this case the required volume (area) and the pointing control requirements are the issues. Even the best solar arrays must be operated in a low intensity low temperature (LILT) environment and high radiation environment at Jupiter with low expected performance (~1.5 W/kg). Thus, to consider supplying power using arrays at Jupiter would require a large area (2 m^2) that would be incompatible with the gravity gradient stabilization and the pointing capability required for the arrays.

2.5.1.5 *Small-RPS Characteristics*

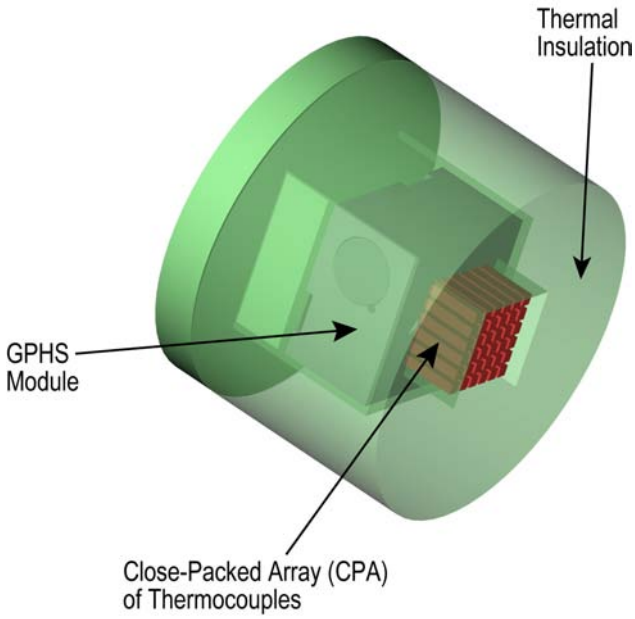

Figure 2.5.1-7. Small-RPS Configuration with End Mounted CPA Thermocouples for the GSO Mission

The small-RPS system considered in this concept (250 Wt/15 We BOL) would have a new arrangement for the thermocouple module as shown in Figure 2.5.1-7. With the introduction of the close-packed array (CPA) thermocouple module [24], the RPS can have a configuration with the end of the RPS as the radiating surface while the remaining surface area is highly insulated as shown in the figure. Having the heat directed toward one end of the RPS housing allows the use of a unique directional radiator. This focused direction for the heat flow is enabling for the GSO spacecraft configuration as discussed in Section 2.5.1.3.

To be compatible with the linear architecture of the spacecraft, the small-RPS configuration uses a "hot end" as shown in Figure 2.5.1-7. This concept has been proposed in DOE studies [24] for use with a CPA of thermocouples at one end of the RPS housing. This arrangement enables a radiator from that end surface. Thus, the long boom attached to this end surface forms a thermal radiator to conduct and radiate the heat away from the RPS unit. To take advantage of this linear radiator, the heat must have a directional conductivity along the boom. Typical boom materials (e.g., all carbon-carbon) would not have sufficient conductivity to spread the heat along the length of the boom so that it could be radiated to space. Thus, the boom would have a heat pipe (or pipes) inside to assure the proper conductivity along the length of the boom. In addition, a small amount of heat must be conducted to the opposite end from the RPS to provide thermal control for the LCAM there and its related science instruments.

Fundamental to this spacecraft design is the proper management of the power available from the small-RPS source. The RPS is assumed to have 250 W of thermal power and an electrical conversion efficiency of 7% at launch, and the mission duration is assumed to be a total of 13 years for the Europa GSO. The typical losses includes 0.8% loss of thermal power per year (due to radioactive decay) and 0.8% loss of thermocouple efficiency per year. Thus, the electrical power output at the end of 13 years is ~14.2 W.

In addition, a power margin of 30% is assumed for this early conceptual study. Thus, the electrical power design assumption for the spacecraft (worst case) is about 10 We from the RPS at EOM.

As a compliment to the RPS to support peak power periods, a Li-Ion battery would provide the power augmentation. Preliminary studies suggested that a 20-Ah battery would provide an adequate energy margin. With a bus voltage of 5 V and a depth-of-discharge of 33%, the available energy would be 33 W-hr.

Furthermore, the power accounting assumes that the engineering overhead of the spacecraft would include sufficient power from the RPS to recharge the battery between utilization intervals. The combination of power from the RPS and energy from the battery would allow continuous spacecraft overhead operation with periodic science acquisition and playback.

2.5.1.6 *Science Instruments*

A brief summary of the GSO science goals and applicable instruments was given in Table 2.5.1-1. The preliminary description of each instrument is given in the following paragraphs and additional detailed descriptions may be found in [41]. The magnetometer is a triaxial fluxgate having a noise and resolution of less than 0.05 nT and provides a 3-axis measurement of $\pm$ 200 nT per vector. The plasma spectrometer is based on the Ion and Electron Spectrometer (IES) design for the Rosetta mission [42] shown in Figure 2.5.1-8. It can measure both energy and flux of ions and electrons in a range of energies from ~0.001 to 20 keV. The plasma wave detector uses 3 whip antennas as shown in Figure 2.5.1-3. It can detect plasma waves in the frequency range of 5-1000 kHz. The charged particle detector is based on a concept described in [41] that uses a silicon detector to provide a range of particle detection between about 5 to 100 MeV per nucleon. The gravity experiment uses a doppler extractor (similar in concept to the Galileo instrument in [43]) combined with an ultra stable oscillator in the RF module to extract slight variations in the one-way RF carrier from the JIMO spacecraft. This would allow determination of the small doppler changes in the signal caused by the effects of the harmonics of the gravity field of the satellite as well as any effects caused by local mass concentrations in the satellite. It is expected that the doppler variations can be measured with an accuracy of better than 0.01 mm/s. The imaging experiment would be located on the nadir viewing platform (nadir end of the boom) to allow observations of the Galilean satellite surface at low resolution. The camera [40] would have a wide angle field-of-view (approximately 60 degrees) telescope and a detector array size of 1024 × 1024 pixels that are 10 microns in size.

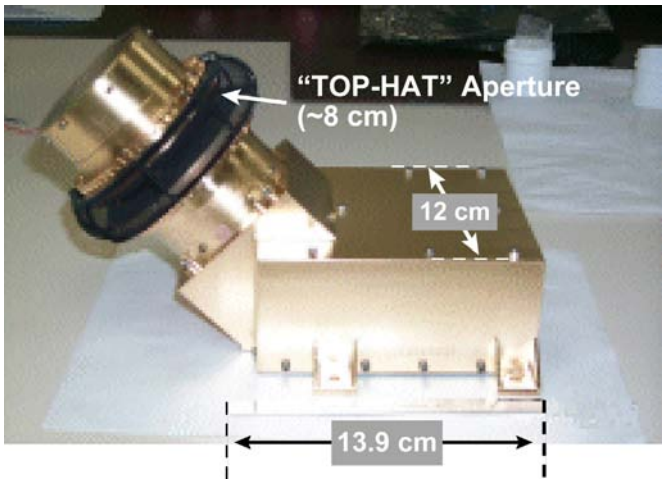

Figure 2.5.1-8. Ion and Electron Spectrometer from Rosetta

Table 2.5.1-2 is a summary of the expected performance and other parameters associated with the GSO payload. Note that the four F & P instruments have a total data rate of about 100 bits/s.

Table 2.5.1-2. GSO Science Instrument Characteristics

Instrument	Instrument Performance	Telemetry Rate (bits/s)	Mass (kg)	Power (W)
Magnetometer	± 200 nT @ 0.05 nT	20	1	1
Plasma Spectrometer	0.001 to 20 keV	50	1	1
Plasma Wave	5 to 1000 kHz	10	1	1
Charged Particles	5 to 100 MeV	10	1	1
Imaging	Wide angle FOV (~60°) 1024 × 1024 pixels	10 frames/day	1	2
Doppler Extractor	~0.01 mm/s	100	1	2

2.5.1.7 *Data*

The small-RPS system would enable a significant science data return using periodic science acquisition and playback modes. Spacecraft avionics would operate continuously with the small-RPS power available. The absence of any active attitude control requirements (because of the gravity gradient stabilization) would enable this operational capability.

The instruments would be operated in an acquisition mode that would depend on the power available from the RPS and the battery while maintaining a steady state operation of the spacecraft. The F&P instruments would require very low power and can operate for very long durations. The gravity field experiments would take advantage of the absence of perturbations from an active attitude control system. However, the receiver and antenna operations would require reasonable power and the duration of the gravity field data sessions could be limited by the power and energy available. Finally, the imaging instrument and its data system would require high power but for only short intervals of time (few seconds per frame and readout). Thus, the overall science acquisition strategy can be managed within the power constraints of the RPS. Table 2.5.1-3 contains a power management scenario for a typical three day operational sequence of science data acquisition.

The science data acquisition modes are designed to use only RPS power ($\leq$ 10 We). The only duty cycle imposed on the science is related to how much data can be returned during the telecom relay link period for data playback that depends on battery energy for its duration. Referring to Table 2.5.1-3, there are three basic science data modes labeled Mode A, B and C. Each mode is a different set of scientific experiments requiring different resources from the spacecraft.

The spacecraft resources for Mode A (*Fields and Particles*) includes the Command and Data Handling (CDH) subsystem (2 We) to provide sequencing (e.g., duty cycling) of the instrument observations and data storage, the Attitude Control System (ACS) (2 We) on for star camera observations (e.g., a 10^4 bit frame every 10 minutes) to identify the attitude during the observations for science experiment reconstruction, and power needed to maintain spacecraft operation (e.g., battery charging, etc.) (2 We). Thus, the spacecraft "engineering" overhead power is about 6 We for Mode A as shown in Table 2.5.1-3 with 4 We allocated for the F & P payload.

The resources for Mode B (*Doppler Science Data*) are similar, but more frequent star camera observations are needed (a frame every minute) to acquire the pointing knowledge necessary to maintain the pointing of the antenna for the receipt of the carrier signal from the JIMO spacecraft; however, the antenna pointing accuracy only has to be sufficient enough to receive the high power signal from JIMO. Also, the telecom receiver must be on (~2 We) to receive the JIMO carrier and send it to the Doppler extractor where the received carrier is compared to the USO and the "beat" frequency containing the gravity field data is digitized (at about 100 bits/s) for return as telemetry later.

Mode C (*Imaging*) is not a continuous mode but is used only periodically to acquire imaging observations for science or inspection purposes. To support the imaging observations, more frequent star camera frames must be taken (~1 frame per minute) to allow reconstruction of the observations.

For each of the science modes, the resulting telemetry data would be stored for playback later when JIMO is available for relay of the data. The summary of the typical data acquired for each mode is given in the table. The largest quantity of stored data is in Mode A assuming a three day acquisition duration. An example of the data playback from Mode A is shown near the bottom of the table. Mode D is the playback mode requiring about 26 We of power because of the high power needs of the RF system. This power would be supplied by a combination of the RPS (10 We) and the battery (16 We). The duration of the playback is limited by the battery depth-of-discharge (33%) and, in this case, is about 2.1 hours. However, the data from Mode A can be returned (at 5 kbits/s) in ~1.6 hours providing a margin of about 23% before battery "depletion" at 33% DOD.

Table 2.5.1-3. GSO Data Modes and Power Constraints

Power Requirements					
Mode	Data Activity		Science Pwr (We)	Engr. Pwr (We)	Total Pwr (We)
A	F&P Science Acquisition		4	6	10
B	Doppler Science Data		2	8	10
C	Imaging		2	6.5	8.5
D	Playback		–	26	26
Power Sources					
RPS Power EOM, Watts			10.1		
Batteries (20 Ah x 5 V x 0.33 DOD), W-hr			33		
Data Acquisition					
Mode	Data Rate (incl. Engr.), bits/s		Duration, hr	Total bits	
A	110		72	2.85 E + 07	
B	100		72	2.59 E + 07	
C	10 frames	0.5 Mbits/ frame		1.00 E + 06	
Playback					
Downlink Rate, bits/s		5000			
Mode A Playback (worst case)					
Total Power Required, We		26			
Power from RPS, We		10			
Power from Battery, We		16			
Battery depletion duration, hr			2.1		
Playback duration, hr			1.584		
Margin, %		23			

The current LCAM flash memory of over 100 Mbits [40] is easily capable of supporting the science storage requirement of about 30 Mbits and has a large margin for other memory needs in the avionics.

2.5.1.8 *Communications*

A separate telecommunications module or subsystem is part of the GSO spacecraft design because of the realization that the small transceiver in the "standard" LCAM module [40] is not sufficient for the GSO to JIMO communications link. The module would contain four fundamental elements: X-band transceiver, X-band amplifier(s), Ultra Stable Oscillator (USO) and a doppler extractor. The transceiver provides a command and telemetry function at X-band and would operate at low power in its receive mode (~2 We). The amplifier would be an advanced solid-state device with high efficiency (~33%) and an RF output of about 5 W (RF), equivalent to ~15 We. The USO would have a stability of better than 1 part in 10^{13} to allow sufficient accuracy for the doppler gravity experiment.

The doppler extractor would receive the uplink signal from JIMO and combine it with the USO signal to extract the difference signal containing the gravity field signature which would be digitized and stored for later playback during a downlink session with JIMO. A similar concept was used during the Galileo probe descent [43] but the detailed design of the GSO gravity measurement system has not been done.

Telemetry would be returned during a relay telecommunications session with the JIMO spacecraft. A telemetry rate of 5 kbits/s can be supported over the maximum distance (3×10^6 km) using the 5 We RF amplifier. The antenna shown in Figure 2.5.1-2 is sized to provide this 28 dB gain. Detailed design of the phase steerable array with this gain capability remains to be done but seems quite feasible. Because the attitude would not be controlled beyond the gravity gradient

range of angles, the phase steerable antenna must point the antenna in the JIMO direction based on the knowledge of the attitude from the celestial sensors (star camera, gyros). The trajectory geometry between GSO and JIMO would be known and predictable at any time and the antenna beam would be pointed in that direction as needed for periodic communications.

Table 2.5.1-4 is a design control table (DCT) for this downlink from the GSO (around Callisto) to the JIMO mothership (assumed around Europa) at the extreme range of 3×10^6 km.

Table 2.5.1-4. Proposed GSO Telecommunications Design Control Table

Configuration of the RF System									Requirement	
5 W SSPA X-Band CLGA GSO Transmitter One-Way TLM channel/RS-Convolutional (7, ½)/PB=1.E-6 Carrier Loop Bandwidth = 10.0 Hz, Bit Rate = 5000 bits/s									3EG	max range
	Link Parameter	**Unit**	**Design**	**Fav Tol**	**Adv Tol**	**Mean**	**Var**	**S**		
	TRANSMITTER PARAMETERS									
1	S/C RF Power Output	dBm	37.00	0.00	–0.20	36.93	0.0022	T	5	Xmtr Pwr, W
2	Total Circuit Loss	dB	–1.00	0.10	–0.10	–1.00	0.0033	U		
3	Antenna Gain (on boresight)	dBi	0.00	0.50	–0.51	0.00	0.0425	T		
4	Ant Pointing Loss	dB	28.00	0.50	–0.51	28.00	0.0854	U	HGA Phase Steerable	
5	EIRP (1+2+3 = 4)	dBm				63.93	0.1334			
	PATH PARAMETERS									
6	Space Loss	dB	–240.49	0.00	0.00	–240.49	0.0000	D	X	RF band
7	Atmospheric Attn	dB	0.00	0.00	0.00	0.00	0.0000	D	8439	Freq, Mhz
	RECEIVER PARAMETERS									
8	JIMO Antenna Gain	dBi	46.90	0.10	–0.10	46.90	0.0017	T	3 m	HGA
9	Ant PointingLoss	dB	–0.10	0.00	0.00	–0.10	0.0000	U		
10	Polarization Loss	dB	–0.04	0.00	0.00	–0.04	0.0000	U		
	TOTAL POWER SUMMARY									
11	Total Rcvd Pwr (Pt) (5+6+7+8+9+10)	dBm				–129.81	0.1351	G		
12	Noise Spec Dens	dBm/Hz	–172.40	0.00	0.00	–172.40	0.0000	G		
	System Noise Temp	K	450.00	–0.30	0.30			G		
	Vacuum	K	20.00	–0.30	0.30			T		
13	Received Pt/No (11–12)	dB-Hz				42.59	0.1351	G		
	CARRIER PERFORMANCE at Req. Pt/No									
	TELEMETRY PERFORMANCE at Required Pt/No									
14	Tlm Data Supp	dB	–0.54	0.07	–0.08	–0.54	0.0010	T		
15	Data Rate	dB	36.99	0.00	0.00	36.00	0.0000	D		
16	Radio Loss	dB	–0.36			–0.36		T		
17	SubCarrier Demod. Loss	dB	–0.29			–0.29		T		
18	Symbol Sync. Loss	dB	–0.02			–0.02		T		
19	Waveform Distortion Loss	dB	0.00			0.00		T		
20	Threshold Eb/No	dB				2.31		D		
21	Required Eb/No	dB				2.98				
22	Required Pt/No	dB-Hz				40.51	0.3035	U		
23	Performance Margin (39-13)	dB				2.08				
24	Sigma	dB				0.66				
25	Margin—2 sigma	dB				0.76				

2.5.1.9 *Thermal*

To provide thermal control for the GSO, flight proven thermal control elements would be used. The GSO thermal control system would use a heat pipe within the boom/radiator and thermal conduction control from the heat pipe to the science payload. This would allow the heat transfer required for the RPS operation, and provide thermal control for the electronics modules and science payload. The thermal conductor system would be used to transfer heat from the cold junction of the RPS thermocouples to the boom/radiator. The system would also include controlled conductance from the end of the heat pipe to the base of the LCAM to provide thermal control to the lower LCAM and science payload. Additionally, MLI, thermal surfaces, thermal conduction control and sensors would be used in the thermal control design.

The boom/radiator would be designed as a thermal conductor radiator to reject the waste heat from the RPS. The heat pipe would be used to transfer the heat along the length of the high emissivity boom surface to be radiated to deep space. Sufficient heat (~10 Wt) would be conducted to the opposite end of the boom to provide adequate thermal control for the lower LCAM and its scientific payload platform.

2.5.1.10 *Power*

The proposed GSO spacecraft power requirements are given in Table 2.5.1-5. The three numerical columns on the left list the current best estimate for the power of each element on the spacecraft. A power margin is given for each item and the sum or total power is also given. In the right three columns the power for each data mode (see Section 2.5.1.7) is given according to what item is used during that mode.

Table 2.5.1-5. GSO Spacecraft Power Requirements

Item	Power			Power per Mode				Heritage
	Power (W)	Margin (W)	Power with Margin (W)	A (W)	B (W)	C (W)	D (W)	
Payload								
Magnetometer	0.5	0.5	1.0	1.0				MSSPM incl. Boom
Plasma Spec.	1.5	0.5	2.0	2.0				IES
Plasma Wave	0.3	0.3	0.6	0.6				Solar Probe
Charged Particles	0.3	0.2	0.5	0.5				MSSPM
Imaging	1.5	0.5	2.0			2.0		LCAM
Doppler 5 Extractor	1.5	0.5	2.0					New
P/L Totals	5.6	2.5	8.1	4.1	2	2		
Spacecraft Bus								
AC Sensors	0.6	0.2	0.8	0.8	0.8	0.8	0.8	LCAM
C&DH	1.5	0.3	1.8	1.8	1.8	1.8	1.8	LCAM
Power	1.0	0.5	1.5	1.5	1.5	1.5	1.5	New
Profs	0.1	0.1	0.2					LCAM
Cabling								New
Structure								LCAM
Thermal Boom (Radiator)								New
JIMO Adapter								New
RF Transceiver	0.5	0.5	1.0		1.0		1.0	New
RF Amplifier	15.0	5.0	20.0				20.0	New
High Gain Antenna	0.5	0.5	1.0		1.0		1.0	New
S/C Totals	19.2	7.1	26.3	4.1	6.1	4.1	26.1	
Overall Totals	24.8	9.6	34.4	8.2	8.1	6.1	26.1	

2.5.1.11 *Mass*

Preliminary mass estimates are shown in Table 2.5.1-6 for the GSO spacecraft items and are based on the LCAM study [40], the MSSPM study [41], and analytical estimates of the new items. Mass margins are included in the estimates and have been identified for each item of the spacecraft. This was done to account for the large margins necessary for radiation shielding in the Jovian environment. Typically, the shielding margin is assumed to be a factor of 3 times the mass of the item if it is susceptible to radiation damage (e.g., electronics).

2.5.1.12 *Radiation*

Traveling to the Jupiter system with a radioisotope power system would impose two different radiation environments on the spacecraft. First, the high energy secondary gamma radiation is

Table 2.5.1-6. Preliminary Estimates of GSO Mass Requirements

Item	Mass (kg)	Margin* (kg)	Mass with Margin (kg)	Heritage
Payload	2.8	3.2	6.0	
Magnetometer (with boom)	1.0	0.6	1.6	MSSPM incl. Boom
Plasma Spectrometer	0.6	0.4	1.0	IES
Plasma Wave	0.5	0.5	1.0	Solar Probe
Charged Particles	0.3	0.6	0.9	MSSPM
Doppler Extractor	0.3	0.6	0.9	New
Imaging	0.1	0.5	0.6	LCAM
Spacecraft Bus	33.6	31.2	64.8	
AC Sensors	0.2	0.6	0.8	LCAM
Command & Data Handling	0.6	1.8	2.4	LCAM
Power	6.0	3.0	9.0	New
Propulsion	0.8	0.8	1.6	LCAM
Cabling	2.0	1.0	3.0	New
Structure	2.0	2.0	4.0	LCAM
Thermal (w/Boom Radiator)	10.0	4.0	14.0	New
JIMO Adapter	2.0	1.0	3.0	New
RF Transceiver	2.0	6.0	8.0	New
RF Amplifier	3.0	6.0	9.0	New
High Gain Antenna	5.0	5.0	10.0	New
Overall Totals	36.4	34.4	70.8	
Notes: * Mass margin includes radiation shielding				

emitted from the RPS that can affect instrument operation but this is an acceptable background noise to the instruments. A more significant concern related to the RPS is the long term dose [potentially $\geq$ 50 krads (Si)] imposed over the 13-year lifetime of the GSO mission. Figure 2.3.1-12 illustrates the total dose environment for 13 years as a function of the distance from the center of the GPHS module of nuclear material.

This relatively small magnitude of the RPS dose must be compared to the significantly larger magnitude of the high energy particle radiation in the Jovian environment. The final destination of one of the GSOs is in orbit about Europa. This location is one of the most intense regions of the Jovian radiation belts. Over only a short duration (~30 days) in orbit about Europa, the expected dose behind 100 mils of aluminum is about 0.8 Mrad (Si) as shown in Figure 2.3.1-11. Thus, the dose from the Jovian environment is over 10 times larger than that expected from the RPS in the current GSO configuration.

The GSO components that are sensitive to this environment would be radiation hardened designs and would use spot shielding to mitigate the radiation effects.

2.5.1.13 *Alternate RPS Power System*

The unidirectional heat flow configuration of the chosen RPS for the proposed GSO configuration is near optimum for the thermal control and attitude concept for the GSO. Other architectures that rely on radial heat flow through radial mounted thermocouples could be employed, but would be less desirable because of the fin radiator system that is typically used. It is conceivable that the configuration could be designed around a fin-based RPS but more complex thermal control surfaces on the electronics bays would be necessary as well as a heat pipe arrangement that would conduct sufficient heat to the lower payload module for thermal control purposes.

A possible end-mounted Stirling convertor could retain the advantage of the unidirectional heat flow configuration. Also, a significant improvement in efficiency (~15% versus 7%) could provide more power (~20 We) for spacecraft operations. It is not clear, however, that a Stirling system this small (with one GPHS module) is a reasonable design at this time.

2.5.2 Additional RPS-Enabled Subsatellite Missions

Other small magnetospheric missions about the outer planets are possible using a small-RPS and a more capable mother ship such as JIMO. Although no detailed studies have been completed for these other missions, their existence seems possible by analogy to the GSO mission.

One such mission using a small-RPS could be dedicated to long term polar measurements of Jupiter's magnetosphere. A capable F&P payload could return new information about the variations and long term characteristics of the magnetosphere while JIMO continued on to its primary goals of orbiting the Galilean satellites.

Orbiters of other scientifically interesting satellites such as Titan and Triton within the Cronian and Poseidean systems could also be enabled by a GSO-like spacecraft carrying an F&P payload. Delivery by a Nuclear Electric Propulsion (NEP) class mother ship (e.g., JIMO) to these locations could allow the placement and relay communications capabilities required by the satellite orbiter.

Finally, this class of orbiter could act as a local relay satellite from surface stations to allow short-range intermediate relay of telemetry when the mother ship was in another location in the planet's system.

2.5.3 Summary and Conclusions

A scientifically significant orbiter of the satellites of a giant planet is conceptually possible using a small-RPS powered spacecraft in conjunction with a supporting spacecraft within the planet's satellite system. The Galilean Satellite Orbiter (GSO) spacecraft would rely on the JIMO capabilities for delivery to the satellite orbit as well as telecommunications support for scientific experiments and telemetry return via relay. Other enabling capabilities include advanced micro spacecraft components and instruments which are small, lightweight and require very low power.

The small instruments would enable nearly continuous fields and particles data acquisition and storage. The RPS power would be augmented with battery power for brief playback intervals using a relatively high powered telecommunications relay link. A suggested experiment includes a one-way carrier signal from JIMO to measure the gravitational perturbations of the GSO orbit (using Doppler variations in the carrier) thereby measuring the gravitational field and mascons of the satellite. Finally, a small imaging capability exists for periodic observations of the satellite's surface as well as a possible role as an inspector of the JIMO mother ship.

Even with the mission and system design constraints imposed by the small-RPS power source, a viable science mission and spacecraft design is possible in the future era of technology of 2015. It is in this era that the low powered avionics and instruments would be available that would also enable this mission.

Although this design concept is very preliminary, it does suggest that a mission like this would be enabled using a small-RPS power source.

2.6 DEPLOYABLE MINI-PAYLOAD APPLICATIONS

Deployable mini-payloads are envisioned as small, standalone instruments that could be enabled via small-RPS technology and deployed from a mother vehicle such as a rover or proposed JIMO spacecraft to points of interest within the Solar System [44]. They could be used for long-duration science missions or as positional beacons for rovers or other spacecraft. There are two applications considered for this concept: (1) seismic monitoring stations deployed by a rover or aerobot, and (2) passive fields and particles stations delivered by a mother spacecraft. Both applications could be designed to operate in vacuum or in environments with atmosphere.

2.6.1 Seismic Monitoring Stations

Seismic monitoring stations would detect and measure the target body's seismic activity to determine its interior structure, composition, and physical state. These stations could be deployed from a rover or aerobot.

The station as conceived would be designed to be simple, low-cost, low-power, and lightweight. It would contain five key subsystems: a science instrument, avionics, communications, thermal, and power. The station would be powered via small-RPS technology. Figure 2.6.1-1. shows a potential concept for a seismic monitoring station. With the exception of thermal and power, all of the subsystems would be housed within the upper portion of the seismic monitoring station. The small-RPS would make up the bottom structure, along with thermal radiators that are used to reject excess heat to the external environment and to provide a stable base.

2.6.1.1 *Science Goals*

Seismic monitoring stations would allow seismic activity to be monitored on bodies in both the inner and outer solar system, in areas of limited sunlight, over long periods of time.

The outer solar system contains bodies such as the icy Jovian moons, Europa, Callisto, and Ganymede. Scientists believe an ocean may lie beneath Europa's icy surface, making it one of the best candidates for potential life in our solar system [45]. A network of seismic monitoring stations could monitor Europa's seismic activity to determine crustal thickness. The stations could also determine if seismic and perhaps cryovolcanic activity on Europa is driven by tidal forces, as on Earth [46]. Similarly, Ganymede has a distinct grooved terrain that appears to be tectonically produced. Seismic monitoring stations could determine crustal thickness and structure and provide insight on how these grooves were formed.

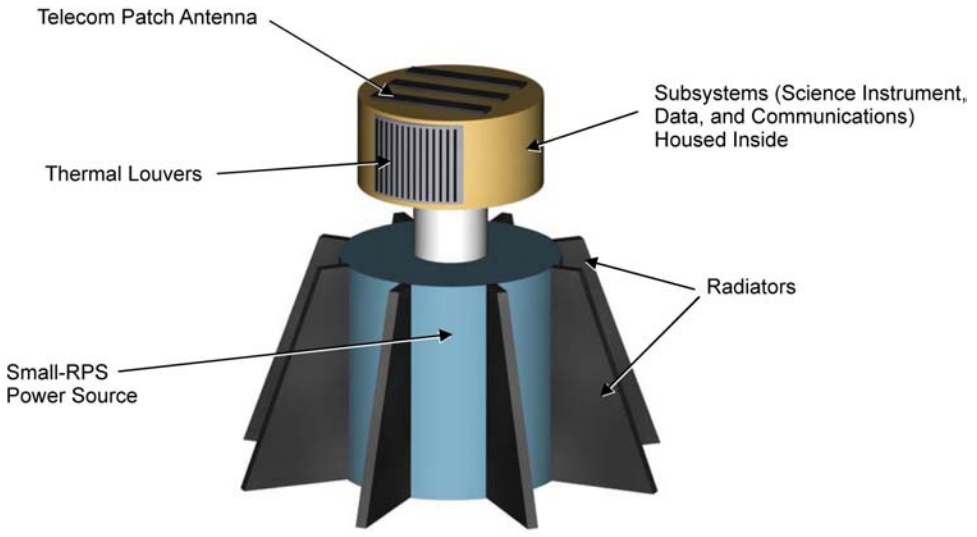

Figure 2.6.1-1. Configuration Concept for a Seismic Monitoring Station

The inner solar system includes areas such as the polar regions of both the Moon and Mars. A seismic monitoring station could be deployed in the shadowed craters of the Moon to observe lunar quakes, learn about subsurface conditions, seismically-image the subsurface, and aid in understanding how the Moon was formed. Seismic activity is also believed to have occurred on Mars, making it another viable candidate for seismic monitoring [47].

2.6.1.2 *Mission Goals*

Seismic monitoring stations could be piggybacked onto larger missions involving a rover or aerobot, the "mother vehicle." The mother vehicle would ultimately deploy an array of seismic monitoring stations for long-term monitoring. The stations would communicate with the mother vehicle, which would relay data back to Earth.

2.6.1.3 *Mission Architecture Overview*

Because they are small and lightweight, many seismic monitoring stations could be loaded onto a rover or aerobot for eventual deployment. The science community could determine where to place the monitoring stations before launch, based on prior knowledge of the planet; or the mother vehicle could determine the location based on information it obtains on or near the surface.

If necessary, the rover could prepare the surface for deployment (e.g., remove debris or obstacles) before the rover arm deploys the station onto a suitable location, ensuring adequate contact with the ground. One rover could deploy the stations to a localized area of the planet for surface mapping, as illustrated in Figure 2.6.1-2. Two rovers could be used to deploy seismic monitoring stations to different regions of a planet, similar to the Mars Exploration Rovers. Deployment via rover could be used to study localized areas and is limited only by the range of the rover itself.

Alternatively, aerobots could deploy the seismic monitoring stations to achieve a more global reach. This concept is similar to the aerial drop-off probes proposed for Titan. A balloon or blimp could descend near the planet's surface, release the seismic monitoring station, ascend towards the next monitoring location and repeat until all of the stations were deployed (Fig. 2.6.1-3.).

Seismic monitoring stations would communicate with a mother vehicle (e.g., an orbiter or rover) that communicates with Earth. The mother vehicle would provide position and attitude information for these stations at the time of drop-off, allowing the stations to be as simple as possible. The

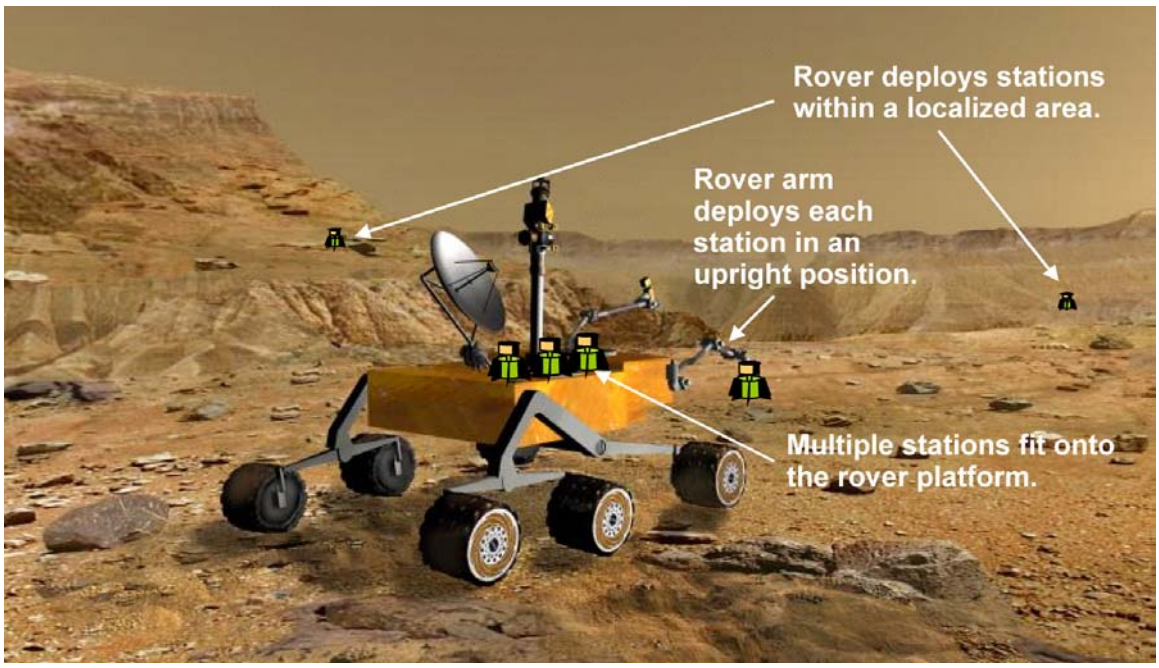

Figure 2.6.1-2. Conceptualization of Seismic Monitoring Stations Being Deployed via a Rover for Monitoring a Localized Area

stations could potentially take measurements for over ten years, conceivably limited only by the lifetime of the relay element.

2.6.1.4 *Power Source Trade Study*

As conceived, seismic monitoring stations using RPS power are ideal for missions that take place anywhere there is limited, intermittent, or no solar insolation. These types of missions cannot practically use solar power and require a long-duration presence that cannot be supported by batteries.

Small-RPS power systems could enable these types of missions because they provide a long-lasting, power source that provides thermal energy (in the form of excess heat), which can be used to maintain electronics within operating temperature ranges.

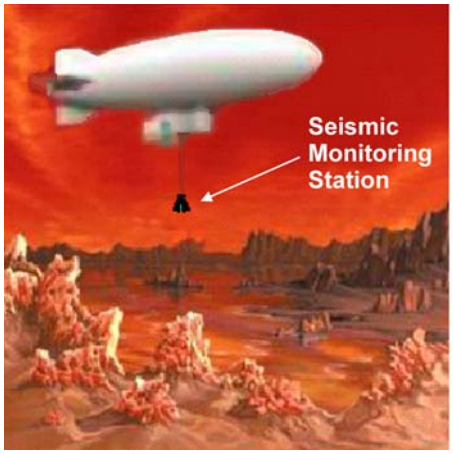

Figure 2.6.1-3. Conceptual Deployment of a Seismic Monitoring Station by an Aerobot

2.6.1.5 *Small-RPS Characteristics*

The power source proposed for this type of mission is a conceptual single-fuel capsule GPHS-derivative using thermoelectric power conversion technology [48], illustrated in Figure 2.6.1-4. It has a mass of approximately 2 kg, produces approximately 60 Wt of thermal output, and has 3 We of electrical output (BOL) with a 5% conversion efficiency. The TE operating temperatures are approximately 550 °C (hot side) and 155 °C (cold side).

2.6.1.6 *Science Instrument*

The science instrument proposed for this application is a JPL microseismometer [44], illustrated in Figure 2.6.1-5. This instrument has a micromachined silicon suspension. The suspension has a 10 Hz resonance, a 6×10^{-9} m/s^2/Hz noise floor, and a UHF capacitive displacement with a sensitivity of 5×10^{-13} m/Hz. The transducers are arranged in a tetrahedral configuration to provide 3 components of acceleration, in addition to a redundant transducer. It measures 5 cm along each edge. Its acceleration sensitivity is better than 10^{-8} m/s^2 over a frequency range of 0.01–100 Hz.

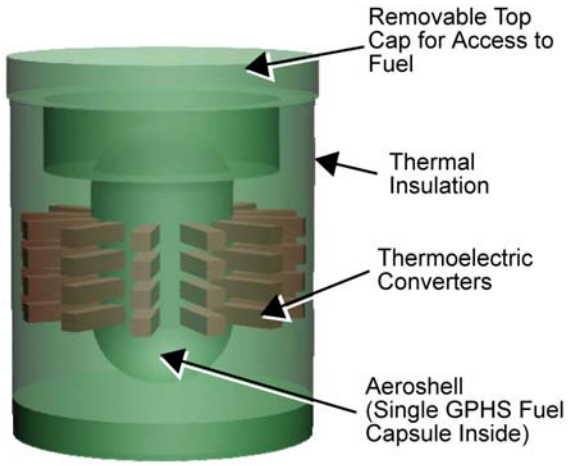

Figure 2.6.1-4. RPS Power Source Concept for the Seismic Monitoring Station

2.6.1.7 *Data*

The microseismometer would continuosly make seismic measurements during the science mission, and the avionics subsystem would process it. The proposed avionics subsystem is based on the one designed for the MUSES-CN Nanorover [3], and would consist of a Mongoose CPU, SRAM, EEPROM, digital/analog input/output, and power supplies and switches. The flight electronics would be based on the Synova R3000 32-bit flight processor, fabricated on the Honeywell Rad-Hard Foundry production line, and a radiation hard custom gate-array. In addition, 2 MBytes of rad-hard RAM and 1 MByte of rad-hard EEPROM would be used.

The output data rate from the microseismometer depends on the sampling rate, which in turn depends on the seismic frequency range of interest. Sampling at 5 Hz with 16-bit samples (each of three axes) yields a total data rate of ~240 bits/s. Achievable data compression for this instrument was not assessed but could potentially reduce the data rate significantly.

2.6.1.8 *Communications*

The communications subsystem at the seismic station would be based on that developed for the MUSES-CN mission. It would consist of an L-band (1900 MHz PCS) transceiver with a matching transceiver on the mother vehicle. This system was designed to provide a 9.6 kbits/s data rate at a range of 20 km at up to 1 radian off-axis of the station top surface normal. The receive antenna must be pointed at the station within 0.1 radian. This system could conceptually provide a data rate on the order of 96 bits/s to an orbiter 200 km away (assuming the data rate scales as $1/R^2$).

The telecom subsystem would be fabricated from commercial rad-hard GaAs packaged parts. Clock recovery and Manchester decoding would be implemented in a radiation hardened field-programmable gate array. The MUSES-CN antenna is a right-hand circularly polarized square patch with an offset-pin feed, but other antenna configurations could also be considered. The seismic station's communication system would occupy a single board with dimensions of approximately 12 cm x 6 cm x 2 cm.

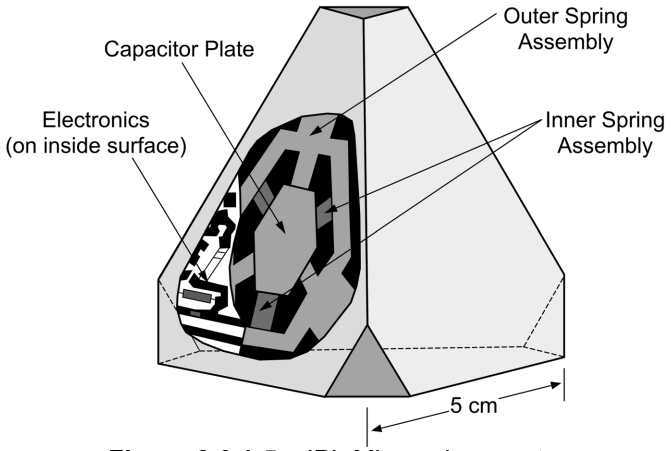

Figure 2.6.1-5. JPL Microseismometer

2.6.1.9 *Thermal*

The baseline thermal control system of the seismic monitoring station would rely on using passive means to maintain and regulate system temperatures, and would include multilayer insulation (MLI), low thermal conductance materials, louvers, and/or thermal coatings. In addition, RPS waste heat could be used to keep the station electronics warm, and radiator fins would be used to radiate (or conduct) excess heat to the local environment. Preliminary conductive heat transfer calculations indicate that on the surface of Titan (T~94 K), one of these stations could passively maintain an interior temperature of 155°C using ~25 Wt. The remaining waste heat would be rejected via conductive coupling to the Titan atmosphere and regulated using thermal louvers. A detailed internal thermal design has not yet been performed.

2.6.1.10 *Power*

The seismic monitoring station would have two basic power modes: *Science Data Acquisition* (Mode A), or *Science Data Acquisition with Downlink* (Mode B). In Mode A, the station collects seismic data continuously and stores it in internal memory. This mode uses 1.37 We of power (including a 50% contingency). In Mode B, the station collects data continuously while downlinking it to the rover or orbiter for eventual relay to Earth. This mode uses 2.49 We of power (including a 50% contingency). These modes are summarized in Table 2.6.1-1, along with the power required for each subsystem.

Table 2.6.1-1. Seismic Monitoring Station Power Modes

Subsystem	Mode A (W)	Mode B (W)
Instrument	0.10	0.10
C&DH	0.81	0.81
Telecom	(off)	0.75
Subtotal (CBE)	0.91	1.67
50% contingency	0.46	0.83
Total	1.37	2.49

The power subsystem hardware is based on a concept developed by JPL's Team A for a microrover milliwatt radioisotope power source [49]. The power subsystem would take the electrical power output from the small-RPS and convert it to the different voltages required for the various seismic monitoring station subsystems. It would also provide power regulation and switching functions. This particular design includes a small Li-Ion battery to accommodate applications with short periods of higher power use. Figure 2.6.1-6. shows a block diagram of the seismic monitoring station's power electronics and subsystems.

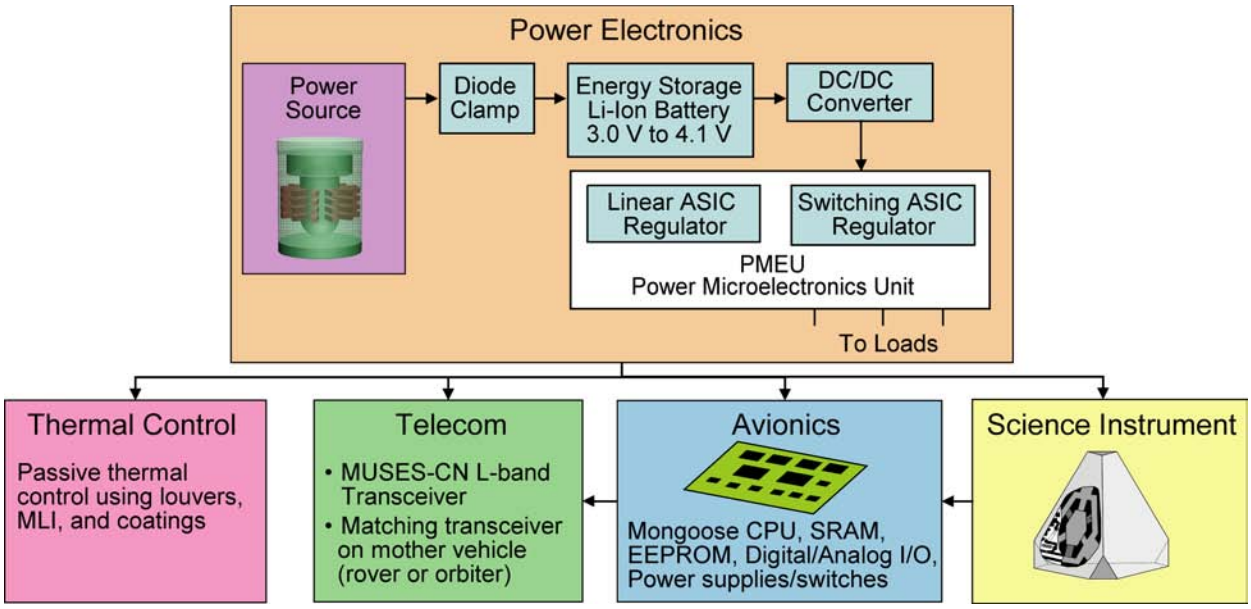

Figure 2.6.1-6. Block Diagram Showing How the Seismic Monitoring Station's Subsystems Integrate Together

2.6.1.11 *Mass*

Seismic monitoring stations would be designed to be lightweight, with a total mass of only 7.1 kg including 50% contingency (Table 2.6.1-2). The heaviest subsystem of the seismic station would be the RPS power source estimated at 3 kg, followed by the structure (with integrated thermal control fins) weighing ~2 kg. The remaining subsystems (instruments, avionics, communications, battery and power distribution, and thermal) would jointly weigh less than 1.5 kg.

Table 2.6.1-2. Seismic Monitoring Station Mass Summary

Subsystem	Mass (kg)	Margin (50%) (kg)	Mass with Margin (kg)
JPL Microseismometer	0.10	0.05	0.15
Avionics	0.15	0.08	0.23
Communications	0.53	0.26	0.79
Thermal	0.30	0.15	0.45
Small-RPS	2.00	1.00	3.00
Battery and Power Distribution	0.30	0.15	0.45
Structure	1.32	0.66	1.98
TOTAL:	**4.7**	**2.35**	**7.1**

2.6.1.12 *Radiation*

The seismic monitoring station would be exposed to externally produced (natural) and internally produced radiation during the course of its mission. Key sources of natural radiation include the Van Allen radiation belts traversed during the Earth egress, cosmic radiation received during the cruise phase, and the inherent radiation environment of the final mission destination. As a result, the seismic station would potentially be exposed to gammas, neutrons, and other high-energy particles. Internal radiation would be generated from the decay of the plutonium fuel within the GPHS fuel capsules and from resulting secondary fission reactions that occur due to fuel impurities.

The seismic monitoring station would be inherently radiation tolerant due to the selected use of radiation hardened components and subsystems as previously discussed. However, as external radiation levels are site specific, they would need to be assesed for a specified location and dura-

tion in order to determine whether any additional shielding would be necessary to meet the station's lifetime requirements. It is expected that the external radiation environment, not the relatively mild RPS environment, would drive the total radiation dose and any shielding requirements.

2.6.1.13 *Alternate RPS Power System*

Other RPS power systems that could be used for this concept include a GPHS module-based RPS using only one fuel capsule (with the remaining three capsule "slots" containing inert fuel capsules to maintain the overall GPHS mass properties). However, the larger size and mass of such an RPS would not be as efficient as the one-capsule RPS assumed in this study.

2.6.2 Passive Fields and Particles Monitoring Station

Passive fields and particles (PFP) monitoring stations could be used to study magnetic fields and radiation levels, and would be deployed from a rover or mother vehicle.

As with the seismic monitoring stations, each PFP station would be designed to be a simple, low-cost, and lightweight, and would be powered by a small-RPS power source. Each station would contain five main subsystems: science instruments, avionics, communications, thermal, and power.

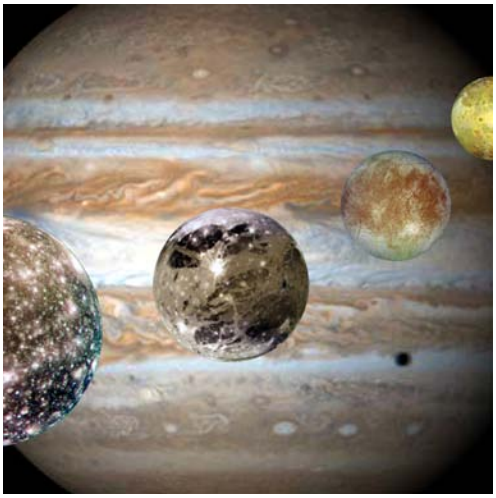

Figure 2.6.2-1. Jupiter and its Galilean Satellites

2.6.2.1 *Science Goals*

Passive fields and particles monitoring stations could be deployed in Jupiter's magnetosphere, a large region of electrically charged particles and magnetic fields surrounding the planet (Fig. 2.6.2-1.). Jupiter's magnetosphere resembles a smaller version of that of the Sun, and thus studying it would contribute to our knowledge of the behavior and evolution of magnetospheres in general [50].

The science goals of the passive fields and particles (PFP) monitoring station would be to conduct F&P experiments observing the plasma environment in Jupiter's magnetosphere either in orbit around Jupiter itself or around its inner moons (e.g., Io, Europa, Ganymede). This could involve a search for evidence of subsurface liquid water in Jupiter's icy moons using magnetic field measurements, the interaction of the moons with the Jovian magnetosphere, the radiation environment of the inner moons, and studying the structure of the satellites' magnetospheres and ionospheres.

2.6.2.2 *Mission Goals*

This would be a simplified version of the fields and particles subsatellite concept (Section 2.5), having no propulsion, using passive gravity gradient stabilization, and having a small Active Pixel Sensor (APS) star camera to provide attitude knowledge.

2.6.2.3 *Mission Architecture Overview*

The PFP stations would rely on a mother vehicle for launch, deployment, and data transmission back to Earth. They could be launched on a spacecraft as part of a larger mission involving a rover or mother vehicle. Because they would be designed to be small and lightweight, multiple passive fields and particles monitoring stations could be loaded onto the mother vehicle. Deployment of the PFP stations would be performed by the mother vehicle once the desired Jovian orbit had been obtained.

2.6.2.4 *Power Source Trade Study*

RPS-powered PFP monitoring stations could be used on missions that cannot use conventional solar power (e.g., due to limited or no insolation) and on missions that would require a long-dura-

tion presence that could not be supported by batteries. The RPS power system would be well-suited for PFP missions at Jupiter and beyond.

Small-RPS power systems could enable these type of missions because they are long-lasting and reliable, and would provide thermal energy (in the form of excess heat) that could be used to maintain electronics within operating temperature ranges without resorting to electric heaters.

2.6.2.5 *Small-RPS Characteristics*

The power source for this type of mission would be a conceptual GPHS-derivative using 2 fuel capsules and TE power conversion technology [48]. As conceived, it would have a mass of approximately 3 kg, produce approximately 125 We of thermal output (BOL), and generate 6.25 We of electrical output (BOL) with a 5% conversion efficiency. The TE operating temperatures are assumed to be approximately 550°C (hot side) and 155°C (cold side).

2.6.2.6 *Science Instruments*

The payload envisioned for this mission is based on the Multimission Space and Solar Physics Microspacecraft [41], and would consist of an energetic particle detector, an electron and ion analyzer, and a magnetometer.

2.6.2.7 *Data*

The data rates for the conceptual PFP monitoring stations would be similar to those of the larger GSO spacecraft discussed in Section 2.5.1.6.

2.6.2.8 *Communications*

All data generated by the PFP station would be stored on a solid state recorder (SSR) until it was possible to transmit the data back to the mother vehicle using the PFP station low-power communication system. The mother vehicle, assumed to possess a high-power communication system, would then relay the data back to Earth for scientific analysis.

2.6.2.9 *Thermal*

Thermal control would be accomplished by a combination of thermal insulation, heat pipes, and louvers. Excess heat from the RPS could be used to keep critical subsystems warm. Radiators would be used to reject excess heat.

2.6.2.10 *Power*

The PFP monitoring station would be operated in one of two mutually exclusive power modes. Mode A would be the nominal operating mode (Table 2.6.2-1) where all four instruments would be powered-on and either taking measurements or in hot standby (i.e., to stay warm during the long cruise phase). Sufficient electrical power would be available from the RPS unit (5.2 We at EOM) such that this mode could be sustained.

Mode B would be the nominal telecom mode, and is similar to Mode A except that the PFP communications system would be activated for transmitting or receiving data from the mother vehicle. This mode would require ~8.6 We of total power, which is 3.4 We more than the EOM power output of the RPS. Thus, a supplemental battery would be required to carry the peak loads during the communications events.

2.6.2.11 *Mass*

Each PFP station would have a total mass of approximately 10.8 kg, including 50% margin (Table 2.6.2-2). The RPS system would comprise 40% of the system mass at 4.5 kg, followed by the structure at 3.2 kg and the instruments at 2 kg. The remaining subsystems (avionics, communications, and thermal) would together have a mass of ~1 kg.

Table 2.6.2-2. Passive Fields & Particles Monitoring Station Mass Summary

Subsystem:	Mass (kg)	Margin (50%) (kg)	Mass with Margin (kg)
Instruments			
Energetic Particle Detector	0.30	0.15	0.45
Electron and Ion Analyzer	0.68	0.34	1.02
Magnetometer	0.29	0.14	0.43
Active Pixel Sensor Camera	0.06	0.03	0.09
Instrument Electronics Module	0.10	0.05	0.15
Avionics (incl. Power Electronics)	0.15	0.08	0.23
Power Source (2-Fuel-Capsule GPHS Derivative)	3.00	1.50	4.50
Communications	0.15	0.08	0.23
Thermal Control	0.30	0.15	0.45
Structure	2.16	1.08	3.24
TOTAL:	7.2	3.6	10.8

Table 2.6.2-1. Passive Fields & Particles Monitoring Station Power Modes

Subsystem	Mode A (W)	Mode B (W)
Instruments		
Energetic Particle Detector	0.3	0.3
Electron and Ion Analyzer	1.1	1.1
Magnetometer	0.3	0.3
Active Pixel Sensor Camera	0.4	0.4
Instrument Electronics Module	0.3	0.3
Avionics (incl. Power Electronics)	0.8	0.8
Communications	(OFF)	2.5
Subtotal:	3.2	5.7
50% Contingency	1.6	2.9
TOTAL:	4.8	8.6

2.6.2.12 *Radiation*

The external radiation environment would generally dominate the total dose to the passive fields and particles monitoring station. The baseline PFP would use radiation-hardened components in order to tolerate the radiation exposure during the long cruise phase and the strong radiation environment about Jupiter. Future detailed analyses would need to be performed to assess whether additional shielding would be required to meet the mission lifetime requirements.

2.6.2.13 *Alternate RPS Power System*

This concept could potentially use an RPS using two fuel capsules in an existing GPHS module (with the remaining two capsule slots filled with inert material to maintain the GPHS module mass properties). This could have the advantage of a design with an existing aeroshell, but would likely have greater mass and volume than the two-capsule RPS baselined in this study.

2.6.3 Summary and Conclusions

This study has introduced a new class of conceptual low power, long-lived deployable mini payloads that could potentially be enabled using small radioisotope power systems. One such science payload is a seismic monitoring station that would be powered by a conceptual small-RPS unit for up to 10 years using a single GPHS fuel capsule with an estimated 2.6 We (EOM) output. The technology for the seismic stations is at a moderately high state of development with the exception of the RPS. Significant design heritage would be borrowed from the MUSES-CN Nanorover, upon which both the avionics and communications subsystems are based. Therefore, it is con-

cluded that seismic monitoring stations could potentially be capable of supporting missions as early as 2011, given the availability of the specified RPS power system. A second science payload introduced was a conceptual passive fields and particles station designed to operate about Jupiter with a nominal 10-year mission lifetime. This payload would be powered by a conceptual RPS using two GPHS fuel capsules with an estimated 5.2 We (EOM) output, and would be supplemented by a secondary battery system used to carry the peak loads during communications events. Both the seismic monitoring station and the passive fields and particles monitoring station concepts would utilize a mother vehicle for delivery to the target destination and for communications back to Earth. Based on this initial analysis, it is believed that deployable mini-payloads powered by small-RPS systems could provide an exciting new capability for the science and mission communities.

2.7 MISSION STUDIES SUMMARY

The results of the mission studies, literature survey, and the survey of the Mars scientific community indicate that there are numerous scientifically valuable missions and applications that could be enabled by small-RPS technology. A total of fifty-one mission concepts were identified, with 24 using GPHS-class RPSs, 13 using fractional GPHS-based RPSs, and 14 using RHU-based RPSs (Table 2.7.1-1). As the capability of each mission increased, so generally did the power requirements. Supplementary batteries or super-capacitors were required for most designs to accommodate the peak loads encountered during high-power activities, most notably, communications, mobility (rovers) and certain instruments.

The GPHS-class RPS can potentially enable twenty-four missions (47% of total) that have power demands in the range of 12.5 We to ~50 We. This power range corresponds to an RPS using one to four GPHS-modules with a 5% efficient thermoelectric converter. An RPS using a single GPHS-module (12.5 We) was found sufficient to power Lander spacecraft and subsatellites with relatively sophisticated instrumentation suites including Raman spectroscopes, LIBS, plasma wave spectrometers and Doppler extractors. An RPS using two to four GPHS-modules is sufficient to power a Mars Exploration Rover (MER)-class vehicle with instrumentation similar to that utilized on MER (e.g., imagers, APXS, RAT and Mini-TES). Nearly eighty percent of the GPHS-class missions could be enabled with an RPS using a single GPHS module, whereas the remaining twenty percent (typically Rover concepts) required two to four GPHS modules.

Mission concepts requiring more than 12.5 We of power assumed a stackable RPS design, with each RPS containing one GPHS module. Depending on the power level, additional RPS modules could be stacked together in a building block approach, thus maintaining a standardized RPS design. Acceleration load tolerance is a significant issue, and nearly half of the GPHS-class missions require the RPS be capable of surviving spacecraft accelerations greater than 40g, typically due to launch and landing loads. Seven concepts require spacecraft acceleration tolerance up to 600g, and four concepts (known as Rough-Landers) require a maximum g-tolerance of 5000g. Mission environments include both vacuum (e.g., Lunar rover, Europa lander) and atmosphere (e.g., Mars and Titan rovers). Consequently, the ideal multi-mission GPHS-class RPS is lightweight, stackable, capable of withstanding a maximum spacecraft acceleration of 5000g, and can operate in atmosphere or vacuum.

Fractional GPHS RPSs (using 1 to 3 fuel capsules) were found sufficient for small standalone seismic and weather monitoring stations, as well as Pathfinder-class mini-rovers. The moderate power output (~3 to 9 We) of this RPS would be ideal for deployable mini-payloads using low-power instrumentation and communicating over a relatively short-range. Rovers using a fractional GPHS-based RPS are feasible, but somewhat limited by the need for longer and more frequent battery charging to accommodate the relatively large power draws during traverse and communications. The smaller size of the fractional GPHS-powered rover also limits the range of terrain over which the rover can navigate due to smaller wheel size and large mobility power requirements. Approximately 25% of the fractional GPHS RPS missions required the RPS to tolerate spacecraft accelerations up to 600g. The mission environment was evenly distributed between vacuum and atmosphere. Thus, the ideal multi-mission fractional-GPHS RPS would tolerate spacecraft accelerations up to 600g, and operate in vacuum and atmosphere.

The RHU-based RPS potentially enables a specialized class of micro-landers and micro-rovers requiring between 10 mWe to several hundred milliwatts of electrical power. This RPS concept uses 1 or more RHUs depending on the required power level and efficiency of the power converter and thermal insulation. The RHU-based RPS is sufficient to power a Pascal-type micro-lander and its derivatives that use low-power electronics and instrumentation. Micro-rovers based on the Muses-CN architecture [3] are conceptually feasible using an RPS powered from just one RHU [3], with additional capability afforded by more RHUs. Mission concepts using low power RHU-RPSs rely strongly upon rechargeable batteries or ultra-capacitors to meet the basic power

Table 2.7.1-1. Mission Concepts and Applications Potentially Enabled by Small-RPS Technology

Mission #	Heat Source	Mission or Application	Power Level (Electrical)	RTG Configuration (Note1)	Spacecraft G-Load	Environmt	Mission Class (Estimated) (Note 2)	Time Frame
1	RHU	Pascal Micro-Lander (Mars)**	27 to 40 mW	1 to 2 RHUs	40 to 600g	Atmosphere	Scout	2009
2	RHU	Pascal-Type Micro-Lander (Other Bodies)*	27 to 40 mW	1 to 2 RHUs	40 to 600g	Vacuum	Scout	2009
3	RHU	Pascal Micro-Lander (Mars)**	100 mW	4 RHUs	40 to 600g	Atmosphere	Scout	2011
4	RHU	Europa Impactor Micro-Lander*	10 to ~100 mW	1 to 4 RHUs	>5000g	Vacuum	Discovery (PB) or Flagship (SA)	2015
5	RHU	Lunar Micro-Lander**	500 mW	~12 RHUs	40 to 600g	Vacuum	Discovery	2009
6	RHU	Prospecting Asteroid Mission (PAM) Micro-Sat***	300 to 400 mW	7-9 RHUs	<40g	Vacuum	New Frontiers	2020-2030
7	RHU	Saturn Autonomous Ring Array Micro-Sat***	300 to 400 mW	7-9 RHUs	<40g	Vacuum	New Frontiers	2025-2035
8	RHU	MUSES-CN Micro-Rover (RPS Derivative)*	10 to ~100 mW	1 to 4 RHUs	40 to 600g	Vacuum	Discovery	2009
9	RHU	Mars Micro-Rover (* and **)	10 to ~100 mW	1 to 4 RHUs	40 to 600g	Atmosphere	Scout	2009
10	RHU	Lunar Micro-Rover*	10 to ~100 mW	1 to 4 RHUs	40 to 600g	Vacuum	Discovery	2009
11	RHU	Titan Micro-Rover*	10 to ~100 mW	1 to 4 RHUs	40 to 600g	Atmosphere	Discovery	2015
12	RHU	Mars Science Micro-Instrument**	5 to 50 mW	1 to 2 RHUs	<40g	Atmosphere	Piggyback (PB) on MSL	2009
13	RHU	Mars Deployable Micro-Seismic Station**	10 to ~100 mW	1 to 4 RHUs	<40g	Atmosphere	Scout	2011
14	RHU	Mars Deployable Micro-Payload**	27-40 mW	1 to 2 RHUs	<40g	Atmosphere	Piggyback (PB) on MSL	2009
15	Fractional-GPHS	Lander Amorphor. Rover Array Mini-Lander***	3 to 9 W	1–3 Capsules	<40g	Vacuum	Scout	2010-2020
16	Fractional-GPHS	Mars Mini-Rover**	3 W	1 Capsule	<40g	Atmosphere	Scout	2011
17	Fractional-GPHS	Mars Deployable Seismic Station**	3 W	1 Capsule	<40g	Atmosphere	Scout	2011
18	Fractional-GPHS	Mars Mini-Rover (* and **)	6 W	2 Capsules	<40g	Atmosphere	Scout	2011
19	Fractional-GPHS	Lunar Mini-Rover*	6 W	2 Capsules	<40g	Vacuum	Discovery (Comsat Extra)	2011
20	Fractional-GPHS	Titan Mini-Rover*	6 W	2 Capsules	<40g	Atmosphere	Discovery (PB) or Flagship (SA)	2015
21	Fractional-GPHS	Mars Moon Mini-Rover*	6 W	2 Capsules	<40g	Vacuum	Scout	2011
22	Fractional-GPHS	Mars Cryobot**	3 to 6 W	1–2 Capsules	<40g	Atmosphere	Scout	2011
23	Fractional-GPHS	Seismic Station Mini-Payload*	3 W	1 Capsule	40 to 600g	Atmosphere	SMEX (PB)	2009
24	Fractional-GPHS	Weather Station Mini-Payload*	3 W	1 Capsule	40 to 600g	Atmosphere	SMEX (PB)	2009
25	Fractional-GPHS	Seismometer Station Mini-Payload*	3 W	1 Capsule	40 to 600g	Vacuum	SMEX (PB)	2009
26	Fractional-GPHS	Mars Mini-satellite**	3 W	1 Capsule	<40g	Vacuum	TBD	2011
27	Fractional-GPHS	Fields and Particles Mini-Payload*	6 W	2 Capsules	40 to 600g	Vacuum	SMEX (PB)	2009
28	GPHS	Lunar Soft Lander*	12.5 W	1 GPHS	< 40g	Vacuum	Discovery	2009
29	GPHS	Europa Lander*	12.5 W	1 GPHS	40 to 600g	Vacuum	Discovery (PB) or Flagship (SA)	2015
30	GPHS	Titan Moon Lander*	12.5 W	1 GPHS	40 to 600g	Atmosphere	Discovery (PB) or Flagship (SA)	2015
31	GPHS	Ganymede Lander*	12.5 W	1 GPHS	40 to 600g	Vacuum	Discovery (PB) or Flagship (SA)	2015
32	GPHS	Callisto Lander*	12.5 W	1 GPHS	40 to 600g	Vacuum	Discovery (PB) or Flagship (SA)	2015
33	GPHS	Lunar Lander*	12.5 W	1 GPHS	40 to 600g	Vacuum	Mid-X	2009
34	GPHS	Landers for other bodies in vacuum*	12.5 W	1 GPHS	40 to 600g	Vacuum	Discovery (PB) or Flagship (SA)	2009
35	GPHS	Landers for other bodies with atmosphere*	12.5 W	1 GPHS	40 to 600g	Atmosphere	Discovery (PB) or Flagship (SA)	2009
36	GPHS	Mars Rough Lander*	12.5 W	1 GPHS	600 to 5000g	Atmosphere	Mid-X	2009
37	GPHS	Mars Network Rough Lander*	12.5 W	1 GPHS	600 to 5000g	Atmosphere	Mid-X	2009
38	GPHS	Titan Rough Lander*	12.5 W	1 GPHS	600 to 5000g	Atmosphere	Discovery (PB) or Flagship (SA)	2015
39	GPHS	Europa Rough Lander*	12.5 W	1 GPHS	600 to 5000g	Vacuum	Discovery (PB) or Flagship (SA)	2015
40	GPHS	Callisto Orbiter Subsatellite*	12.5 W	1 GPHS	< 40g	Vacuum	Mid-X (PB)	2015
41	GPHS	Ganymede Orbiter Subsatellite*	12.5 W	1 GPHS	< 40g	Vacuum	Mid-X (PB)	2015
42	GPHS	Europa Orbiter Subsatellite*	12.5 W	1 GPHS	< 40g	Vacuum	Mid-X (PB)	2015
43	GPHS	Communications Relay Satellite*	12.5 W	1 GPHS	< 40g	Vacuum	Discovery	2009
44	GPHS	Outer Planets Magetosphere Subsatellite*	12.5 W	1 GPHS	< 40g	Vacuum	Mid-X (PB)	2015
45	GPHS	Mars Rover*	25 to 50 W	2 to 4 GPHSs	< 40g	Atmosphere	New Frontiers	2011
46	GPHS	Lunar Rover*	25 to 50 W	2 to 4 GPHSs	< 40g	Vacuum	New Frontiers (excludes ComSat)	2011
47	GPHS	Titan Rover*	25 to 50 W	2 to 4 GPHSs	< 40g	Atmosphere	New Frontiers	2015
48	GPHS	Titan Amphibious Rover*	12.5 W	1 GPHS	< 40g	Atmosphere	SMEX (PB) or Flagship (SA)	2015
49	GPHS	Mars Moon Rover (Phobos and Deimos)*	25 to 50 W	2 to 4 GPHSs	< 40g	Vacuum	New Frontiers	2011
50	GPHS	Rovers for other bodes in vacuum*	25 W	2 GPHSs	< 40g	Vacuum	New Frontiers	2011
51	GPHS	Venus Aerobot*	12.5 to 25 W	1 to 2 GPHSs	< 40g	Atmosphere	New Frontiers	2011

Legend

* = Mission concept identified or studied by JPL
** = Mission concept identified or studied by NASA ARC (Mars missions identified by Mars MEPAG community)
*** = Mission concept identified or studied by NASA GSFC

PB = Denotes that Indicated mission piggybacks (PB) on another mission, and does not require a separate launch vehicle or communications relay to Earth.
SA = Denotes a standalone mission that requires its own launch vehicle and communications relay to Earth.

All indicated missions are assumed to be stand-alone unless otherwise stated.
Note 1: The RTG configuration assumes a thermoelectric-based system with 5% conversion efficiency.
Note 2: Capped cost limit as a function of mission class as of last announcement of opportunity (AO):

SMEX	$120M
Mid-X	$180M
Discovery	$360M
Scout	$325M
New Frontiers	$700M
Flagship	>$700M

needs for communications, mobility and operation of instrumentation. Significant recharging times can be required to perform short duration tasks; for example, one hour of recharge may be necessary to accomplish one minute of activity. However, a key benefit of RPS technology is its long life (measured in decades); thus, infrequent operation times may be an acceptable trade in return for diminutive size. For rovers, the size of the vehicle must also be traded against terrain type, as the small wheel size of the micro-rover significantly affects its traversibility.

Fourteen RHU-based candidate missions were identified, and most have spacecraft acceleration requirements exceeding 40g (Table 2.7.1-1), due primarily to the landing loads associated with the use of airbags. One specialized lander concept forgoes the use of airbags and, instead, strikes the ground at high velocity, burying itself below the surface where it performs its mission. This concept is known as an impactor, and requires a spacecraft acceleration tolerance exceeding 5000g. Operating environment is another key consideration, and missions have been identified in vacuum (Lunar micro-rover, Europa Impactor, etc.) and in atmosphere (Pascal lander, Titan micro-rover, etc.) Consequently, the ideal multi-mission RHU-based RPS would be designed to tolerate spacecraft landing loads exceeding >5000g, and be capable of operating in vacuum and within an atmosphere.

An assessment was performed to identify Mars science community interest in small-RPS technology. Principle Investigators and Co-Is of the MEPAG were asked to provide RPS power requirements for missions they are proposing (or considering proposing) beginning as early as 2009. Eighty percent of PIs stated they could use RPS if it was available, and 12 missions were identified (Table 2.7.1-2) in the MEPAG survey. Two missions were identified by Co-Is that would ride piggyback on the proposed MSL; one as an instrument within the rover wheel (5-50 mWe), and the other a deployable science payload (27-40 mW) that would be dropped off by a rover. Two PIs were definitely planning 2011 Scout proposals for a low-power rover mission (3 We) and for multiple science stations (27-40 mWe). Five other PIs and Co-Is were considering proposals for Scout-class missions in 2011 that include a seismic network (10 mWe to 3 We), multiple science stations (100 mWe), a cryobot concept (3 to 6 W) and a mini-rover (6 We). Lastly, PIs stated they could utilize RPS power for rover concepts (10 mWe to 3 We) and for a mini-satellite (3 W). In summary, the survey of the MEPAG team has identified a user community with mission objectives that would be enabled by small-RPS technology in the range of milliwatts to a few watts (electrical), corresponding to RHU and fractional GPHS-class RPS systems.

Table 2.7.1-2. Survey of MEPAG Science Members Regarding RPS Requirements

#Missions	Class	PI and Co-I Comments	Mission # in Table 2.7.1-1
2	MSL Piggyback	Co-Is considering proposals for MSL	12, 14
2	Scout	PIs definitely planning proposals for 2011	1, 16
5	Scout	PIs and Co-Is considering proposals for 2011	3, 13, 17, 18, 22
3	Scout	PIs stated they would utilize RPS if available	9, 16, 26

3. POWER CONVERSION TECHNOLOGIES FOR SMALL-RPS SYSTEMS

The power conversion options considered for the small-RPS mission studies were restricted to technologies that were flight-proven or could be flight-qualified in time to support a 2011 mission. Thermoelectrics (TEs) and Stirling cycle engines were the only technologies deemed mature enough to meet this requirement. The following subsections review and describe the performance features of each technology.

3.1 THERMOELECTRICS

Thermoelectrics (TEs) is the only power conversion technology that has been used in the RPSs flown on past and present U.S. space missions. Radioisotope Thermoelectric Generators (RTGs), a type of RPS, have played a key role as power sources for Earth satellites, lunar surface experiments, and robotic planetary exploration. RTGs launched in the 1970s are still operating today, the two Voyager probes and the Pioneer 10 spacecraft have accrued over 25 years and 30 years of operation, respectively. Thermoelectric converters are highly reliable, easily scalable, and can be designed to be highly redundant. Furthermore, TEs generate a power output that is load following" and consequently easy to regulate. TEs technology are compact, rugged, radiation resistant, and produce no noise, vibration or torque during operation. The disadvantage of existing thermoelectrics is their relatively modest conversion efficiencies (5 to 7%), resulting in lower power densities and greater fuel requirements compared to dynamic power converters.

The fundamental physical process involved in thermoelectrics is the Seebeck effect, which is the electromotive force that arises between two dissimilar materials (i.e., metals or semi-conductors) when they are subjected to a temperature difference. Thermocouples are a common application of this effect, which is used to measure temperature. The electromotive force generated by the thermocouple is counteracted by an applied voltage, which can be used to power an electric circuit or, if large enough, a spacecraft.

A schematic representation of a thermoelectric unicouple is illustrated in Figure 3-1, and an actual unicouple is shown in Figure 3-2. The unicouple consists of individual legs of an n-type and p-type semiconductor material. The hot junction between the n and p legs is formed by bonding both legs to a hot shoe. Cold shoes are bonded to each leg and an external load completes the circuit. In an actual RTG system, multiple thermoelectrics are connected in series to produce a desired electrical voltage. Parallel connections between multiple thermoelectrics are typically made to improve reliability.

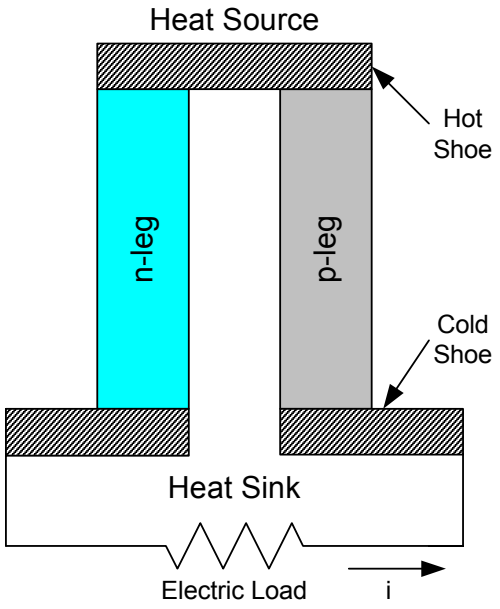

Figure 3-1. Schematic of Unicouple Powering an Electronic Circuit

Flight-proven RTGs have used two different unicouple materials: Silicon Germanium (SiGe) and Lead Telluride (PbTe) / Tellurides of Antimony, Germanium and Silver (TAGS). SiGe-based RTGs are typically used in vacuum environments (i.e., outer space) and operate at high temperatures (hot shoe ~1100°C) using a GPHS module heat source. The Voyager, Galileo, Ulysses and Cassini spacecraft all used SiGe unicouples in large (multi-hundred watt-range) RTGs. The system efficiency of an SiGe RTG can approach ~7%.

RTGs that employ PbTe–TAGS thermoelectrics can be designed to function in both vacuum and atmosphere, and typically operate at lower temperatures than SiGe RTGs (hot shoe temperature ~550°C). The GPHS heat source is used to power the PbTe–TAGS RTG, and an inert cover gas is required to prevent sublimation of the TE material. The Viking Lander, and Pioneer 10 and 11 spacecraft used PbTe–TAGS unicouples in large (multi-hundred watt-range) RTGs. The system efficiency of a PbTe–TAGS system can approach ~6.2%, but is assumed to be 5% for the mission studies documented herein.

Figure 3-2. Thermoelectric Unicouple

Bismuth Telluride (BiTe) is the third type of TE material considered in this study. BiTe has been designed for a number of terrestrial applications, and is under consideration for low power space missions using an RHU as the heat source. BiTe unicouples are designed to operate at temperatures even lower than PbTe–TAGS, with a hot shoe temperature ~250°C. To maximize efficiency, the cold-junction temperature must be as low as possible (~0°C). To minimize the required radiator area, this system is best utilized for low power applications (mWatts to few Watts) in deep space or on the surface of outer planets where the temperature is very low. The system efficiency of the BiTe RTG is highly dependent upon its operating temperature, choice of insulation, and operating environment (atmosphere or vacuum), and is assumed to be 4.5% in vacuum (using multilayer insulation) and 2.5% in a Martian atmosphere (using bulk insulation) for a small RTG system.

3.2 STIRLING

The Stirling convertor is a dynamic power conversion technology currently under development for space-based applications [10]. It is comprised of a free-piston Stirling engine and linear alternator for power conversion. The major advantages of Stirling technology are its relatively high conversion efficiency ($\geq$18%), high power density, compact size and scalability. Greater conversion efficiency means that a Stirling-based RPS would require less plutonium fuel than an equivalent-power thermoelectric RPS, which potentially translates into lower cost. The major disadvantage of Stirling is its lack of space qualification. No Stirling convertor has ever been flown in space for power generation. However, 24 Stirling units have flown for cryocooler applications on spacecraft for both industry and government, with 684,000 operating hours in space and 759,000 operating hours total (space and ground test). Of these 24 Stirling units, 19 are still in operation.

The Stirling convertor involves a double piston system, one of which does the actual thermodynamic work of compression and expansion, and the other simply acts as a displacer to move the working fluid (typically helium) from the heating chamber to the cooling chamber. A typical free-piston Stirling convertor is shown in Figure 3-3. The low-mass displacer piston shuttles the working fluid between the hot and cold spaces of the engine through a regenerator, and the high-mass power piston delivers the mechanical work to a linear alternator. The alternator, in turn, produces AC power at a controlled frequency and voltage depending on needs of the loads. A radioisotope heat source provides the heat to the heater head of the Stirling convertor, and radiator fins or other cooling mechanisms reject the heat from the cold end. The preferred type of Stirling convertor for space power is the free piston Stirling engine (FPSE), coupled with a linear alternator, which can be configured within a hermetically sealed vessel to prevent helium loss. The FPSE would require no lubricants as there would be no contact between any moving parts.

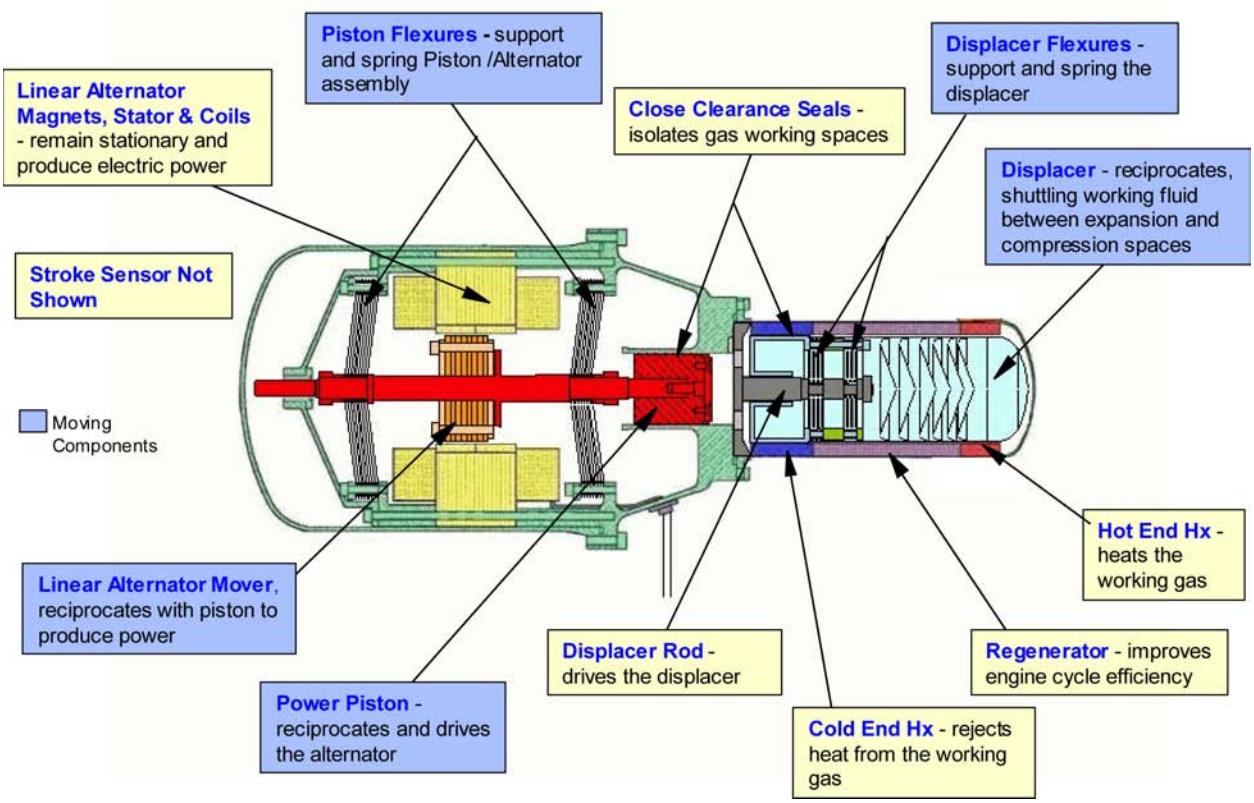

Figure 3-3. Cutaway of Stirling Convertor Integrated with a Linear Alternator in a Hermetically Sealed Pressure Vessel

Only one Stirling convertor (Figure 3-4) in the small-RPS category (mW to 10s of Watts) was identified to potentially support a 2011 mission [51]. This is a 10 We system with 18.5% conversion efficiency, and has experienced over 88,000 hours of test. This unit was designed for terrestrial use, and would need to be significantly adapted for space use. Key modifications could include using lower-mass components and increasing the acceleration tolerance to withstand launch and landing loads. The 10 We Stirling convertor requires a fractional GPHS module (single fuel capsule), or its equivalent, to generate the required 54 We of thermal power.

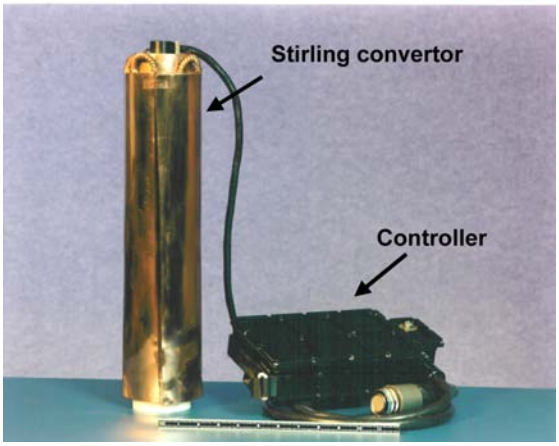

Figure 3-4. 10 We Stirling Convertor and Controller Designed for Terrestrial Applications

4. SMALL-RPS CONCEPTS

NASA has identified potential needs for small, multi-purpose RPSs for science applications on planetary surfaces and in deep space. As a result, NASA, the Department of Energy, and industry have begun to explore the range of small-RPS concepts that could use existing heat source technologies in order to satisfy near-term mission applications.

This section summarizes the small-RPS concepts that have been developed by Hi-Z, JPL/Swales, ARC, BIAPOS, and DOE/OSC over the last decade using thermoelectric conversion combined with RHU and GPHS heat sources and their derivatives. RPS system characteristics, efficiencies and key performance data are provided for each RPS concept described herein.

4.1 HI-Z MILLIWATT RPS CONCEPT

The Hi-Z RPS is a concept that was developed for general use in space, and for a number of conceptual Mars atmospheric probes and surface landers [52, 53]. This RPS system is based on a single RHU using a BiTe thermoelectric (TE) converter, and is designed to generate 40 mWe in a vacuum environment with a system efficiency of 4% (Fig. 4-1). The mass of this RPS is estimated at 0.325 kg. Tension wires and multi-layer insulation (MLI) are used to minimize heat leakage to the environment and thus enhance the system conversion efficiency. The Hi-Z design has been tested by NASA ARC under high acceleration loads as a function of impact angle relative to the RPS axis (alpha angle), and found to be capable of sustaining over 2000g of uniaxial acceleration at an alpha of 0 degrees (Fig. 4-2). For impact angles greater than 0 degrees, the maximum survival acceleration decreases quickly as a function of angle as shown in the figure. The nominal hot-side TE operating temperature is 250°C, and there is a 200 K temperature drop between hot and cold shoes. The specific power of the Hi-Z RPS is 0.123 We/kg.

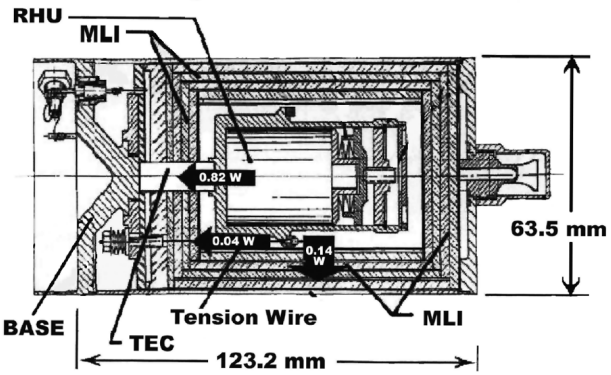

Figure 4-1. Hi-Z 40-mWe RPS Using an RHU Heat Source and BiTe Thermoelectric Conversion

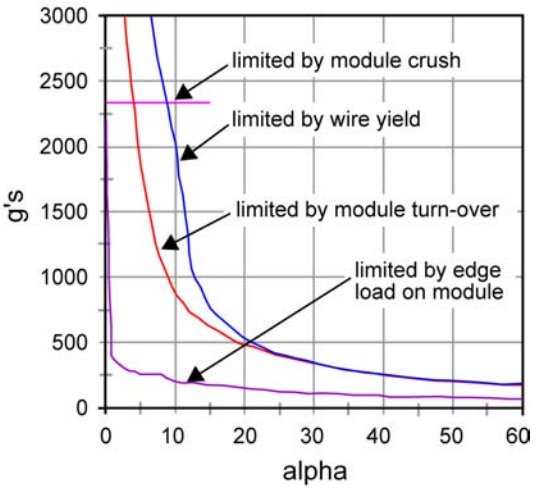

Figure 4-2. Acceleration Tolerance of the Hi-Z Milliwatt RPS as a Function of Impact Angle Relative to RPS Long-Axis

4.2 JPL/SWALES MILLIWATT RPS CONCEPT

The JPL/Swales RPS concept in based on a single RHU using BiTe thermoelectric conversion (Figs. 4-3 and 4-4). Tests conducted by Swales have demonstrated an electrical output of 20 mWe in a vacuum environment, corresponding to a system conversion efficiency of 2% [54]. The size of this RPS design is 6.4 cm diameter by 8.1 cm long (Fig. 4-3), and the total RPS mass is 0.3 kg. This unit is designed for operation in vacuum, and uses reflective heat shields and 6 titanium support wires as thermal

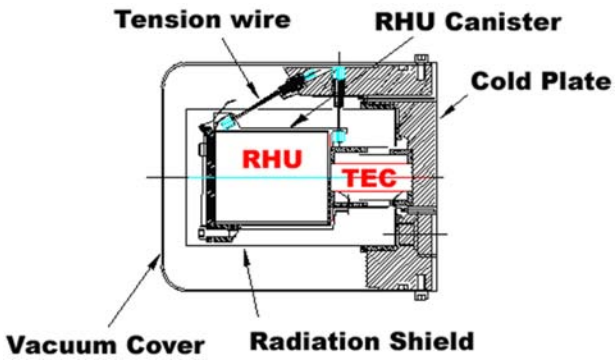

Figure 4-3. JPL/Swales Conceptual Milliwatt RPS using an RHU and BiTe Thermelectric Convertor to Generate 20 mWe

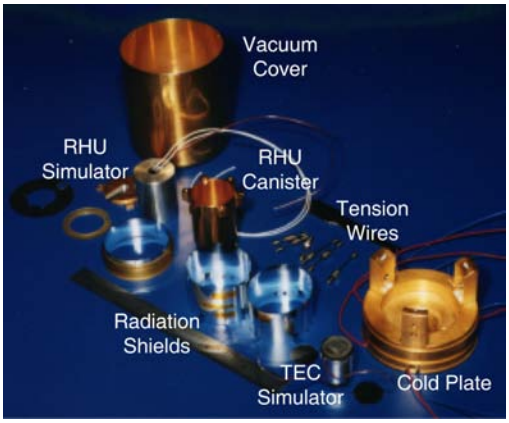

Figure 4-4. Photograph of the JPL/Swales 20 mWe RPS Design

insulation. This RPS system operates with a hot side temperature of 200°C, and a cold side temperature of 30°C. The specific power of the JPL/Swales RPS is 0.067 We/kg.

4.3 ARC MILLIWATT RPS CONCEPT

The Ames Research Center (ARC) RPS concept is based on a single RHU using a BiTe thermoelectric converter. It was initiated for the Pascal Lander mission as a system capable of generating 40 mWe of power under high acceleration loads (up to 500g). This system uses a wire suspension system (Figs. 4-5 and 4-6) that has been tested by ARC under impact loads that have the same duration as the impacts expected from the air-bag cushions for Mars missions [55]. The ARC RPS uses wire ties and multilayer insulation under vacuum to minimize heat loss and enhance system efficiency. The mass of this RPS concept is 0.121 kg, and the specific power is 0.33 We/kg.

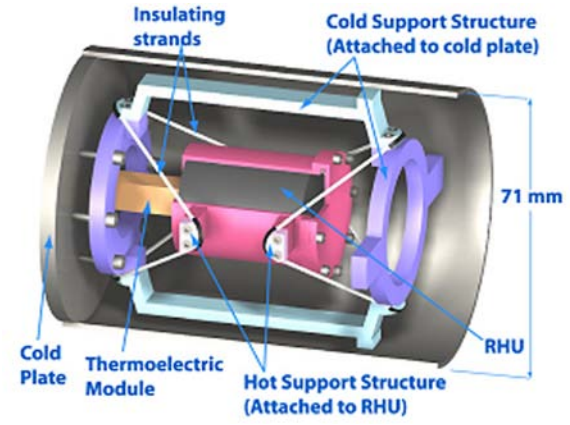

Figure 4-5. ARC Milliwatt RPS Concept Using an RHU and BiTe Thermoelectric Convertor to Generate 40 mWe

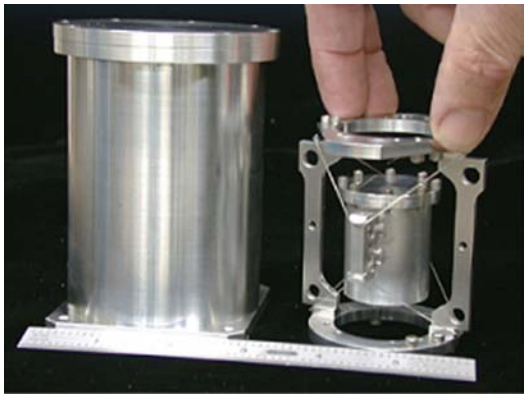

Figure 4-6. Photograph of conceptual 40 mWe ARC RPS

4.4 BIAPOS MILLIWATT RPS CONCEPT

The BIAPOS RPS concept was built and tested in Russia. It is based on the existing RHU heat source and BiTe thermoelectric converter, and comes in 1-RHU and 2-RHU configurations [56, 57]. Analyses and tests indicated that the 1-RHU design (designated PS-1) can produce 25 mWe of power, corresponding to a system efficiency of 2.5%. The associated dimensions are 85 mm (diameter) by 100 mm (height), with an estimated mass of 0.270 kg. The specific power of PS-1 is 0.093 We/kg.

The 2-RHU variant (designated PS-2) is predicted to be capable of generating 70 mWe output, corresponding to a 3.45% system efficiency. The dimensions of the PS-2 concept (Fig. 4-7) are 85 mm (diameter) by 130 mm (height), with an estimated mass of 0.37 kg. The specific power of PS-2 is 0.189 We/kg.

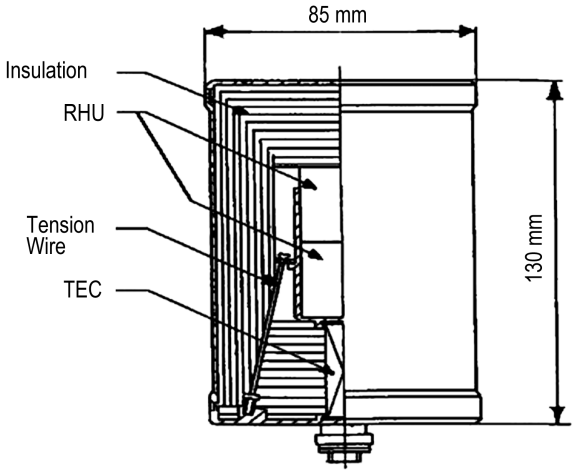

Figure 4-7. BIAPOS Milliwatt RPS Concept Using 2 RHUs to Generate 70 mWe

4.5 DOE/OSC RPS CONCEPTS

This section summarizes the results of a set of comprehensive tests and studies performed by DOE/Orbital Sciences that assessed the performance and configuration of several conceptual small-RPS systems in the milliwatt to tens of watts power range. The concepts in the tens of watts range use the existing GPHS heat source (250 Wt) and advanced thermoelectrics made from segmented PbTe–TAGS/BiTe. This technology is currently in the research and development phase, and thus beyond the scope of what was considered within the mission studies. However, segmented TE technology (PbTe–TAGS/BiTe and Skutterudite-based unicouples) offer a next generation capability with enhanced conversion efficiencies (>9%). The concepts in the milliwatt range use the existing RHU heat source (1 Wt) and their derivatives with BiTe thermoelectrics. The baseline heat sources used in the study and their corresponding electrical power levels are as follows:

1. The General Purpose Heat Source (GPHS) is used with advanced TE converters to produce electrical outputs in the range of 18–24 We.
2. The Radioisotope Heater Unit (RHU) and its derivatives are used with BiTe TE converters to produce electrical outputs in the range of 40 to 160 mWe.

The GPHS, in a multi-module configuration, has been used in RPSs for the NASA Galileo, Ulysses and Cassini missions and is slated for the upcoming Pluto New Horizons mission. The enhanced GPHS, which is to be used on later missions, contains a 0.10 inch central web and 0.10 inch increased graphite thickness on the broad faces for additional strength and reentry ablation protection (Fig.4-9). As of this writing, over 250 RHUs have been used for thermal control in spacecraft, including the NASA Galileo and Cassini spacecraft. The choice of TE materials in the DOE/OSC study was preferentially selected for system compatibility in a Mars atmosphere and in outer planetary space environments, and to maximize thermoelectric efficiency. The selected TE materials were segmented PbTe-TAGS/BiTe for power outputs in the range of 20 We (i.e., using GPHS-Based RPSs) and BiTe for RPSs in the range of 40 to 160 mWe (i.e., using RHU-based RPSs).

Figure 4-8 shows a typical arrangement of the major components of an RPS using thermoelectric conversion.

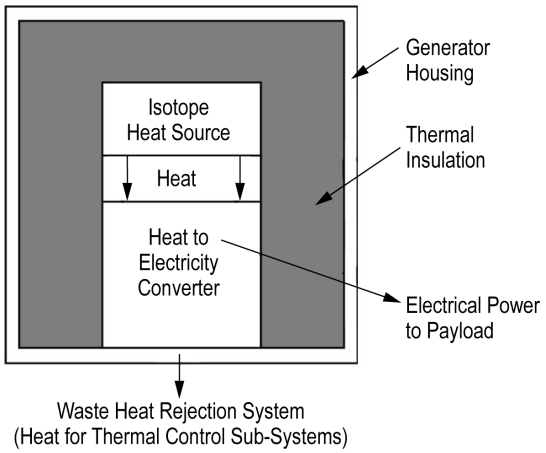

Figure 4-8. RPS Major Components

4.5.1 GPHS-Based RPS Concepts

The components of the GPHS-based RPS are (i) General Purpose Heat Source, (ii) Thermoelectric Converter, (iii) Thermal Insulation, (iv) Generator Housing, (v) Housing Closure/Seals, (vi) Internal Cover Gas/Vacuum, (vii) Gas Management Devices, (viii) Getter, (ix) Heat Source Support, (x) Electrical Power Cabling/Connector, (xi) Mounting/ Handling Provisions, and (xii) Waste Heat Rejection System.

The heat source for the GPHS-based RPS was assumed to be the enhanced GPHS module (250 Wt @ BOL), as shown in Figure 4-9.

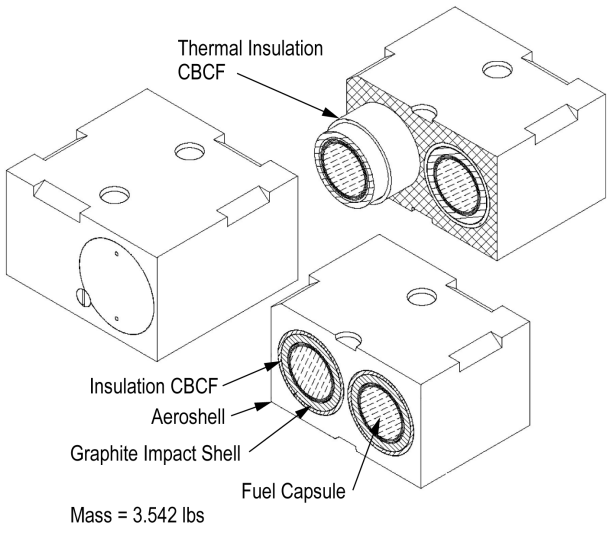

Figure 4-9. Enhanced GPHS 3-D View

Within the DOE/OSC study, the RPS was assumed to be capable of operating in the Earth's atmosphere (prior to launch), in deep space vacuum, or on the surface of Mars. The RPS cold-end temperature was maintained via a cold plate, in which the heat removal approach is tailored to the specific application. The mechanical loads that were considered include: (i) handling loads, (ii) transportation, and (iii) launch loads. The payload voltage was assumed to be at least 5 V_{DC} under matched load. Bio-sterilization was not addressed specifically.

Based on the results of the study, the Close-Packed Array (CPA) thermoelectric module (Fig. 4-10a) was determined to be the preferred developmental approach. It could provide higher system performance in terms of efficiency and specific power, and is mature enough to enable implementation on spacecraft in the 2010 time-frame. Spring-loaded thermoelectric couples / modules (Fig. 4-10b) as used in the SNAP 19 Pioneer and Viking RPSs could be selected for more near-term applications.

Other component selections used in the design study were:

- Thermal Insulation
  - MinK-1400 for load bearing needs, Microtherm HT for non-load bearing locations
  - Compatible with operating temperatures and cover gas environment
- Generator Housing Material
  - Be-38% Al (to be used in MMRTG)
  - Be-23% lighter than 6061 Al alloy (backup)
- Housing Closure/Seals
  - Bolt flange/Viton O-ring/seal welded after fueling (used in SNAP-19)

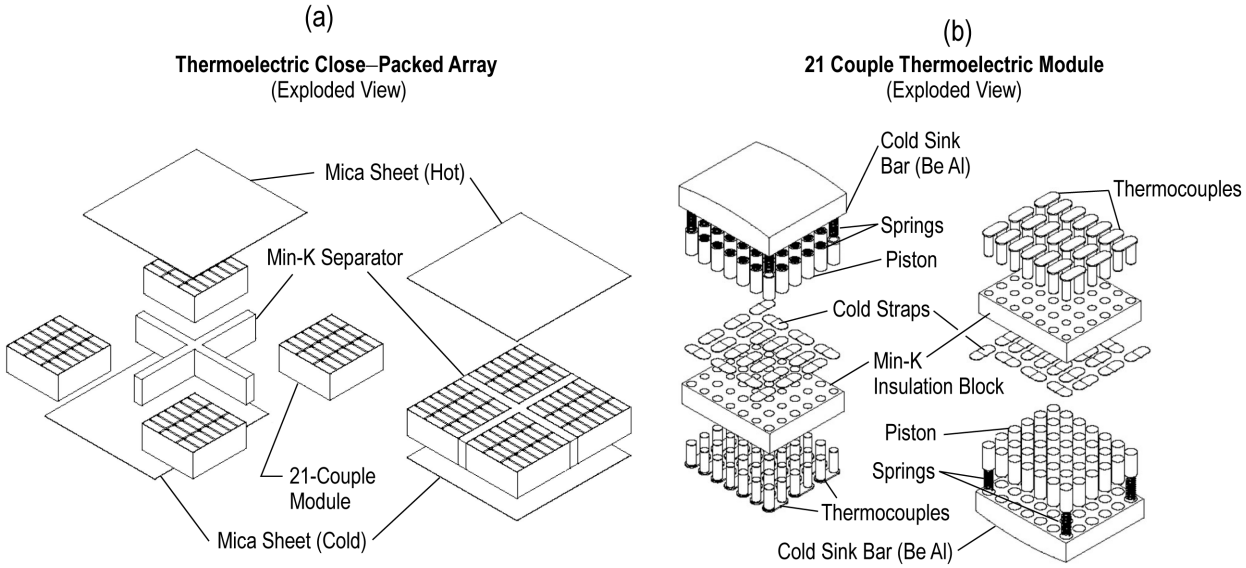

Figure 4-10. Detailed Illustrations of (a) Close-Packed Array (CPA) Thermoelectric Modules and (b) 21-Couple Spring-Loaded Thermoelectric Modules

- Internal Gas Environment
  - Inert xenon gas fill with small amount of helium for leak-checking seals
  - Zirconium getter in palladium holder
- Helium Management
  - Thin sealed Haynes-25 canister with pigtail vent tube through housing
  - Keeps helium out of converter section, reduces heat losses
- Heat Source Support
  - Preload provided by compression of MinK-1400 insulation
- Heat Accumulation Block
  - Four-sided POCO graphite for spring-loaded modules (at least 0.25-inch thick)

An RPS design concept for an advanced technology CPA-based RPS configuration is provided in Figure 4-11(a), and a spring-loaded thermoelectric module is shown in Figure 4-11(b).

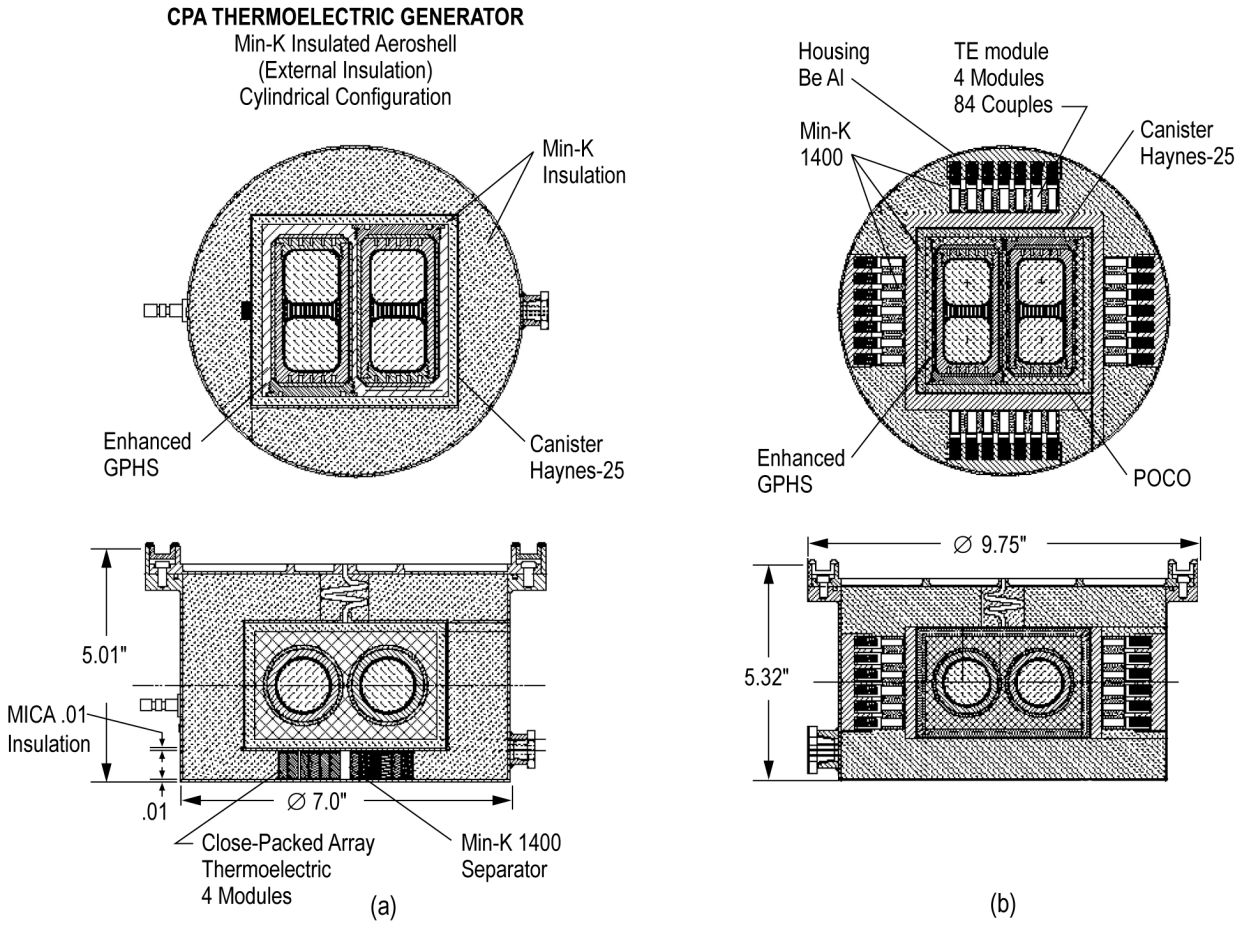

Figure 4-11. GPHS-Based RPS Concepts from the DOE/OSC Study using (a) Close-Packed Array (CPA) Thermoelectric Modules and (b) Spring-Loaded TE Unicouples Along All Four Sides

Results of the early studies predicted power output levels at approximately 18 We, as shown in Table 4-1 with system efficiencies of 7.5% and specific powers of 3.3 to 6.1 We/kg. (Note that specific powers in this study do not include radiator mass since a cold plate is assumed for waste heat removal.) The reference to internal and external insulation within the table refers to the method of maintaining acceptable temperatures for the iridium cladding on the fuel capsules. External insulation is inserted between the GPHS and thermoelectric. Internal insulation is a cylindrical layer around the fuel capsule itself, internal to the GPHS. Although internal insulation results in lower system mass, it requires a change in the GPHS design that would require further evaluation.

Table 4-1. Low-Power RTG Characteristics (BOL)

	SPRING-LOADED		CLOSE-PACKED ARRAY	
Insulation	External	Internal	External	Internal
Q_{HS} (W)	250	250	250	250
$T_{AS,}$ C	883.6	552.9	805.5	503.6
$T_{HOT,}$ C	424.4	427.5	429.8	426.9
$T_{COLD,}$ C	50.4	50.4	50	50
$Q_{TE,}$ W	184.8	186.8	189	186.6
η_{TH} (%)	73.92	74.72	75.6	74.62
η_{TE} (%)	9.98	10.03	10.03	10.03
V_{OC} (V_{DC})	12.3	12.4	12.6	12.5
V_{LOAD} (V_{DC})	7.5	7.6	7.6	7.5
Power (W_E)	18.44	18.74	18.96	18.72
η_{SYS} (%)	7.38	7.5	7.58	7.49
Weight (kg)	5.62	5.26	3.481	3.073
Specific Power, W/kg	3.28	3.57	5.446	6.09

An additional study was performed for a higher output voltage CPA design, shown in Figure 4-12. The optimum CPA RPS configuration was found to have an output power of 22.96 We at 28.52 V_{DC}, corresponding to a specific power of 5.24 We/kg (Table 4-2).

In summary, the results of the DOE/OSC study indicate that a conservative, near-term development approach based on segmented PbTe-TAGS/BiTe spring-loaded couples would provide an RPS with a (i) beginning of life (BOL) electrical power of ~18.7 We, (ii) Mass of ~5.3 kg, (iii) BOL Efficiency of 7.5%, and (iv) BOL specific power of 3.6 We/kg (Table).

For longer-term consideration, a segmented CPA RPS with improved performance (i.e., ~23 We) is possible, but development of the segmented CPA is required.

4.5.2 RHU-Based RPS Concepts (40 mWe)

The RHU-class RPS is based on the RHU heat source and its derivatives. Three heat source configurations were considered in the DOE/OSC study, namely (i) Multiple RHUs, (ii) Multiple RHU fuel capsules in a larger aeroshell, and (iii) a larger multi-watt(t) fuel capsule in a larger aeroshell. An RHU fuel capsule is comprised of a fuel pellet and platinum clad. The standard RHU is shown in Figure 4-13.

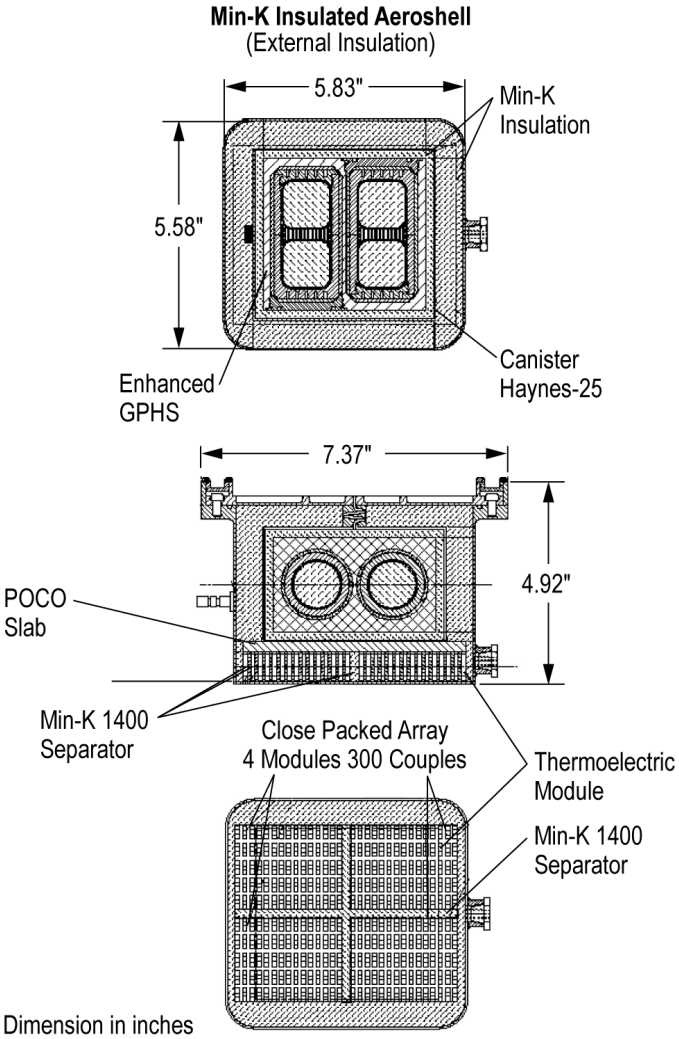

Figure 4-12. GPHS-based RPS Concept Using CPA TEs to Generate 22 We at ~28 VDC

Table 4-2. Performance Characteristics of Higher-Voltage GPHS-Based RPSs from the DOE/OSC Study (Optimum Configuration Highlighted)

HIGHER VOLTAGE CPA RTG CHARACTERISTICS							
T_{COLD} MAINTAINED AT 25°C, ALL OTHER SIDES ADIABATIC: T_{HOT}-427 C							
Number of Couples	264	280	288	300	308	312	320
BOL Power (We)	20.30	21.38	22.11	22.96	23.46	23.82	24.41
Load Voltage (V)	25.18	26.59	27.46	28.52	29.21	29.63	30.35
System Efficiency (%)	8.12	8.55	8.84	9.18	9.38	9.53	9.76
Overall Size (in)							
X-Dimension	5.98	5.89	6.85	6.75	7.08	8.6	7.62
Y-Dimension	6.73	7.11	7.20	7.81	8.06	8.62	8.85
Z-Dimension	4.38	4.34	4.495	4.46	4.65	4.85	4.81
RTG Weight (lb)							
HS/Canister	4.65	4.65	4.65	4.65	4.65	4.65	4.65
POCO Slab	0.39	0.38	0.421	0.39	0.40	0.45	0.38
TE CPA	1.5	1.56	1.64	1.67	1.71	1.77	1.73
MinK Insulation	0.51	1.14	0.90	1.04	1.31	2.18	1.89
Housing	0.82	0.84	0.98	1.03	1.12	1.42	1.31
Misc. (10%)	0.79	0.86	0.86	0.88	0.92	1.05	0.10
Total RTG Wt (lb)	8.64	9.43	9.44	9.67	10.12	11.51	10.96
Total RTG Wt (kg)	3.92	4.28	4.28	4.39	4.59	5.22	4.97
BOL Specific Power							
(W/lb)	2.35	2.27	2.34	2.38	2.32	2.07	2.23
(W/kg)	5.18	5.00	5.16	5.24	5.11	4.56	4.91

The 40 mWe generator (and multiples thereof), utilize the BiTe thermoelectric module, shown in Figure 4-14, that was developed by Hi-Z Technology, Inc. Several modules of this type have been tested in the laboratory from 10,000 hours to over 25,000 hours.

Figure 4-15 shows the seven 40 mWe generator options considered in this study. The thermal insulation dimensions are selected to maintain a hot-end temperature of 250°C, while the cold end is maintained at 25°C via a cold plate.

The lightest and most compact 40 mWe RPS design (Fig. 4-15) is Option #7, which has a mass of 0.482 kg and a specific power of 0.083 We/kg. However, this concept would require the development of a new 3.3 Wt fuel capsule.

The preferred 40 mWe RPS designs using existing RHU fuel capsules are listed below in descending order based on specific power:

- Option #6 - 4 RHU fuel capsules in a redesigned aeroshell
  - Specific power of 0.061 We/kg
- Option #4 - 4 RHUs side-by-side
  - Specific power of 0.032 We/kg
- Option #1 - Stack of 4 RHUs,
  - Specific power of 0.030 We/kg

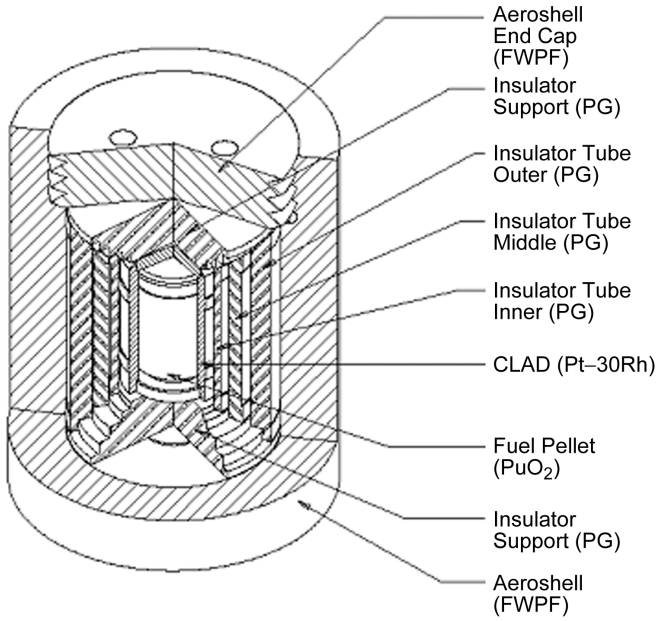

Figure 4-13. Illustration of a Radioisotope Heater Unit (RHU)

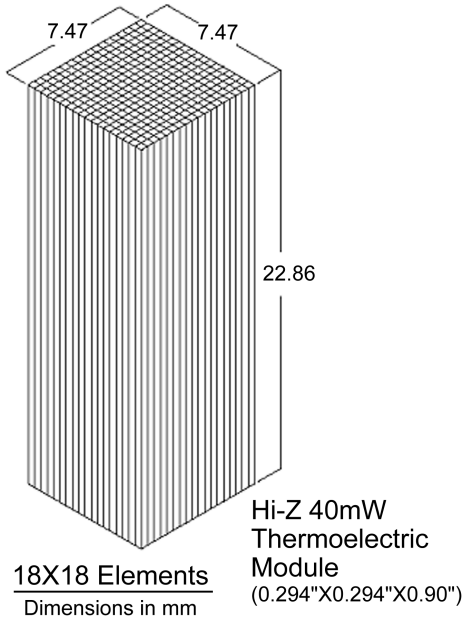

Figure 4-14. Hi-Z 40 mWe CPA Thermoelectric Module Using BiTe

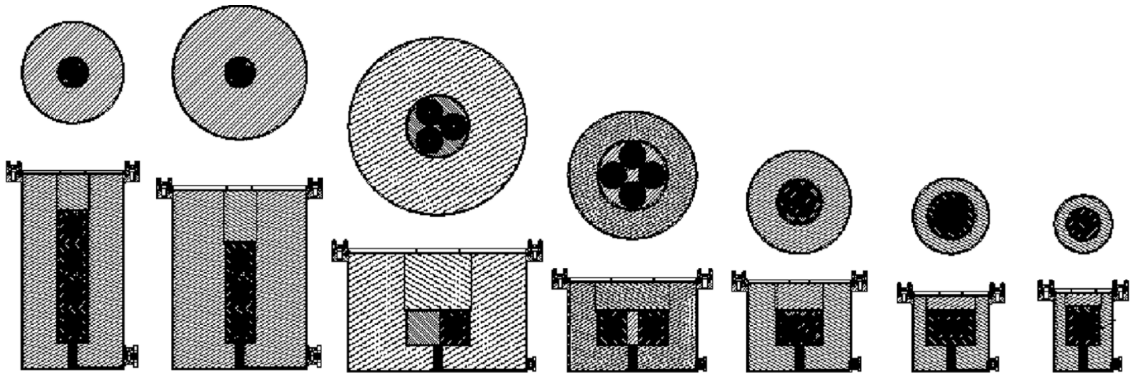

Figure 4-15. Several Conceptual 40 mWe RPS Configurations Assessed in the DOE/OSC Study

In summary, several practical design concepts for a 40 mWe RPS have been assessed in the DOE/OSC study that would require only minimal development in order to support near-term mission applications. The smallest and lightest design, without new fuel capsule development is Option #6 in Figure 4-15, and further detailed in Figure 4-16. The mass of this concept is 0.656 kg, corresponding to a specific power of 0.061 W/kg.

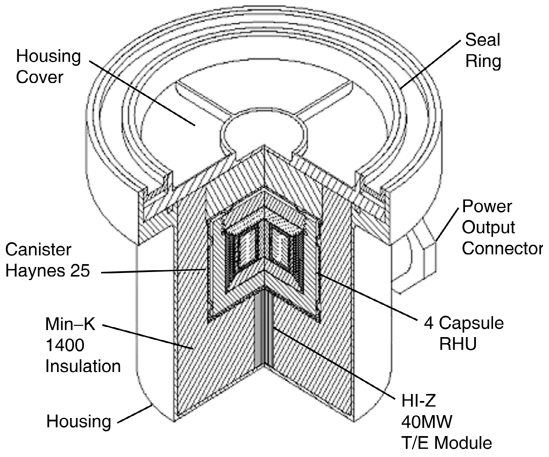

Figure 4-16. Conceptual Design for a 40 mWe RPS Using Existing RHU Fuel Capsules in a Redesigned Aeroshell

4.5.3 RHU-Based RPS Concept (160 mWe)

Several concepts were considered for higher milliwatt RPSs (>40 mWe) based on the Hi-Z BiTe thermoelectric module. The preferred concept is a generator with 160 mWe power output that utilizes seven 1 Wt RHU fuel capsules in a redesigned aeroshell and four Hi-Z 40-mWe thermoelectric modules as shown in Figure 4-17. The mass of this higher power generator system was estimated at 0.854 kg, corresponding to a specific power of 0.187 We/kg.

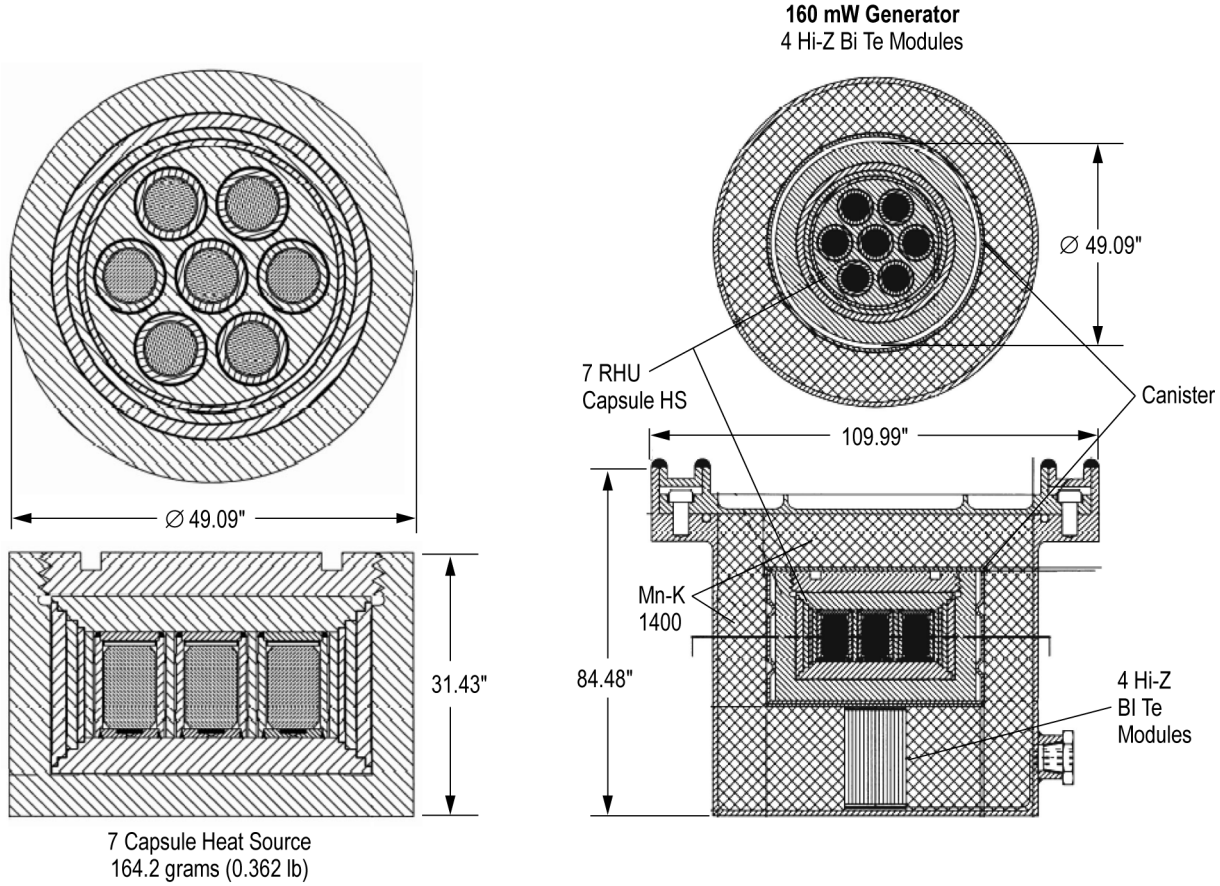

Figure 4-17. RPS Concept Using Seven RHU Capsules and Hi-Z BiTe TE Converters to Generate 160 mWe

4.6 SMALL-RPS CONCEPTS SUMMARY

During the last several years, a significant amount of research has been conducted in designing conceptual small-RPS units and in predicting their performance characteristics. This report summarizes the expected performance values of twenty-four of these conceptual RPS designs, including thirteen milliwatt-range RPSs (Table 4-3) and eleven multiwatt-range RPSs (Table 4-4). Of the milliwatt RPS concepts, five have been designed to operate in deep space (Hi-Z, JPL/Swales, ARC and BIAPOS), and eight have been designed for operations in both deep space and in a Mars atmosphere (DOE/OSC). All milliwatt RPSs described herein would use an RHU heat source (or its derivative) with bismuth telluride thermoelectrics. The estimated specific power of the milliwatt RPSs was estimated to range from 0.020 to 0.330 We/kg, and is greatly influenced by the RPS operating environment, study assumptions, and power levels. Milliwatt RPS units designed solely for deep space environments can make use of light multi-layer insulation (MLI) or thin radiation shields, which significantly decreases their unit mass and increases their specific power relative to the RPSs designed for operation in an atmosphere (which would require heavier bulk thermal insulation). However, bulk insulation has the advantage of being a load-bearing material, which simplifies the RPS design and increases its robustness. Milliwatt-class RPS concepts that assumed a new RHU fuel capsule design (DOE Option #7) or used multiple existing RHU fuel capsules in a redesigned aeroshell (DOE Options #5 and 6) generally had higher specific powers for a given power output than did similar RPS concepts (DOE Options #1 through #4) using exist-

Table 4-3. Summary of Milliwatt-Range RPS Concepts and Estimated Performance Characteristics—All Use BiTe Thermoelectrics.

RPS	Heat Source	System Efficiency	Power Output at BOL (mWe)	Mass (kg)	Specific Power (We/kg)	Notes
NASA and Industry Milliwatt RPS Designs						
Hi-Z	1 RHU	4%	40	0.325	0.123	Designed for cacuum operation, up to 2000g uniaxial acceleration
JPL/Swales	1 RHU	2%	20	0.30	0.067	Designed for vacuum operation.
ARC	1 RHU	4%	40	0.121	0.330	Designed for vacuum operation, Up to 500g acceleration
BIAPOS PS1	1 RHU	2.5%	25	0.27	0.093	Russian organization
BIAPOS PS2	2 RHUs	3.5%	70	0.37	0.189	Russian organization
DOE/OSC Milliwatt RPS Designs - All Designed for Operation in Vacuum or in Atmosphere						
Option#1	4 RHUs	1.0%	40	1.35	0.030	
Option#2	4 RHUs	1.0%	40	1.674	0.024	
Option#3	4 RHUs	1.0%	40	2.001	0.020	
Option#4	4 RHUs	1.0%	40	1.258	0.032	
Option#5	3 RHU Fuel Capsules	1.3%	40	0.868	0.046	Requires a new aeroshell for three RHU fuel capsules.
Option#6	4 RHU Fuel Capsules	1.0%	40	0.656	0.061	Requires a new aeroshell for four RHU fuel capsules.
Option#7	3.3 Wt Fuel Capsule	1.2%	40	0.482	0.083	Optimum configuration for DOE 40-mWe RPS. Requires redesigned fuel capsule and aeroshell.
160mW RPS	7 RHUs	2.3%	160	0.854	0.187	Uses 7 RHUs to generate 160 mWe.

ing RHU fuel capsules and aeroshells. The higher specific power, however, would need to be traded against the additional cost associated with the development of a different RHU fuel capsule or aeroshell. Lastly, milliwatt RPS units running at higher power levels (>40 mWe) generally had higher values of specific power than did similar RPS designs operating at lower power levels (<40 mWe), e.g., BIAPOS PS2 versus BIAPOS PS1, and the DOE's 160mWe concept versus their 40 mWe concepts. This is indicative of the economy of scale associated with going to higher power levels, and is further demonstrated by the specific power levels predicted for the multiwatt RPS concepts studied by DOE/OSC (Table 4-4).

Table 4-4. Summary of Multiwatt-Range RPS Concepts and Estimated Performance Characteristics—All Use segmented PbTe-TAGS/BiTe Thermoelectrics.

#	RPS	Heat Source	System Efficiency	Power Output at BOL (We)	Mass[1] (kg)	Specific Power[1] (We/kg)	Notes
12 VDC Multi-Watt RPS - Designed for Operation in Vacuum or in Atmosphere							
a. Spring-Loaded Configuration (Near-Term Technology)							
1	External	1 GPHS	7.38%	18.44	5.62	3.28	
2	Internal	1 GPHS	7.50%	18.74	5.26	3.57	Optimum configuration for 12V Spring-Loaded configuration based on specific power.
b. CPA Configuration (Further-Term Technology / Requires Additional R&D)							
3	External	1 GPHS	7.58%	18.96	3.481	5.446	
4	Internal	1 GPHS	7.49%	18.72	3.073	6.09	Optimum configuration for 12V CPA configuration based on specific power.
28 VDC CPA Multi-Watt RPS - Designed for Operation in Vacuum or in Atmosphere							
5	264 Couple	1 GPHS	8.12%	20.30	3.92	5.18	Least mass of 28V RPS designs.
6	280 Couple	1 GPHS	8.55%	21.38	4.28	5.00	
7	288 Couple	1 GPHS	8.84%	22.11	4.28	5.16	
8	300 Couple	1 GPHS	9.18%	22.96	4.39	5.24	Optimum configuration for 28V design based on specific power.
9	308 Couple	1 GPHS	9.38%	23.46	4.59	5.11	
10	312 Couple	1 GPHS	9.53%	23.82	5.22	4.56	
11	320 Couple	1 GPHS	9.76%	24.41	4.97	4.91	Highest efficiency and greatest output power of 28V RPS designs..

Note:
1. RPS mass and specific power calculations do not include thermal radiator mass.

Eleven multiwatt RPS concepts were studied by DOE/OSC and their expected performance characteristics summarized herein (Section 4.5 and Table 4-4). These RPS designs include four concepts that would run at ~12 VDC, and seven that would operate at ~28 VDC. All eleven concepts were designed to operate in either deep space or in a Mars atmosphere and would use a single GPHS module with segmented PbTe-TAGS/BiTe thermoelectrics. Furthermore, all are predicted to have specific powers ranging between 3.28 to 6.09 We/kg (excluding radiator fin mass). Of the four 12-VDC RPS concepts, two would use spring-loaded thermoelectric couples/modules as used in the SNAP 19 Pioneer and Viking RPSs, and are expected to have a maximum specific power of 3.57 W/kg (Row 2 in Table 4-4). Using advanced close-packed array thermoelectrics, the specific power of the 12-V RPS concepts could be increased to 6.09 We/kg (Row 4). Of the seven 28-V RPS designs studied by DOE/OSC, the optimum configuration used a 300 couple close-packed array to generate a specific power of 5.24 We/kg (Row #8). Though other 28-V RPS

configurations could yield greater electrical power or lower mass, the 300-couple design yielded the best combination of both parameters.

In summary, the predicted performance characteristics of twenty-four small-RPS concepts have been summarized herein, including eleven milliwatt-class RPS units and eleven multiwatt-class RPS units. While additional research and development needs to be performed to verify, optimize, and refine the RPS concepts studied by NASA, industry and DOE, there is sufficient evidence to suggest that such concepts are indeed feasible and could be developed by the 2009 to 2011 time-frame given adequate resources.

5. ACKNOWLEDGEMENTS

The following individuals contributed significantly to the development of this document.

Section 1
George Schmidt (Author), NASA HQ
Rob Abelson (Author), JPL
Tibor Balint, JPL
Ellis Miner, JPL
Jim Randolph, JPL
Jim Shirley, JPL

Section 2.1 to 2.2
Rob Abelson (Author), JPL
Tibor Balint, JPL
Ellis Miner, JPL
Jim Randolph, JPL
Jim Shirley, JPL

Section 2.3 Landers
Rob Abelson (Author), JPL
Jim Shirley (Co-Author), JPL
Bob Carpenter, OSC
John Elliott, JPL
Jacklyn Green, JPL
Insoo Jun, JPL
Ellis Miner, JPL
Bill Nesmith, JPL
Erik Nilsen, JPL
Tom Spilker , JPL
Rao Surampudi, JPL
Wayne Zimmerman, JPL
JPL Europa Pathfinder Team, JPL

Section 2.4 Rovers
Tibor Balint (Author of Mars rover), JPL
Jim Randolph (Author of lunar rover), JPL
Jim Shirley (Co-Author of lunar rover), JPL
Rob Abelson (Co-Author of lunar rover), JPL
Gary Ball, JPL
Luther Beegle, JPL
Robert Carnright, JPL
Roger Diehl, JPL
Salvador DiStefano, JPL
Raymond Ellyin, JPL
David Hansen, JPL
Robert Haw, JPL
Michael Henry, JPL
Timothy Ho, JPL
Insoo Jun, JPL
Frank Jordan, JPL
Eug-Yun Kwack, JPL
Randel Lindemann, JPL
Greg Mungas, JPL
Daniel Nigg, JPL
Keith Novak, JPL
Guillermo Olarte, JPL
Knut Oxnevad, JPL
Vincent Randolph, JPL
John Rohr, JPL
Cesar Sepulveda, JPL
William Strauss, JPL
Thomas Valdez, JPL
Keith Warfield, JPL
Gail Watson-Ashe, JPL
Eric Wood, JPL

Section 2.5 Sub-Satellites
Jim Randolph (Author), JPL
Leon Alkalai, JPL
David Collins, JPL
Faramaz Davarian, JPL
David Hansen, JPL
Bill Imbriale, JPL
Alex Konopliv, JPL
Jerry Langmaier, JPL
Bob Miyake, JPL
Bill Moore, JPL
Bill Nesmith, JPL
Jon Sims, JPL
Rao Surampudi, JPL
Paul Timmerman, JPL
Brian Wilcox, JPL
Daniel Winterhalter, JPL

Section 2.6 Deployable Mini-Payloads
Celeste Satter (Author), JPL
Rob Abelson (Co-Author), JPL
Kathryn Marshall (Technical Writer), JPL
Bruce Banerdt, JPL
David Collins, JPL
Sal DiStefano, JPL
Mike Newell, JPL
Jan Tarsala, JPL

Section 2.7 Mission Studies Summary
Rob Abelson (Author), JPL
John Allmen, ARC
Pam Clark, GSFC

Section 3 Power Conversion Technologies for Small-RPS Systems
Rob Abelson (Author), JPL
Dick Shaltens, GRC
Jeffrey Schreiber, GRC
Rao Surampudi, JPL

Section 4 Small-RPS Concepts
Rob Abelson, (Author-Sect. 4.1–4.4, 4.6), JPL
Heros Noravian (Author-Sect. 4.5), Analytix
Thierry Caillet, JPL
Jean-Pierre Fleurial, JPL
Vasanth Kumar, Analytix
Bob Wiley, DOE

Documentation Services
Jeanné Washington, Lead, JPL
Jim Jackson, JPL
Kathryn Marshall, JPL
Mary Sue O'Brien
Joseph Spahr, JPL
Mary Young, JPL

6. REFERENCES

1. Hunt, M. E., R. B. Harty, and R. Cataldo, "A Dynamic Isotope Power System for Space Exploration Initiative Surface Transport Systems", AIAA-92-1489, AIAA Space Programs and Technologies Conference, Huntsville, AL, March 24-27, 1992.
2. Furlong, R. P. and E. J. Wahlquist, "U.S. Space Missions Using Radioisotope Power Systems", Nuclear News, April 1999.
3. Jones, R. M., "The MUSES CN Rover and Asteroid Exploration Mission", 22nd International Symposium on Space Technology and Science, Morioka, Japan, May 28–June 4, 2000.
4. President G. W. Bush speech, "A Renewed Spirit of Discovery", January 2004, URL: http://www.whitehouse.gov/space/renewed_spirit.html.
5. "New Frontiers in the Solar System: An Integrated Exploration Strategy", Space Studies Board, National Research Council, National Academics Press, 2003.
6. Greeley, R. and T. Johnson, "Report of the NASA Science Definition Team for the Jupiter Icy Moons Orbiter (JIMO)", NASA, February 13, 2004.
7. Zimmerman, W., J. Green, et.al., "Europa Pathfinder Study", Internal JPL Presentation, 2001.
8. Gershman, R., "Jupiter Icy Moons Orbiter (JIMO) Mission Architecture Document", Jet Propulsion Laboratory, Pasadena, CA, December 3, 2003.
9. Surampudi, R., R. Carpenter, M. El-Genk, L. Herrera, L. Mason, J. Mondt, B. Nesmith, D. Rapp, and R. Wiley, "Advanced Radioisotope Power Systems Report", Report to NASA Code S, March 2001.
10. Hyder, A., K., R. L. Wiley, G. Halpert, D. J. Flood, and S. Sabripour, Spacecraft Power Technologies, Imperial College Press, 2000.
11. Beasley, M. A., S. L. Firebaugh, R. L. Edwards, A. C. Keeney, and R. Osiander, "Microfabricated Thermal Switches for Emittance Control", Space Technology and Applications Forum-STAIF 2004, American Institute of Physics 0-7354-0171-3/04.
12. Kislov, N., H. Grogerm, R. Ponnappan, E. Caldwell, D. Douglas, and T. Swanson, "Electrochromic Variable Emittance Devices on Silicon Wafer for Spacecraft Thermal Control", Space Technology and Applications Forum-STAIF 2004, American Institute of Physics 0-7354-0171-3/04.
13. Biter, W., S. Hess, and S. Oh, "Electrostatic Radiator for Spacecraft Temperature Control", Space Technology and Applications Forum-STAIF 2004, American Institute of Physics 0-7354-0171-3/04.
14. Personal Communication with Wayne Zimmerman, JPL, 2004.
15. Jun, I., "Peer Review of Radiation Shielding Approach for the Jupiter Icy Moons Orbiter (JIMO)", Technical Baseline Review-2, JPL internal presentation, January 29, 2004.
16. Jun, I., "Single Brick GPHS Total Dose Estimates", Mars Smart Lander Study, JPL Internal Presentation, December 23, 2003.
17. NASA, "Mars Exploration Rover Mission", URL: http://marsrovers.jpl.nasa.gov/home/index.html
18. MEPAG (Mars Exploration Program Assessment Group), URL: http://mepag.jpl.nasa.gov.
19. Diehl, R., et al, "AFL Study, MER Expansion Studies", Pre-Projects and Advanced Studies (Office-610), Jet Propulsion Laboratory, Pasadena, CA, April 2004.
20. NASA, "NASA's Mars Exploration Program", URL: http://marsprogram.jpl.nasa.gov/.

21. NASA-KSC, “Launch vehicle database”, URL: http://elvperf.ksc.nasa.gov/elvMap/.
22. Balint, T., “Power System Breakpoints for Mars Exploration”, Pre-Projects and Advanced Studies (Office-610), Jet Propulsion Laboratory, Pasadena, CA, September 24, 2003.
23. Dawson, S., N. Mardesich, and D. Rapp, “Solar Energy on Mars, Volumes 1 to 3”, Jet Propulsion Laboratory, Pasadena, CA, May 2003.
24. Wiley, R., R. Carpenter, “Small Radioisotope Power Source Concepts”, Proc. of Space Technology & Applications International Forum (STAIF-2004), Albuquerque, NM, February 8th–11th, 2004.
25. Golombek, M. P., “Rock Statistics Calculations for the MER Landing Sites”, 3rd MER Landing Site Workshop, Pasadena, CA, March 27, 2002.
26. Oxnevad, K., et al, “A Lunar RPS Rover Study”, JPL Document D-28811, April 29, 2004.
27. Feldman, W. C., et al, “Evidence for water ice near the lunar poles”, J. Geophys. Res. 106, No. E10, 23,231–23,251, 2001.
28. Vasavada, A. R., D. A. Paige, and S. E. Wood, “Near-Surface Temperatures on Mercury and the Moon and the Stability of Polar Ice Deposits”, Icarus 141, 170–193, 1999.
29. Bussey, D. B. J., P. G. Lucey, M. S. Robinson, P. D. Spudis, K. D. Edwards, and D. Steutel, “Permanent Shadow in Simple Craters Near the Lunar Poles”, Lunar. Plan. Sci. Conf. 34, abs.1897, 2003.
30. Bussey, D. B. J., M. S. Robinson, K. Fristad, and P. D. Spudis, “Permanent Sunlight at the Lunar North Pole”, Lunar Plan. Sci. Conf. 35, abs. 1387, 2004.
31. Melosh, H. J., “Impact Cratering”, Shirley, J. H. and R.W. Fairbridge, eds., Encyclopedia of Planetary Sciences, Chapman & Hall, New York, 1997.
32. Cook, A. C., T. R. Watters, M. S. Robinson, P. D. Spudis, and D. B. J. Bussey, “Lunar polar topography derived from Clementine stereoimages”, J. Geophys. Res. 105, No. E5, 12,023–12,033, 2000.
33. Noreen, G., “JPL Lunar Network Architecture Study”, JPL Internal Document, March 15, 2004.
34. Team X, “Lunar Rover MER 2004-02”, Report Number 686, February 5, 2004.
35. Phoenix Project Mission and System Review, JPL Internal Document, March 23, 2004.
36. “Mars Lander Hazard Avoidance Using 3D LADAR,” Lockheed Martin Internal Document, 3 December, 2003.
37. Mills, A. F., Heat Transfer, Irwin Publishers, Chicago, 10992, pp 674-688.
38. Pauken, M. and J. I. Rodriguez, “Performance Characterization and Model Verification of a Loop Heat Pipe”, American Society of Automotive Engineers, Paper# 2000-01-2317, 2000.
39. “JIMO Science Forum Compiled Objectives”, in Forum on Concepts and Approaches for Jupiter Icy Moons Orbiter, June 12, 2003, URL: http://www.lpi.usra.edu/meetings/jimo2003/abstractsvolume.html
40. Collins, D., et al, “Low-Cost Adjunct Microspacecraft Testbed”, JPL Internal Document, October 22, 2003.
41. Collins, D. H., et al, “Multimission Space and Solar Physics Microspacecraft”, JPL Internal Document D-18809-A, April 14, 2000.
42. “SwRI charged particle detector and ultraviolet spectrometer to fly aboard Rosetta”, SwRI News Release, February 20, 2004, URL: http://www.swri.org/9what/releases/2004/rosetta.htm.

43. Atkinson, D. H., "The Galileo Mission to Jupiter and Doppler Wind Measurements", IEEE Antennas and Propagation Magazine, Vol. 33, No. 4., August 1991.
44. Banerdt, W. B. and W. T. Pike, "A Miniaturized Seismometer for Surface Measurements in the Outer Solar System", Forum on Innovative Approaches to Outer Planetary Exploration 2001–2020, Lunar and Planetary Institute, Houston, Texas, February 21–22, 2001.
45. Office of Naval Research, Press Release, September 9, 2001, http://www.onr.navy.mil/media/article.asp?ID=40.
46. Koppes, Steve, "Living' La Vida Europa", Arizona State University E-zine, Fall 1999, http://researchmag.asu.edu/stories/europa.html.
47. Shirley, J. H. and R.W. Fairbridge, eds., Encyclopedia of Planetary Sciences (Encyclopedia of Earth Sciences Series), Kluwer Academic Publishers, Dordrecht, 1997.
48. Schock, A., "Design of Small Impact-Resistant RTGs for Mars Environmental Survey Mission", CONF 920104, American Institute of Physics, 1992.
49. JPL Team A, "μ-Rover Milliwatt Radioisotope Power Source (RPS)", JPL internal report, September 1999.
50. NASA Solar System Exploration Web Site, News Archive, January 2, 2001, http://sse.jpl.nasa.gov/news/display.cfm?News_ID=599.
51. Schreiber, J., "Stirling Isotope Power Conversion Options Presentation", Glenn Research Center, Cleveland, OH, January 2004.
52. Bass, J. C. and D. T. Allen, "Milliwatt Radioisotope Power Supply for Space Applications", 18th International Conference on Thermoelectrics, IEEE, 1999.
53. Allen, D. T. and M. S. Murbach, "Milliwatt Radioisotope Power Supply for the PASCAL Mars Surface Stations", Space Technology and Applications International Forum (STAIF), 2001.
54. Snyder, G. J., A. Borshchecsky, et.al., "Testing of Milliwatt Power Source Components", ICT, 2002.
55. Roach, P. R., P. Kittel, J. Feller, and B. Helvensteijn, "Thermal Isolator with Strong Mechanical Support for a Radioisotope Heater Unit", Space Technology and Applications International Forum - STAIF, 2004.
56. Pustovalov, A., V. Gusev, A. Borshchevsky, and A. Chmielewski, "Experimental Confirmation of Milliwatt Power Source Concept", 18th International Conference on Thermoelectrics, 1999.
57. Pustovalov, A., "MiniRTGs on Plutonium-238: Development and Application", 18th International Conference on Thermoelectrics, 1999.

7. ACRONYMS AND ABBREVIATIONS

AC	attitude control
ACS	Attitude Control System
ALRH	Apollo Lunar Radioisotope Heater
ALSEP	Apollo Lunar Surface Experiments Package
ARC	Ames Research Center
APS	Active Pixel Sensor
APXS	Alpha Particle X-ray Spectrometer
BiTe	bismuth-telluride
BOL	beginning of life
C&DG	command and data handling
CBE	current best estimate
Co-I	Co-Investigator
CPA	close-packed array
CPU	central processing unit
DC/DC	direct current/direct current
DCT	design control table
DOE	Department of Energy
DOI	descent orbital insertion
DSN	Deep Space Network
DTE	direct to Earth
EDL	entry, descent, and landing
EEPROM	electrically erasable programmable read-only memory
ELM	Europa Lander Mission

EOL	end of life
EOM	end of mission
EPF	Europa Pathfinder
F&P	fields and particles
FPGA	Field Programmable Gate Array
G&C	guidance and control
GaAs	gallium arsenide
GaInP/SiAs/Ge	gallium indium phosphorous/silicon aresenic/germanium
GCMS	Gas Chomoatograph Mass Spectrometer
GPHS	General Purpose Heat Source
GSFC	Goddard Space Flight Center
GRC	Glenn Research Center
GSO	Galiliean Satellite Orbiter
HGA	high-gain antenna
HRS	heat rejection system
IES	Ion and Electron Spectrometer
JIMO	Jupiter Icy Moons Orbiter
JPL	Jet Propulsion Laboratory
LADAR	Laser Detection and Ranging
LCAM	low-cost adjunct microspacecraft
LGA	low-gain antenna
LIBS	Laser-Induced Breakdown Spectroscopy

LIDAR	Light Detection and Ranging
LILT	low intensity low temperature
LOS	line of sight
LV	launch vehicle
ME	mobility electronics
MEPAG	Mars Exploration Program Assessment Group
MER	Mars Exploration Rovers
MHW	multi-hundred Watt
Mini-TES	Mini-Thermal Emission Spectrometer
MLI	multi-layer insulation
MMRS	Mars Microbeam Raman Spectroscope
MMRTG	Multi-Mission RTG
MSL	Mars Science Laboratory
MSSPM	Multimission Space and Solar Physics Microspacecra
MTO	Mars Telecom Orbiter
NASA	National Aeronautics and Space Administration
NEP	Nuclear Electric Propulsion
NRC	National Research Council
Pancam	panoramic camera
PbTe	lead telluride
PCS	Power Conversion System
PI	Principal Investigator
P/L	payload
RAT	rock abrasion tool

REM	Rover Electronics Module
RF	radio frequency
RHU	radioisotope heater unit
RPS	radioisotope power systems
RTG	Radioisotope Thermoelectric Generators
SA	solar array
S/C	spacecraft
SEC	Single-Engine Centaur
SiGe	silicon-germanium
SMEX	Small Explorer
SNAP	systems for nuclear auxiliary power
SRAM	static random access memory
SRG	Stirling Radioisotope Generator
SSR	solid-state recorder
TAGS	tellurides of antimony, germanium, and silver
TE	thermoelectric
TID	total ioniznig dose
TV	thermal valves
TLM/CMD	telemetry and command
TOF-MS	Time-of-Flight Mass Spectrometer
UHF	ultra-high frequency
URL	uniform resource locator
USO	ultra stable oscillator
We	electrical watts

Wt	thermal watts
WEB	warm electronics box
XRD/XRF	X-ray Diffractometer/X-ray Fluorescence Spectrometer